ROLES AND REGULATION OF STAT3 IN INNATE IMMUNITY

Hung-Ching Hsia

A dissertation submitted to the faculty of the University of North Carolina at Chapel Hill in partial fulfillment of the requirements for the degree of Doctor of Philosophy in the department of Cell Biology and Physiology in the School of Medicine

Chapel Hill
2017

Approved by:

Albert Baldwin

Douglas Cyr

Blossom Damania

Ben Major

Yue Xiong

ABSTRACT

Hung-Ching Hsia: Roles and Regulation of STAT3 in Innate Immunity
(Under the direction of Albert Baldwin)

Innate immunity is the first line of host defense to microbial infections. The rapid induction of the innate immune response is achieved through recognition of pathogen-associated molecular patterns (PAMPs) and danger-associated molecular patterns (DAMPs). Upon recognition of PAMPs and DAMPs, cells initiate immune responses by expressing type I interferons (IFN) and interferon-stimulated genes (ISGs) to establish an antiviral and antimicrobial state, and by secreting cytokines and chemokines to recruit and activate immune cells such as macrophages and monocytes. These processes are precisely regulated to initiate a swift and effective defense against pathogens.

My dissertation focuses on the roles and regulation of signal transducer and activator of transcription 3 (STAT3) in these responses. In the first project, I investigated the role of STAT3 in myeloid cells with regards to innate immune responses during viral infection. We discovered that STAT3 knockout mice are more susceptible to herpes simplex virus-1 (HSV-1) due to an attenuated IFN response and to defects in dendritic cell and natural killer cell activation, revealing a requirement of STAT3 in eliciting an effective innate immune response against HSV-1. The second project focused on dissecting the signaling pathways activated by cytosolic DNA, a DAMP, and the regulation of downstream transcription factors. I identified a novel signaling axis involving an inhibitory phosphorylation in STAT3 by TANK-binding kinase 1 (TBK1).

This TBK1-mediated phosphorylation restricts STAT3 activation and expression of selective STAT3 target genes in response to cytosolic DNA. Collectively, the research presented in this dissertation demonstrates a pivotal role of STAT3 in host innate immunity against viral infection, and uncovers a novel mechanism whereby the activity of STAT3 can be fine-tuned by innate immune response pathways.

To my parents and grandma

ACKNOWLEDGEMENTS

This dissertation would not have been possible without the help from a lot of wonderful people. First and foremost, I would like to express my gratitude to my advisor, Dr. Al Baldwin, for providing a supportive environment that allowed me to pursue interesting scientific questions. He guided me through the process of dissertation research and cultivated my critical thinking skills to become a good scientist. The trainings I received from him are invaluable and will be forever useful. I am also grateful to my committee members, Dr. Doug Cyr, Dr. Blossom Damania, Dr. Ben Major, and Dr. Yue Xiong, for offering their time and knowledgeable insights. Their constructive feedbacks helped shape my research tremendously. Special thanks are owed to Dr. Damania, who provided expert knowledge and supports in immunology and virology as I wandered into unfamiliar territories. Thanks are also due to Dr. Jessica Hutti for her numerous thoughtful inputs, Dr. Zhe Ma and Dr. Zhigang Zhang for their suggestions and assistance in viral infection experiments, and Mr. Aaron Ebbs, Mr. Jose Roques, and Mr. Charles Stopford for their superb support in animal studies. I wish to thank the past and current members of the Baldwin Lab for constant feedbacks, daily support, and awesome happy hour that made science even more exciting. I am also fortunate to have a group of amazing friends, who are my best emotional support system no matter where in the world they are. Finally, I would like to thank my grandma and parents, who have no idea what I do but still believe in me and love me unconditionally, my sister, for getting her PhD first and urging me to catch up, and my husband, who is my best friend and partner in this very long journey of doctoral research and life.

TABLE OF CONTENTS

LIST OF TABLES ..... **x**

LIST OF FIGURES ..... **xi**

LIST OF ABBREVIATIONS ..... **xiii**

CHAPTER 1: INTRODUCTION **1**

1.1 STAT3 ..... **1**

1.1.1 General introduction *1*

1.1.2 STAT3 in human diseases *2*

1.2 TBK1 and IKKε **4**

1.2.1 General introduction *4*

1.2.2 TBK1 and IKKε in innate immunity *5*

1.2.3 TBK1 and IKKε in cancers *6*

1.3 Responses Elicited by Cytosolic DNA **7**

1.3.1 Induction of the inflammasomes by cytosolic DNA *7*

1.3.2 Induction of interferons by cytosolic DNA *8*

1.3.3 Induction of the NF-κB pathway by cytosolic DNA *12*

1.3.4 Cytosolic DNA and autoimmunity *12*

1.3.5 Cytosolic DNA and microbial infections *13*

1.4 Regulation of STATs by Innate Immune Signaling Pathways **13**

REFERENCES **17**

CHAPTER 2: STAT3 REGULATES HOST DEFENSE AND PROTECTS MICE AGAINST HERPES SIMPLEX VIRUS-1 INFECTION 29

2.1 Summary 29

2.2 Introduction 30

2.3 Results 33

2.3.1 Characterization of Stat3$^{fl/fl}$ LysM-Cre$^{+/+}$ mice 33

2.3.2 Stat3 knockout BMMs show attenuated type I interferon response to HSV-1 infection 34

2.3.3 Myeloid Stat3 knockout mice are more susceptible to HSV-1 infection 36

2.3.4 Susceptibility of Stat3 knockout mice is not caused by immunopathology in the brain 37

2.3.5 Stat3 knockout mice express reduced levels of antiviral cytokines in the spleen ... 38

2.3.6 Stat3 knockout mice have decreased CD8^{+} cDC frequency during HSV-1 infection 39

2.3.7 Stat3 knockout mice have impaired NK and T cell activation during HSV-1 infection 40

2.4 Discussion 41

2.5 Materials and Methods 46

REFERENCES 60

CHAPTER 3: CYTOSOLIC DNA PROMOTES STAT3 PHOSPHORYLATION BY TBK1 TO RESTRAIN STAT3 ACTIVITY 66

3.1 Summary 66

3.2 Introduction 67

3.3 Results 69

3.3.1 TBK1 directly phosphorylates STAT3 at serine 754 69

3.3.2 STAT3 is phosphorylated at S754 in response to cytosolic dsDNA 70

3.3.3 TBK1 is required for cytosolic DNA-induced STAT3 phosphorylation at S754 72

3.3.4 The cGAS-STING-TBK1 pathway induces STAT3 S754 phosphorylation in response to cytosolic DNA 73

3.3.5 Secreted cytokines induce activation of STAT3 in response to cytosolic DNA..... 74

3.3.6 S754 phosphorylation of STAT3 restricts cytosolic DNA-induced STAT3 target gene expression 75

3.3.7 S754 phosphorylation suppresses the transcriptional activity of STAT3 76

3.4 Discussion 78

3.5 Materials and Methods 82

REFERENCES 102

CHAPTER 4: FUTURE DIRECTIONS AND CONCLUSIONS 107

4.1 Roles and Regulation of STAT3 Activity in Diseases 107

4.1.1 Regulation of STAT3 activity: A balancing act..... 107

4.1.2 Regulation of STAT3 activity in viral Infection 109

4.1.3 Regulation of STAT3 activity in tumors and the tumor microenvironment 109

4.2 The Mechanism of STAT3 Inhibition by S754 Phosphorylation 112

4.3 Concluding Remarks 114

4.4 Materials and Methods 115

REFERENCES 120

LIST OF TABLES

Table 2.1 Cellular composition of the spleen[a] 50

Table 2.2 Cellular composition of the bone marrow[a]. 51

Table 4.1 Upregulation of stimulatory co-receptors in BMDC by DNA transfection 119

LIST OF FIGURES

Figure 1.1 A schematic overview of the STAT3 pathway 15

Figure 1.2 Signaling pathways induced by cytosolic DNA 16

Figure 2.1 STAT3 knockout BMMs show attenuated type I interferon response to HSV-1 infection 52

Figure 2.2 Myeloid STAT3 knockout mice are more susceptible to HSV-1 infection 53

Figure 2.3 Susceptibility of STAT3 knockout mice is not caused by immunopathology in the brain 54

Figure 2.4 STAT3 knockout mice express reduced levels of antiviral cytokines in the spleen 55

Figure 2.5 STAT3 knockout mice have decreased $CD8^+$ cDC frequency during HSV-1 infection 56

Figure 2.6 STAT3 knockout mice have impaired NK and T cell activation during HSV-1 infection 57

Supplemental Figure 2.1 Myeloid-specific deletion of STAT3 58

Supplemental Figure 2.2 KO mice showed marginally higher viral loads in the brain 59

Figure 3.1 IKKε and TBK1 induce STAT3 phosphorylation at S754 88

Figure 3.2 Cytosolic DNA induces STAT3 activation and phosphorylation at S754 89

Figure 3.3 TBK1 activity is required for cytosolic DNA-induced S754 phosphorylation of STAT3 90

Figure 3.4 Cytosolic DNA induces pS754-STAT3 via the cGAS/STING axis 91

Figure 3.5 Cytosolic DNA-induced STAT3 activation is mediated by *de novo* synthesized secreted factors 92

Figure 3.6 . S754 phosphorylation restricts STAT3 activation in response to cytosolic DNA 94

Figure 3.7 S754 phosphorylation inhibits transcriptional activity of STAT3 96

Figure 3.8 Schematic overview of STAT3 activation and regulation downstream of the cytosolic DNA pathway 98

Supplemental Figure 3.1 Cytosolic DNA induces expression of IFNβ and IL-6 99

Supplemental Figure 3.2 CRISPR-mediated knockout of STAT3 in HEK293T and THP-1 100

Supplemental Figure 3.3 STAT3 inhibits IFNβ-induced ISRE reporter expression..... 101

Figure 4.1 Cytosolic DNA induces STAT3 S754 phosphorylation and promotes DC maturation 117

Figure 4.2 S754 phosphomimetic interferes with STAT3 dimerization..... 118

LIST OF ABBREVIATIONS

AD-HIES	Autosomal dominant hyper IgE syndrome
AIM2	Absent in melanoma 2
BMDC	Bone marrow-derived dendritic cells
BMM	Bone marrow-derived macrophages
cDC	Conventional dendritic cells
cGAS	Cyclic GAMP synthase
CTL	Cytotoxic T lymphocytes
DAMP	Danger-associated molecular pattern
DBD	DNA-binding domain
DDX41	DEAD-box helicase 41
GAS	Gamma-activated sequence
HSV-1	Herpes simplex virus-1
IFI16	Interferon gamma inducible protein
IFN	Interferon
IκB	Inhibitor of kappaB
IKK	IκB kinase
IRF	Interferon regulatory factor
ISG	Interferon stimulated genes
ISGF3	Interferon-stimulated gene factor 3
ISRE	Interferon-stimulated responsive element
JAK	Janus kinase
LPS	lipopolysaccharide

MMMΦ	Marginal metallophilic macrophages
MOI	Multiplicity of infection
MZMΦ	Marginal zone macrophages
NCOA1	Nuclear receptor coactivator 1
NF-κB	Nuclear factor-kappaB
NK	Natural killer cells
NTD	N-terminal domain
pDC	plasmacytoid dendritic cells
PAMP	Pathogen-associated molecular pattern
PTM	Post-translational modification
SH2	SRC homology 2
STAT3	Signal transducer and activator of transcription 3
STING	Stimulator of interferon genes
TAD	Transactivation domain
TBK1	TANK-binding kinase 1
TNFα	Tumor necrosis factor alpha
TREX1	3’ repair exonuclease 1
ZBP1	Z-DNA binding protein 1

CHAPTER 1: INTRODUCTION

1.1 STAT3

1.1.1 General introduction

Members of the signal transducer and transcription activator (STAT) family are dimeric transcription factors that regulate cellular differentiation, proliferation, survival, and immunity by responding to a variety of cytokines and growth factors. STAT proteins share the domain structure of an N-terminal domain (NTD) that promotes dimerization, followed by a DNA-binding domain (DBD), an SRC-homology 2 (SH2) domain, and a C-terminal transactivation domain (TAD). Seven STAT genes have been identified in human and mouse, and STAT3 is the third member identified. Like other STAT family members, the activity of STAT3 is regulated by tyrosine phosphorylation, which facilitates STAT3 dimerization by interacting with the SH2 domain within another STAT3 molecule. STAT3 is activated downstream of a number of cytokines and growth factors, such as leukemia inhibitory factor (LIF), IL-6, IL-10, and epidermal growth factor (EGF) (1,2). The most well known activators of STAT3 are the IL-6 family cytokines, with IL-6 being the prototype. Binding of IL-6 to the IL-6 receptor associated with the transmembrane protein gp130 activates Janus kinase 2 (JAK2), one of the four kinases in the JAK family. Activated JAK2 subsequently phosphorylates Y705 of STAT3, facilitating its dimerization and activation. Similarly, type I interferons (IFN) also induce STAT3 activation through JAKs, while EGF and other growth factors activate STAT3 by receptor tyrosine kinases (RTKs) and SRC (3,4). Recent studies revealed that a sphingolipid, spingosine-1-phosphate (S1P) also activates STAT3 via G-protein coupled receptor (GPCR) and JAK2 (5).

Unphosphorylated STAT3 exists as stable dimers prior to activation because of the homotypic interaction mediated by the NTDs of two STAT3 molecules, but inactive STAT3 dimers are constantly being shuttled in between the nucleus and the cytoplasm (6-9). While activated, Y705 phosphorylation enhances the DNA binding activity of STAT3 and thus the nuclear retention (8,10). Active STAT3 homodimers bind to a 9-bp palindromic sequence with the consensus of TTCNNNGAA (11). However, this gamma-interferon activating sequence (GAS) recognized by STAT3 is very similar to that of STAT1. In fact, STAT3 and STAT1 share identical optimal GAS sequence when analyzed *in vitro*, but variation in endogenous core and flanking sequences leads to differential recognition by STAT1 and STAT3, resulting in distinct but overlapping target genes controlled by STAT1 and STAT3 (12,13). In the nucleus, STAT3 promotes the transcription of genes involved in inflammation, survival, and cell cycle, such as C-C motif ligand 2 (CCL2), Bcl-xL, metallomatrix protease 2 (MMP2), Survivin, and Cyclin D1 (4) (Figure 1.1). With target genes involved in these essential cellular processes, constitutive activation of STAT3 has been implicated in tumorigenesis and various types of cancers (4,14,15), as discussed in the following paragraphs.

1.1.2 STAT3 in human diseases

Dysregulation of STAT3 has profound implications in human diseases. For example, germline dominant negative STAT3 mutations have been identified in patients with autosomal dominant hyper IgE syndrome (AD-HIES), an immunodeficiency disorder. AD-HIES patients are characterized by symptoms such as elevated serum IgE titer, increased TNFα and IL-12 production from leukocytes, susceptibility to recurrent bacterial and fungal pneumonia, and impaired ability to control herpesvirus latency (16,17). Similarly, in mice, targeted deletion of

STAT3 in myeloid cells results in elevated TNFα and IL-12 in response to bacterial components and susceptibility to bacterial infections (18,19). These mice are also more susceptible to herpes simplex virus-1 (HSV-1) infection, as discussed in Chapter 2 of this dissertation (20). Conversely, somatic activating mutations of STAT3 have been associated with lymphoproliferative disorders and hepatocellular adenomas (21-23), whereas germline activating mutations of STAT3 contribute to early-onset autoimmune disorders that affect multiple organs (24), underscoring dysregulated STAT3 activation as a causative factor in enhanced cell proliferation and aberrant activation of immune cells.

Constitutive activation of STAT3 has been documented in many types of cancers, and the consequences of such dysregulation are multifaceted. Through target genes involved in inflammation, anti-apoptosis, cell cycle, and invasion and migration, STAT3 supports tumorigenesis, survival, proliferation, and metastasis of cancer cells (4,25,26). Expression of a constitutively active STAT3 mutant is sufficient to transform immortalized cells (14,27). In K-RAS driven pancreatic cancers, STAT3 is required for the initiation and progression of tumorigenesis (28), although studies have reported conflicting roles of STAT3 in K-RAS driven lung cancers (29,30). Elevated STAT3 activity in glioblastoma and prostate cancer correlates with cancer stem cell-like properties, including enhanced tumorigenecity and resistance to therapy (31,32). STAT3 also promotes metastasis by upregulating genes implicated in migration and invasion in tumor cells (33), and by priming and preparing fibroblasts at distal sites for metastatic cancer cells (34). STAT3 often fuels inflammation, exacerbates inflammation-associated cancers, and promotes survival of cancer cells in collaboration with nuclear factor-kappaB (NF-κB). The interaction between STAT3 and NF-κB occurs at several levels. For one, STAT3 and NF-κB share overlapping target genes, including anti-apoptotic genes and

inflammatory cytokines (15). STAT3 physically interacts with NF-κB and retains NF-κB in the nucleus for sustained activation and expression of IL-6, which further activates STAT3 and forms an amplification loop (35-39). Finally, STAT3 inhibits the expression of immunostimulatory genes in cancer cells (40), and induces the expression of IL-23 to activate regulatory T cells (Treg) in the tumor microenvironment, thereby dampening the anti-tumor immune responses through a concerted effort (41). Moreover, IL-10 from tumor cells inhibits activation of immune cells via STAT3 signaling, and genetic deletion of STAT3 in hematopoietic cells enhances anti-tumor immunity, demonstrating an immunosuppressive role of STAT3 in the tumor microenvironment (42,43).

1.2 TBK1 and IKKε

1.2.1 General introduction

NF-κB is a family of dimeric transcription factors comprising five subunits: p65 (RelA), p100/p52, p105/p50, RelB, and c-Rel. In the canonical NF-κB pathway, the activity of the p65-p50 dimer is tightly regulated by inhibitor of kappaB (IκB) and two IκB kinases (IKKs), IKKα and IKKβ. Under basal conditions, the p65-p50 NF-κB dimers are inactive and bound by IκBα in the cytosol. Various environmental cues and cytokines such as IL-1 and TNFα can lead to activation of the IKK complex comprising of IKKα, IKKβ, and IKKγ (NF-κB essential modifier/NEMO). The activated IKK complex phosphorylates IκBα at S32 and S36, which triggers proteasome-dependent degradation of IκBα. The liberated p65-p50 dimers then translocate to the nucleus and activate transcription of target genes involved in inflammation and survival, such as IL-6 and Bcl-xL, and genes involved in the negative feedback of NF-κB, such as A20 and IκBα. In the non-canonical pathway, RelB-p100 dimers are inactive due to the

inhibitory ankyrin repeats in p100 subunit. Phosphorylation of p100 by IKKα induces proteasomal processing of p100 into p52, resulting in the active RelB-p52 dimers (Reviewed in (44)). Genetic experiments demonstrated that the IKKs, especially IKKβ, are required for NF-κB activation by lipopolysaccharide (LPS), IL-1, and TNFα (45-47). Following the identification of IKKα and IKKβ, two more related kinases were identified. TANK-binding kinase 1 (TBK1) was originally identified in a screen for proteins interacting with TANK, a TRAF-binding protein that modulates TRAF-mediated NF-κB signaling (48), and IKKε was identified as an IKK-related kinase whose expression can be highly induced by LPS (49). The sequences of TBK1 and IKKε share approximately 50% identity with each other, and approximately 30% identity with IKKα and IKKβ (50). The domain structures of TBK1 and IKKε are similar to IKKα and IKKβ, but TBK1 and IKKε lack the NEMO-binding domain in the C terminus.

1.2.2 TBK1 and IKKε in innate immunity

Unlike IKKα and IKKβ that phosphorylate both S32 and S36 of IκBα, TBK1 and IKKε only phosphorylate S32 of IκBα in *in vitro* assays (49,51), and TBK1 and IKKε are not required for IκBα degradation or NF-κB activation induced by IL-1 and TNFα (48,49). While dispensable for IL-1 and TNFα-induced NF-κB activation, TBK1 is required for the induction of the type I IFN in response to a variety of pathogen-associated or danger-associated molecular patterns (PAMPs and DAMPs), including poly (I:C), intracellular double-stranded DNA (dsDNA), LPS, and viral infections, whereas IKKε has minimal or redundant functions in these scenarios (52-56). As an interferon-stimulated gene (ISG) itself, IKKε plays a more significant role at the late stage of IFN response after its expression is upregulated by the first wave of IFN (57). PAMPs and DAMPs activate TBK1 and IKKε through engagement of an array of toll-like receptors

(TLRs) and TLR-independent receptors (58). In general, the activating signals from these receptors lead to the assembly of ubiquitin ligase complexes, which bind to and K63-ubiquitinate TBK1 and IKKε. The K63-polyubiquitin chains then cooperate with ubiquitin binding proteins to promote TBK1 and IKKε oligomerization and facilitate their autophosphorylation (59-63). Once activated by autophosphorylation, TBK1 and IKKε mediate IFN expression by directly phosphorylating interferon regulatory factors IRF3 and IRF7 at a number of serine residues, allowing IRFs to homodimerize and translocate to the nucleus to induce type I IFN transcription (52,64). In addition to its pivotal role in IFN induction, TBK1 also promotes autophagy-mediated clearance of intracellular bacteria by phosphorylating adaptors that target bacteria for the autophagosome (65,66). With their ability to respond to the presence of PAMPs and DAMPs to induce IFN expression and autophagy, TBK1, and to a lesser extent IKKε, are critical molecules that establish the first line of host defense against pathogens at the cellular level.

1.2.3 TBK1 and IKKε in cancers

In addition to their well-established roles in initiating IFN responses, several studies reported an oncogenic role for TBK1 and IKKε. An RNAi screening showed that KRAS-transformed cancer cell lines require TBK1-mediated activation of NF-κB and transcription of anti-apoptotic genes for survival (67). TBK1 also inhibits oncogenic stress-induced apoptosis via NF-κB independent pathways (68,69). Similarly, IKKε is often overexpressed or amplified in human breast cancers (70), and inhibition of IKKε in related breast cancer cell-lines results in halted growth and cell death (70,71). IKKε facilitates oncogenesis by indirectly promoting NF-κB activity through phosphorylating and inhibiting CYLD, a negative regulator of the NF-κB pathway (72).

1.3 Responses Elicited by Cytosolic DNA

The subcellular compartmentalization of mammalian cells normally sequesters DNA in the nucleus and mitochondria. DNA in the cytosol is thus a DAMP that signals abnormality and triggers cell-intrinsic immune responses (56,73). Cytosolic DNA can be derived from self-DNA in normal physiological conditions, such as phagocytosed materials, including dead cells and ejected nuclei from erythroid precrusors, or re-activated endogenous retroelements. Additionally, viral or intracellular bacterial infections lead to the presence of foreign DNA in the cytosol (74). Recognition of cytosolic DNA by cellular sensors leads to activation of two major pathways: (i) inflammasome-driven mechanisms that produce IL-1β and IL-18, and (ii) IRF activation that induces IFN expression. The major players in the cytosolic DNA pathway are introduced in the following paragraphs, with emphases on the IFN response (Figure 1.2).

1.3.1 Induction of the inflammasomes by cytosolic DNA

The inflammasome is a molecular complex that regulates the activation of caspase-1 and induces inflammation in response to a variety of PAMPs and DAMPs. Assembly of inflammasomes is mediated by polymerization of apoptosis-associated speck-like protein containing a CARD (ASC) proteins and the subsequent recruitment of pro-caspase 1. After self-activating proteolytic cleavage, caspase 1 processes the cytokine precursors pro-IL-1β and pro-IL-18 into active IL-1β and IL-18 (75). Cytosolic DNA induces IL-1β and IL-18 secretion through inflammasome formation mediated by the protein absent in melanoma 2 (AIM2). AIM2 is a member of the Pyrin and HIN domain (PYHIN) family (76-78) and binds to dsDNA directly via its HIN domain. The Pyrin domain and HIN domain of AIM2 form an autoinhibitory conformation via intramolecular interaction under basal conditions, but direct dsDNA binding by

the HIN domain liberates the Pyrin domain, allowing it to interact with ASC. Using a DNA molecule as a platform, multiple AIM2 proteins bind to and nucleate on the DNA, thereby facilitating the polymerization of ASC and the formation of inflammasomes in response to cytosolic DNA (77-79).

1.3.2 Induction of interferons by cytosolic DNA

While detection of cytosolic DNA by AIM2 induces inflammasome formation through polymerization of the adaptor ASC, other cytosolic DNA sensors engage different adaptor proteins to promote TBK1 and IRF3 activation, thereby leading to interferon production. The roles of various cytosolic DNA sensors and the quintessential adaptor stimulator of interferon genes (STING) in cytosolic DNA-induced IFN response are discussed as follows.

STING. It has been known that introduction of foreign DNA into the cytosol triggers TBK1-mediated IFNβ production, but it was unclear how TBK1 becomes activated (56,73). It was later found that an ER resident protein STING, encoded by the *TMEM173* gene, is a critical adaptor required to activate TBK1 upon cytosolic DNA challenge (80-82). Structural and in vitro analyses suggested that STING does not act as a DNA sensor in the cells (83,84). Instead, it binds to cyclic GMP-AMP (cGAMP) generated by the DNA-dependent cytosolic enzyme cyclic GMP-AMP synthase (cGAS) (85). Binding to cGAMP induces STING oligomerization and enhances its interaction with TBK1 (85), thereby promoting TBK1 autophosphorylation and activation, presumably by increasing the local concentration of TBK1 (62). Active TBK1 subsequently phosphorylates the C terminus of STING, creating a docking site for recruiting IRF3, which is then phosphorylated and activated by TBK1 (86-88). Interestingly, STING seems to be a convergence point for the cytosolic DNA pathway, because it is also required for an IFN

response mediated by other cytosolic DNA sensors, such as IFI16 and DDX41 (83,89). In addition to cGAMP, STING also recognizes other cyclic di-nucleotides (CDNs) generated by bacteria (90,91). Therefore, STING has an integral role in defending against intracellular bacterial infection by directly sensing bacterial CDN and by indirectly responding to bacterial DNA via cGAS. Several frequent single nucleotide polymorphisms (SNPs) have been identified in the human *TMEM173* allele. These SNPs lead to amino acid substitutions that decrease the affinity of STING to bacterial CDNs, and may have implications in the susceptibility to bacterial diseases and autoimmunity of different individuals (92,93).

IFI16. Similar to AIM2, interferon-gamma inducible protein 16 (IFI16) is a member of the PYHIN family. IFI16 interacts with STING upon binding to DNA via its two HIN domains, and promotes IRF3 and NF-κB activation in a STING-dependent manner (83). IFI16 is unique because of its cytoplasmic and nuclear distribution, with nuclear localization being predominant (78,83,94). This unique distribution pattern allows IFI16 to detect foreign DNA not only in the cytoplasm but also in the nucleus. Indeed, IFI16 limits HSV-1 replication by targeting naked HSV-1 DNA genome in the nucleus for heterochromatinzation and silencing (95). However, nuclear IFI16 has to discriminate self-DNA from foreign DNA to prevent self-reactivity. Biochemical studies revealed that the cooperative binding mechanism of IFI16 to DNA is the key to its selectivity (96). The two HIN domains of IFI16 bind to dsDNA with a mild affinity independent of the DNA sequences, while the Pyrin domain promotes cooperative binding between the two HIN domains. As a result, IFI16 selectively oligomerizes on naked DNA over ~150 bp in length with very high affinity and efficiency (96), allowing IFI16 to preferentially bind to naked foreign DNA even in the presence of excessive self-DNA that is chromatinized.

ZBP1. Z-DNA binding protein 1 (ZBP1) is a DNA-binding protein that was initially identified in macrophages as being encoded by an IFN-inducible gene (97,98). A cytosolic protein, ZBP1 binds to cytosolic dsDNA and contributes to optimal IFN expression in MEFs and L929 cells by promoting TBK1-IRF3 interaction (99). ZBP1 also contributes to IFN responses and resistance to cytomegalovirus, a DNA virus (100). However, it is unlikely that ZBP1 is the principle cytosolic DNA sensor, since genetic deletion of ZBP1 has minimal impact on the ability of cells to respond to cytosolic DNA (83,101).

DDX41. The DEAD-box helicase 41 (DDX41) protein has been demonstrated to participate in the cytosolic DNA-induced IFN response in dendritic cells (89). DDX41 binds to dsDNA through its DEAD-box domain, and interacts and colocalizes with STING upon dsDNA transfection (89). It was later shown that Bruton's tyrosine kinase (BTK) phosphorylates DDX41 and induces its binding with STING upon cytosolic dsDNA stimulation, leading to activation of the TBK1-IRF3 signaling axis (102). Moreover, DDX41 also binds to cyclic di-GMP and cyclic di-AMP with even higher affinity than STING, and is required for cyclic di-GMP and cyclic di-AMP-induced, STING-dependent IFN responses (103). It is worth noting that while expression of IFI16 and ZBP1 remains low unless induced by IFNs, the constitutive expression of DDX41 in cells such as DCs and monocytes suggest a critical role for DDX41 in the first line of cytosolic DNA sensing.

RNA polymerase III. STING has an essential role in IFN expression induced by cytosolic DNA regardless of DNA sequences or sources with one exception (104). Transfection of poly(dA:dT) induces moderate IFN expression even in the absence of STING (104), suggesting the existence of STING-independent cytosolic DNA pathways specific to AT-rich dsDNA. Two groups independently discovered that cytosolic poly(dA:dT) is detected and

transcribed by RNA polymerase III in the cytosol (105,106). The resulting 5' triphosphate-capped RNA products are recognized by retinoic acid inducible gene-I (RIG-I), thereby inducing IFN expression through a mitochondrial antiviral signaling protein (MAVS)-dependent mechanism (105,106).

cGAS. While the aforementioned cytosolic DNA sensors are all involved in relaying the presence of cytosolic DNA to IFN induction, knockdown of individual sensors rarely achieves complete abrogation of cytosolic DNA-induced IFN, indicating redundancy between these cytosolic DNA sensors. Moreover, their inducible expression (IFI16, ZBP1), limited distribution pattern in specific cell types (DDX41), and specificity toward AT-rich substrates (RNA Pol III) suggested the existence of additional unidentified cytosolic DNA sensors that are more ubiquitously expressed and less sequence-specific in DNA recognition. The identification of cGAS (encoded by the *MB21D1* gene) provides a missing piece to this puzzle. cGAS is a cytoplasmic nucleotidyltransferase with dsDNA-dependent enzymatic activity. The enzymatic core of cGAS catalyzes the formation of cyclic GMP-AMP (cGAMP) using GTP and ATP as substrates, whereas the C-terminal domain interacts with DNA (107-110). cGAS specifically binds to DNA but not RNA, with strong preference to dsDNA over ssDNA in a sequence-independent manner (108). Structural changes induced by dsDNA binding activate cGAS to produce a non-canonical cGAMP, [G(2'-5')pA(3'-5')], which in turn binds to and activates the downstream adaptor STING, thereby initiating the STING-TBK1-IRF3 signaling cascade and IFN responses (108-113). Genetic deletion of cGAS abrogates the IFN response of a number of cell types to cytosolic DNA with different sequence compositions, suggesting that cGAS has a more universal and critical role in the cytosolic DNA pathway comparing to other sensors (114).

1.3.3 Induction of the NF-κB pathway by cytosolic DNA

In addition to type I IFN, cytosolic DNA also activates NF-κB in a STING-depedent manner. STING overexpression is sufficient to activate NF-κB, whereas STING deficiency abolishes cytosolic DNA-induced NF-κB activation (81,104). Further studies demonstrated that both canonical (p65-p50) and non-canonical (RelB-p52) NF-κB are activated downstream of STING, and NF-κB is required for IL-6 expression and contributes to IFNβ expression induced by cytosolic DNA (115). Activation of NF-κB requires IKKα, IKKβ, and the E3 ligases TRAF3 and TRAF6 but, depending on the cell type, TBK1 may or may not be required for activation of IKKβ by cytosolic DNA ((115) and Chapter 3).

1.3.4 Cytosolic DNA and autoimmunity

Clearance of self-DNA in the cytosol under physiological conditions is achieved by DNases in the cytosol and lysosome, and failure to clear self-DNA causes substantial inflammatory and IFN responses as well as autoimmune conditions. For example, loss-of-function mutations of cytosolic DNase III (3' repair exonuclease 1, TREX1) have been identified as a causative factor of the neurological autoimmune disease Aicardi-Goutières Syndrome (AGS) (116,117). Genetic manipulation in mice showed that deletion of lysosomal DNase II results in accumulation of undigested nuclei in liver macrophages and embryonic lethality characterized by unchecked interferon and inflammatory responses, and that deletion of TREX1 leads to severe autoimmune conditions recapitulating the symptoms in human diseases (118-122). The etiological role of cytosolic DNA in these scenarios is demonstrated by rescue experiments, whereby deletion of cGAS or STING can rescue the autoimmunity observed in these DNase-deficient mice (123-127).

1.3.5 Cytosolic DNA and microbial infections

Cytosolic DNA can also arise from viral or intracellular microbial infections. The DNA genome of herpesvirus and vaccinia virus, as well as the reverse-transcribed HIV DNA, are recognized by intracellular DNA sensors, thereby triggering IFN responses and host antiviral mechanisms (83,100,114,128-133). Not surprisingly, a number of viral proteins have been identified by their ability to target and inhibit the cytosolic DNA pathway to evade host immune surveillance (Reviewed in (134)). Interestingly, an unbiased screening revealed that in addition to its role in controlling DNA virus pathogenesis, cGAS also contributes to limiting RNA virus replication (135). This suggests an unidentified mechanism by which viral RNA activates cGAS. Alternatively, it is possible that low levels of cGAS activation by self-DNA pre-establish a suboptimal antiviral state, such that cGAS deficiency makes cells more susceptible to RNA virus infection. Intracellular bacteria, such as *Mycobacterium tuberculosis*, induce IFNβ production in a cGAS-STING-dependent manner (136,137). Activation of TBK1 in this scenario also induces ubiquitin-mediated autophagy that targets the *M. tuberculosis* to lysosome for degradation, thereby serving as an important tool in controlling intracellular mycobacteria replication (138). Similarly, intracellular infection of *Legionella*, *Listeria*, and *Francisella* all engage the cytosolic DNA pathway, while *Listeria* also produces cyclic-di-AMP that directly activates STING (136,139-141).

1.4 Regulation of STATs by Innate Immune Signaling Pathways

Recent studies identified several novel mechanisms that regulate activity of STATs by innate immune signaling pathways. For example, TBK1 and STING-mediated phosphorylation of the STAT6 DNA binding domain (DBD) is required for virus-induced STAT6 activation,

which promotes efficient antiviral responses by inducing CCL2, CCL20, and CCL26 (142). Type I IFN (IFNα and IFNβ) induces STAT1 homodimers to promote GAS-driven gene expression, while type II IFN (IFNγ) induces STAT1-STAT2-IRF9 heterotrimers, which bind to the interferon-stimulated response element (ISRE) and promote a different ISG expression profile. IKKε fine-tunes the balance between GAS-driven and ISRE-driven ISGs by phosphorylating S708 of STAT1. This phosphorylation disrupts STAT1 homodimerization and favors the heterotrimer formation, thereby shifting the IFN-induced gene expression profile toward ISRE-driven ISGs (143,144). It has also been noted that STING deficiency in autoimmune-prone mice leads to hyperactivation of STAT1-mediated IFN responses and exacerbated autoimmunity symptoms, suggesting a negative role of STING in regulation of STAT1 (145). This regulation may be partially mediated by the ability of STING to activate SH2 domain-containing phosphatases (SHPs), which dephosphorylate and inactivate STAT1 (146). Finally, my work presented in Chapter 3 reveals another signaling axis, in which TBK1 phosphorylates STAT3 at S754 in the transactivation domain (TAD) to restrict STAT3 activity in response to cytosolic DNA.

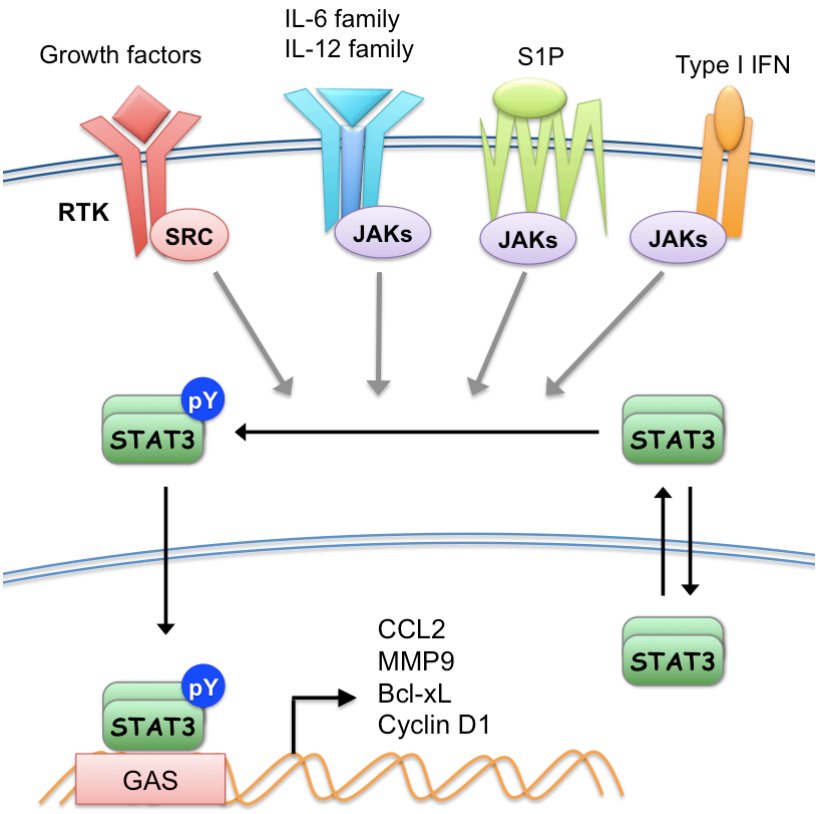

Figure 1.1 A schematic overview of the STAT3 pathway
Preformed STAT3 dimers are constantly being shuttled between the nucleus and the cytoplasm unless activated. STAT3 can be activated by growth factors, several families of interleukins such as IL-6 and IL-12, sphingosine-1-phosphate (S1P), and type I IFNs. Receptor engagement of these ligands induces STAT3 Y705 phosphorylation by receptor tyrosine kinases (RTK), SRC, or Janus kinases (JAK). Phosphorylated STAT3 dimers have enhanced DNA binding affinity and stay in the nucleus, bind to the gamma-activated sequence (GAS) in the promoters, and drive the expression of target genes, such as CCL2, MMP9, Bcl-xL, and Cyclin D1.

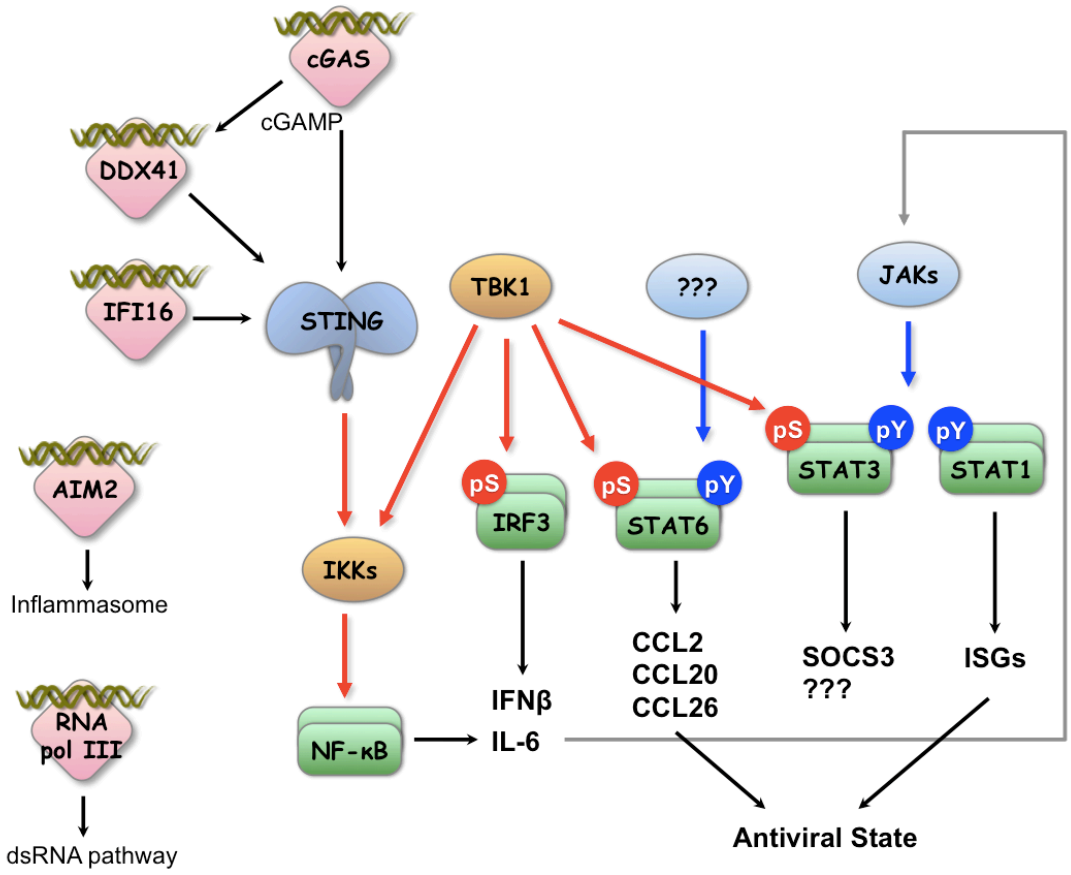

Figure 1.2 Signaling pathways induced by cytosolic DNA
The presence of cytosolic DNA is detected by a variety of sensors: cGAS, IFI16, DDX41, AIM2, and RNA polymerase III. While AIM2 induces inflammasome formation and RNA polymerase III activates the dsRNA pathway, the other sensors engage STING to activate TBK1, leading to IRF3 phosphorylation and IFNβ production. IFNβ establishes an antiviral state through activation of STAT1 and expression of IFN-stimulated genes (ISGs). Additionally, TBK1 also promotes NF-kB and STAT6 activation, but restricts IL-6 and IFNβ-mediated STAT3 activation (Chapter 3). The red arrows denote serine phosphorylation, and the blue arrows denote tyrosine phosphorylation.

REFERENCES

1. Zhong Z, Wen Z, Darnell JE. Stat3: a STAT family member activated by tyrosine phosphorylation in response to epidermal growth factor and interleukin-6. Science. 1994 Apr 1;264(5155):95–8.

2. Akira S, Nishio Y, Inoue M, Wang XJ, Wei S, Matsusaka T, et al. Molecular cloning of APRF, a novel IFN-stimulated gene factor 3 p91-related transcription factor involved in the gp130-mediated signaling pathway. Cell. 1994 Apr 8;77(1):63–71.

3. Yu H, Lee H, Herrmann A, Buettner R, Jove R. Revisiting STAT3 signalling in cancer: new and unexpected biological functions. Nat Rev Cancer. 2014 Oct 24;14(11):736–46.

4. Yu H, Pardoll D, Jove R. STATs in cancer inflammation and immunity: a leading role for STAT3. Nat Rev Cancer. 2009 Nov;9(11):798–809.

5. Lee H, Deng J, Kujawski M, Yang C, Liu Y, Herrmann A, et al. STAT3-induced S1PR1 expression is crucial for persistent STAT3 activation in tumors. Nat Med. 2010 Dec;16(12):1421–8.

6. Haan S, Kortylewski M, Behrmann I, Müller-Esterl W, Heinrich PC, Schaper F. Cytoplasmic STAT proteins associate prior to activation. Biochem J. 2000 Feb 1;345 Pt 3:417–21.

7. Braunstein J, Brutsaert S, Olson R, Schindler C. STATs dimerize in the absence of phosphorylation. J Biol Chem. 2003 Sep 5;278(36):34133–40.

8. Kretzschmar AK, Dinger MC, Henze C, Brocke-Heidrich K, Horn F. Analysis of Stat3 (signal transducer and activator of transcription 3) dimerization by fluorescence resonance energy transfer in living cells. Biochem J. 2004 Jan 15;377(Pt 2):289–97.

9. Reich NC, Liu L. Tracking STAT nuclear traffic. Nat Rev Immunol. 2006 Aug;6(8):602–12.

10. Sasse J, Hemmann U, Schwartz C, Schniertshauer U, Heesel B, Landgraf C, et al. Mutational analysis of acute-phase response factor/Stat3 activation and dimerization. Mol Cell Biol. 1997 Aug;17(8):4677–86.

11. Becker S, Groner B, Müller CW. Three-dimensional structure of the Stat3beta homodimer bound to DNA. Nature. 1998 Jul 9;394(6689):145–51.

12. Horvath CM, Wen Z, Darnell JE. A STAT protein domain that determines DNA sequence recognition suggests a novel DNA-binding domain. Genes Dev. 1995 Apr 15;9(8):984–94.

13. Ehret GB, Reichenbach P, Schindler U, Horvath CM, Fritz S, Nabholz M, et al. DNA binding specificity of different STAT proteins. Comparison of in vitro specificity with natural target sites. J Biol Chem. 2001 Mar 2;276(9):6675–88.

14. Bromberg JF, Wrzeszczynska MH, Devgan G, Zhao Y, Pestell RG, Albanese C, et al. Stat3 as an oncogene. Cell. 1999 Aug 6;98(3):295–303.

15. Grivennikov SI, Karin M. Dangerous liaisons: STAT3 and NF-kappaB collaboration and crosstalk in cancer. Cytokine and Growth Factor Reviews. 2010 Feb;21(1):11–9.

16. Holland SM, DeLeo FR, Elloumi HZ, Hsu AP, Uzel G, Brodsky N, et al. STAT3 mutations in the hyper-IgE syndrome. N Engl J Med. 2007 Oct 18;357(16):1608–19.

17. Siegel AM, Heimall J, Freeman AF, Hsu AP, Brittain E, Brenchley JM, et al. A critical role for STAT3 transcription factor signaling in the development and maintenance of human T cell memory. Immunity. 2011 Nov 23;35(5):806–18.

18. Takeda K, Clausen BE, Kaisho T, Tsujimura T, Terada N, Förster I, et al. Enhanced Th1 activity and development of chronic enterocolitis in mice devoid of Stat3 in macrophages and neutrophils. Immunity. 1999 Jan;10(1):39–49.

19. Matsukawa A, Takeda K, Kudo S, Maeda T, Kagayama M, Akira S. Aberrant inflammation and lethality to septic peritonitis in mice lacking STAT3 in macrophages and neutrophils. J Immunol. 2003 Dec 1;171(11):6198–205.

20. Hsia H-C, Stopford CM, Zhang Z, Damania B, Baldwin AS. Signal transducer and activator of transcription 3 (Stat3) regulates host defense and protects mice against herpes simplex virus-1 (HSV-1) infection. Journal of Leukocyte Biology. 2016 Dec 13.

21. Koskela HLM, Eldfors S, Ellonen P, van Adrichem AJ, Kuusanmäki H, Andersson EI, et al. Somatic STAT3 mutations in large granular lymphocytic leukemia. N Engl J Med. 2012 May 17;366(20):1905–13.

22. Jerez A, Clemente MJ, Makishima H, Koskela H, LeBlanc F, Peng Ng K, et al. STAT3 mutations unify the pathogenesis of chronic lymphoproliferative disorders of NK cells and T-cell large granular lymphocyte leukemia. Blood. 2012 Oct 11;120(15):3048–57.

23. Pilati C, Amessou M, Bihl MP, Balabaud C, Van Nhieu JT, Paradis V, et al. Somatic mutations activating STAT3 in human inflammatory hepatocellular adenomas. J Exp Med. 2011 Jul 4;208(7):1359–66.

24. Flanagan SE, Haapaniemi E, Russell MA, Caswell R, Lango Allen H, De Franco E, et al. Activating germline mutations in STAT3 cause early-onset multi-organ autoimmune disease. Nat Genet. 2014 Aug;46(8):812–4.

25. Yuan J, Zhang F, Niu R. Multiple regulation pathways and pivotal biological functions of STAT3 in cancer. Sci Rep. 2015;5:17663.

26. Dauer DJ, Ferraro B, Song L, Yu B, Mora L, Buettner R, et al. Stat3 regulates genes common to both wound healing and cancer. Oncogene. 2005 Feb 28;24(21):3397–408.

27. Demaria M, Misale S, Giorgi C, Miano V, Camporeale A, Campisi J, et al. STAT3 can

serve as a hit in the process of malignant transformation of primary cells. Cell Death Differ. 2012 Aug;19(8):1390–7.

28. Corcoran RB, Contino G, Deshpande V, Tzatsos A, Conrad C, Benes CH, et al. STAT3 Plays a Critical Role in KRAS-Induced Pancreatic Tumorigenesis. Cancer Res. 2011 Jul 14;71(14):5020–9.

29. Grabner B, Schramek D, Mueller KM, Moll HP, Svinka J, Hoffmann T, et al. Disruption of STAT3 signalling promotes KRAS-induced lung tumorigenesis. Nat Commun. 2015;6:6285.

30. Zhou J, Qu Z, Yan S, Sun F, Whitsett JA, Shapiro SD, et al. Differential roles of STAT3 in the initiation and growth of lung cancer. Oncogene. 2015 Jul;34(29):3804–14.

31. Kim E, Kim M, Woo D-H, Shin Y, Shin J, Chang N, et al. Phosphorylation of EZH2 activates STAT3 signaling via STAT3 methylation and promotes tumorigenicity of glioblastoma stem-like cells. Cancer Cell. 2013 Jun 10;23(6):839–52.

32. Schroeder A, Herrmann A, Cherryholmes G, Kowolik C, Buettner R, Pal S, et al. Loss of Androgen Receptor Expression Promotes a Stem-like Cell Phenotype in Prostate Cancer through STAT3 Signaling. Cancer Res. 2014 Feb 16;74(4):1227–37.

33. Kesanakurti D, Chetty C, Rajasekhar Maddirela D, Gujrati M, Rao JS. Essential role of cooperative NF-κB and Stat3 recruitment to ICAM-1 intronic consensus elements in the regulation of radiation-induced invasion and migration in glioma. Oncogene. 2013 Oct 24;32(43):5144–55.

34. Deng J, Liu Y, Lee H, Herrmann A, Zhang W, Zhang C, et al. S1PR1-STAT3 signaling is crucial for myeloid cell colonization at future metastatic sites. Cancer Cell. 2012 May 15;21(5):642–54.

35. Grivennikov S, Karin E, Terzic J, Mucida D, Yu G-Y, Vallabhapurapu S, et al. IL-6 and Stat3 are required for survival of intestinal epithelial cells and development of colitis-associated cancer. Cancer Cell. 2009 Feb 3;15(2):103–13.

36. Yoon S, Woo SU, Kang JH, Kim K, Shin H-J, Gwak H-S, et al. NF-κB and STAT3 cooperatively induce IL6 in starved cancer cells. Oncogene. 2012 Jul 19;31(29):3467–81.

37. Hutti JE, Pfefferle AD, Russell SC, Sircar M, Perou CM, Baldwin AS. Oncogenic PI3K mutations lead to NF-κB-dependent cytokine expression following growth factor deprivation. Cancer Res. 2012 Jul 1;72(13):3260–9.

38. Lee H, Herrmann A, Deng J-H, Kujawski M, Niu G, LI Z, et al. Persistently activated Stat3 maintains constitutive NF-kappaB activity in tumors. Cancer Cell. 2009 Apr 7;15(4):283–93.

39. Liang J, Nagahashi M, Kim EY, Harikumar KB, Yamada A, Huang W-C, et al. Sphingosine-1-phosphate links persistent STAT3 activation, chronic intestinal

inflammation, and development of colitis-associated cancer. Cancer Cell. 2013 Jan 14;23(1):107–20.

40. Lee H, Deng J, Xin H, Liu Y, Pardoll D, Yu H. A requirement of STAT3 DNA binding precludes Th-1 immunostimulatory gene expression by NF-κB in tumors. Cancer Res. 2011 Jun 1;71(11):3772–80.

41. Kortylewski M, Xin H, Kujawski M, Lee H, Liu Y, Harris T, et al. Regulation of the IL-23 and IL-12 balance by Stat3 signaling in the tumor microenvironment. Cancer Cell. 2009 Feb 3;15(2):114–23.

42. Wang T, Niu G, Kortylewski M, Burdelya L, Shain K, Zhang S, et al. Regulation of the innate and adaptive immune responses by Stat-3 signaling in tumor cells. Nat Med. 2003 Dec 21;10(1):48–54.

43. Kortylewski M, Kujawski M, Wang T, Wei S, Zhang S, Pilon-Thomas S, et al. Inhibiting Stat3 signaling in the hematopoietic system elicits multicomponent antitumor immunity. Nat Med. 2005 Nov 20;11(12):1314–21.

44. Rinkenbaugh A, Baldwin A. The NF-κB Pathway and Cancer Stem Cells. Cells. 2016 Jun;5(2):16.

45. Li Q, Lu Q, Hwang JY, Büscher D, Lee KF, Izpisua-Belmonte JC, et al. IKK1-deficient mice exhibit abnormal development of skin and skeleton. Genes Dev. 1999 May 15;13(10):1322–8.

46. Li Q, Van Antwerp D, Mercurio F, Lee KF, Verma IM. Severe liver degeneration in mice lacking the IkappaB kinase 2 gene. Science. 1999 Apr 9;284(5412):321–5.

47. Li Q, Estepa G, Memet S, Israel A, Verma IM. Complete lack of NF-kappaB activity in IKK1 and IKK2 double-deficient mice: additional defect in neurulation. Genes Dev. 2000 Jul 15;14(14):1729–33.

48. Pomerantz JL, Baltimore D. NF-kappaB activation by a signaling complex containing TRAF2, TANK and TBK1, a novel IKK-related kinase. EMBO J. 1999 Dec 1;18(23):6694–704.

49. Shimada T, Kawai T, Takeda K, Matsumoto M, Inoue J, Tatsumi Y, et al. IKK-i, a novel lipopolysaccharide-inducible kinase that is related to IkappaB kinases. International Immunology. 1999 Aug;11(8):1357–62.

50. Shen RR, Hahn WC. Emerging roles for the non-canonical IKKs in cancer. Oncogene. 2010 Nov 1;30(6):631–41.

51. Tojima Y, Fujimoto A, Delhase M, Chen Y, Hatakeyama S, Nakayama K, et al. NAK is an IkappaB kinase-activating kinase. Nature. 2000 Apr 13;404(6779):778–82.

52. Sharma S, Tenoever BR, Grandvaux N, Zhou G-P, Lin R, Hiscott J. Triggering the

interferon antiviral response through an IKK-related pathway. Science. 2003 May 16;300(5622):1148–51.

53. Fitzgerald KA, McWhirter SM, Faia KL, Rowe DC, Latz E, Golenbock DT, et al. IKKε and TBK1 are essential components of the IRF3 signaling pathway. Nat Immunol. 2003 Apr 14;4(5):491–6.

54. Hemmi H, Takeuchi O, Sato S, Yamamoto M, Kaisho T, Sanjo H, et al. The roles of two IkappaB kinase-related kinases in lipopolysaccharide and double stranded RNA signaling and viral infection. J Exp Med. 2004 Jun 21;199(12):1641–50.

55. Perry AK, Chow EK, Goodnough JB, Yeh W-C, Cheng G. Differential Requirement for TANK-binding Kinase-1 in Type I Interferon Responses to Toll-like Receptor Activation and Viral Infection. J Exp Med. 2004 Jun 21;199(12):1651–8.

56. Ishii KJ, Coban C, Kato H, Takahashi K, Torii Y, Takeshita F, et al. A Toll-like receptor–independent antiviral response induced by double-stranded B-form DNA. Nat Immunol. 2005 Nov 13;7(1):40–8.

57. Solis M, Romieu-Mourez R, Goubau D, Grandvaux N, Mesplede T, Julkunen I, et al. Involvement of TBK1 and IKKε in lipopolysaccharide-induced activation of the interferon response in primary human macrophages. Eur J Immunol. 2007 Feb;37(2):528–39.

58. Chau T-L, Gioia R, Gatot J-S, Patrascu F, Carpentier I, Chapelle J-P, et al. Are the IKKs and IKK-related kinases TBK1 and IKK-epsilon similarly activated? Trends Biochem Sci. 2008 Apr 1;33(4):171–80.

59. Zhou AY, Shen RR, Kim E, Lock YJ, Xu M, Chen ZJ, et al. IKKε-mediated tumorigenesis requires K63-linked polyubiquitination by a cIAP1/cIAP2/TRAF2 E3 ubiquitin ligase complex. Cell Rep. 2013 Mar 28;3(3):724–33.

60. Tu D, Zhu Z, Zhou AY, Yun C-H, Lee K-E, Toms AV, et al. Structure and Ubiquitination-Dependent Activation of TANK-Binding Kinase 1. Cell Rep. The Authors; 2013 Mar 28;3(3):747–58.

61. Larabi A, Devos JM, Ng S-L, Nanao MH, Round A, Maniatis T, et al. Crystal structure and mechanism of activation of TANK-binding kinase 1. Cell Rep. 2013 Mar 28;3(3):734–46.

62. Ma X, Helgason E, Phung QT, Quan CL, Iyer RS, Lee MW, et al. Molecular basis of Tank-binding kinase 1 activation by transautophosphorylation. Proc Natl Acad Sci USA. 2012 Jun 12;109(24):9378–83.

63. Wang L, Li S, Dorf ME. NEMO Binds Ubiquitinated TANK-Binding Kinase 1 (TBK1) to Regulate Innate Immune Responses to RNA Viruses. Meurs EF, editor. PLoS ONE. 2012 Sep 18;7(9):e43756.

64. McWhirter SM, Fitzgerald KA, Rosains J, Rowe DC, Golenbock DT, Maniatis T. IFN-

regulatory factor 3-dependent gene expression is defective in Tbk1-deficient mouse embryonic fibroblasts. Proc Natl Acad Sci USA. 2004 Jan 6;101(1):233–8.

65. Wild P, Farhan H, McEwan DG, Wagner S, Rogov VV, Brady NR, et al. Phosphorylation of the Autophagy Receptor Optineurin Restricts Salmonella Growth. Science. 2011 Jul 7;333(6039):228–33.

66. Pilli M, Arko-Mensah J, Ponpuak M, Roberts E, Master S, Mandell MA, et al. TBK-1 promotes autophagy-mediated antimicrobial defense by controlling autophagosome maturation. Immunity. 2012 Aug 24;37(2):223–34.

67. Barbie DA, Tamayo P, Boehm JS, Kim SY, Moody SE, Dunn IF, et al. Systematic RNA interference reveals that oncogenic KRAS-driven cancers require TBK1. Nature. 2009 Nov 5;462(7269):108–12.

68. Chien Y, Kim S, Bumeister R, Loo Y-M, Kwon SW, Johnson CL, et al. RalB GTPase-mediated activation of the IkappaB family kinase TBK1 couples innate immune signaling to tumor cell survival. Cell. 2006 Oct 6;127(1):157–70.

69. Ou Y-H, Torres M, Ram R, Formstecher E, Roland C, Cheng T, et al. TBK1 Directly Engages Akt/PKB Survival Signaling to Support Oncogenic Transformation. Mol Cell. 2011 Feb 18;41(4):458–70.

70. Boehm JS, Zhao JJ, Yao J, Kim SY, Firestein R, Dunn IF, et al. Integrative Genomic Approaches Identify IKBKE as a Breast Cancer Oncogene. Cell. 2007 Jun;129(6):1065–79.

71. Barbie TU, Alexe G, Aref AR, Li S, Zhu Z, Zhang X, et al. Targeting an IKBKE cytokine network impairs triple-negative breast cancer growth. J Clin Invest. 2014 Nov 3.

72. Hutti JE, Shen RR, Abbott DW, Zhou AY, Sprott KM, Asara JM, et al. Phosphorylation of the tumor suppressor CYLD by the breast cancer oncogene IKKepsilon promotes cell transformation. Mol Cell. 2009 May 14;34(4):461–72.

73. Stetson DB, Medzhitov R. Recognition of cytosolic DNA activates an IRF3-dependent innate immune response. Immunity. 2006 Jan;24(1):93–103.

74. Paludan SR, Bowie AG. Immune sensing of DNA. Immunity. 2013 May 23;38(5):870–80.

75. Guo H, Callaway JB, Ting JP-Y. Inflammasomes: mechanism of action, role in disease, and therapeutics. Nat Med. 2015 Jun 29;21(7):677–87.

76. Muruve DA, Pétrilli V, Zaiss AK, White LR, Clark SA, Ross PJ, et al. The inflammasome recognizes cytosolic microbial and host DNA and triggers an innate immune response. Nature. 2008 Feb 20;452(7183):103–7.

77. Fernandes-Alnemri T, Yu J-W, Datta P, Wu J, Alnemri ES. AIM2 activates the inflammasome and cell death in response to cytoplasmic DNA. Nature. 2009 Mar

26;458(7237):509–13.

78. Hornung V, Ablasser A, Charrel-Dennis M, Bauernfeind F, Horvath G, Caffrey DR, et al. AIM2 recognizes cytosolic dsDNA and forms a caspase-1-activating inflammasome with ASC. Nature. 2009 Mar 26;458(7237):514–8.

79. Jin T, Perry A, Jiang J, Smith P, Curry JA, Unterholzner L, et al. Structures of the HIN domain:DNA complexes reveal ligand binding and activation mechanisms of the AIM2 inflammasome and IFI16 receptor. Immunity. 2012 Apr 20;36(4):561–71.

80. Zhong B, Yang Y, Li S, Wang Y-Y, Li Y, Diao F, et al. The adaptor protein MITA links virus-sensing receptors to IRF3 transcription factor activation. Immunity. 2008 Oct 17;29(4):538–50.

81. Ishikawa H, Barber GN. STING is an endoplasmic reticulum adaptor that facilitates innate immune signalling. Nature. 2008 Aug 24;455(7213):674–8.

82. Sun W, Li Y, Chen L, Chen H, You F, Zhou X, et al. ERIS, an endoplasmic reticulum IFN stimulator, activates innate immune signaling through dimerization. Proc Natl Acad Sci USA. 2009 May 26;106(21):8653–8.

83. Unterholzner L, Keating SE, Baran M, Horan KA, Jensen SB, Sharma S, et al. IFI16 is an innate immune sensor for intracellular DNA. Nat Immunol. 2010 Nov;11(11):997–1004.

84. Burdette DL, Vance RE. STING and the innate immune response to nucleic acids in the cytosol. Nat Immunol. 2012 Dec 14;14(1):19–26.

85. Ouyang S, Song X, Wang Y, Ru H, Shaw N, Jiang Y, et al. Structural analysis of the STING adaptor protein reveals a hydrophobic dimer interface and mode of cyclic di-GMP binding. Immunity. 2012 Jun 29;36(6):1073–86.

86. Tanaka Y, Chen ZJ. STING Specifies IRF3 Phosphorylation by TBK1 in the Cytosolic DNA Signaling Pathway. Sci Signal. 2012 Mar 6;5(214):ra20–0.

87. Zhao B, Shu C, Gao X, Sankaran B, Du F, Shelton CL, et al. Structural basis for concerted recruitment and activation of IRF-3 by innate immune adaptor proteins. Proc Natl Acad Sci USA. 2016 Jun 14;113(24):E3403–12.

88. Liu S, Cai X, Wu J, Cong Q, Chen X, Li T, et al. Phosphorylation of innate immune adaptor proteins MAVS, STING, and TRIF induces IRF3 activation. Science. 2015 Mar 13;347(6227):aaa2630.

89. Zhang Z, Yuan B, Bao M, Lu N, Kim T, Liu Y-J. The helicase DDX41 senses intracellular DNA mediated by the adaptor STING in dendritic cells. Nat Immunol. 2011 Sep 4;12(10):959–65.

90. Sauer JD, Sotelo-Troha K, Moltke von J, Monroe KM, Rae CS, Brubaker SW, et al. The N-Ethyl-N-Nitrosourea-Induced Goldenticket Mouse Mutant Reveals an Essential

Function of Sting in the In Vivo Interferon Response to Listeria monocytogenes and Cyclic Dinucleotides. Infection and Immunity. 2011 Jan 21;79(2):688–94.

91. Burdette DL, Monroe KM, Sotelo-Troha K, Iwig JS, Eckert B, Hyodo M, et al. STING is a direct innate immune sensor of cyclic di-GMP. Nature. 2011 Sep 25;478(7370):515–8.

92. Yi G, Brendel VP, Shu C, Li P, Palanathan S, Cheng Kao C. Single nucleotide polymorphisms of human STING can affect innate immune response to cyclic dinucleotides. PLoS ONE. 2013;8(10):e77846.

93. Jin L, Xu L-G, Yang IV, Davidson EJ, Schwartz DA, Wurfel MM, et al. Identification and characterization of a loss-of-function human MPYS variant. Genes Immun. 2011 Jun;12(4):263–9.

94. Aglipay JA, Lee SW, Okada S, Fujiuchi N, Ohtsuka T, Kwak JC, et al. A member of the Pyrin family, IFI16, is a novel BRCA1-associated protein involved in the p53-mediated apoptosis pathway. Oncogene. 2003 Dec 4;22(55):8931–8.

95. Orzalli MH, Conwell SE, Berrios C, DeCaprio JA, Knipe DM. Nuclear interferon-inducible protein 16 promotes silencing of herpesviral and transfected DNA. Proc Natl Acad Sci USA. 2013 Nov 19;110(47):E4492–501.

96. Morrone SR, Wang T, Constantoulakis LM, Hooy RM, Delannoy MJ, Sohn J. Cooperative assembly of IFI16 filaments on dsDNA provides insights into host defense strategy. Proc Natl Acad Sci USA. 2014 Jan 7;111(1):E62–71.

97. Fu Y, Comella N, Tognazzi K, Brown LF, Dvorak HF, Kocher O. Cloning of DLM-1, a novel gene that is up-regulated in activated macrophages, using RNA differential display. Nature. 1999 Nov;240(1):157–63.

98. Schwartz T, Behlke J, Lowenhaupt K, Heinemann U, Rich A. Structure of the DLM-1-Z-DNA complex reveals a conserved family of Z-DNA-binding proteins. Nat Struct Biol. 2001 Sep;8(9):761–5.

99. Takaoka A, Wang Z, Choi MK, Yanai H, Negishi H, Ban T, et al. DAI (DLM-1/ZBP1) is a cytosolic DNA sensor and an activator of innate immune response. Nature. 2007 Jul 26;448(7152):501–5.

100. DeFilippis VR, Alvarado D, Sali T, Rothenburg S, Fruh K. Human Cytomegalovirus Induces the Interferon Response via the DNA Sensor ZBP1. J Virol. 2009 Dec 9;84(1):585–98.

101. Ishii KJ, Kawagoe T, Koyama S, Matsui K, Kumar H, Kawai T, et al. TANK-binding kinase-1 delineates innate and adaptive immune responses to DNA vaccines. Nature. 2008 Feb 7;451(7179):725–9.

102. Lee K-G, Kim SS-Y, Kui L, Voon DC-C, Mauduit M, Bist P, et al. Bruton's tyrosine kinase phosphorylates DDX41 and activates its binding of dsDNA and STING to initiate

type 1 interferon response. Cell Rep. 2015 Feb 24;10(7):1055–65.

103. Parvatiyar K, Zhang Z, Teles RM, Ouyang S, Jiang Y, Iyer SS, et al. The helicase DDX41 recognizes the bacterial secondary messengers cyclic di-GMP and cyclic di-AMP to activate a type I interferon immune response. Nat Immunol. 2012 Nov 11;13(12):1155–61.

104. Ishikawa H, Ma Z, Barber GN. STING regulates intracellular DNA-mediated, type I interferon-dependent innate immunity. Nature. 2009 Oct 8;461(7265):788–92.

105. Chiu Y-H, MacMillan JB, Chen ZJ. RNA polymerase III detects cytosolic DNA and induces type I interferons through the RIG-I pathway. Cell. 2009 Aug 7;138(3):576–91.

106. Ablasser A, Bauernfeind F, Hartmann G, Latz E, Fitzgerald KA, Hornung V. RIG-I-dependent sensing of poly(dA:dT) through the induction of an RNA polymerase III-transcribed RNA intermediate. Nat Immunol. 2009 Oct;10(10):1065–72.

107. Sun L, Wu J, Du F, Chen X, Chen ZJ. Cyclic GMP-AMP Synthase Is a Cytosolic DNA Sensor That Activates the Type I Interferon Pathway. Science. 2013 Feb 14;339(6121):786–91.

108. Kranzusch PJ, Lee AS-Y, Berger JM, Doudna JA. Structure of human cGAS reveals a conserved family of second-messenger enzymes in innate immunity. Cell Rep. 2013 May 30;3(5):1362–8.

109. Civril F, Deimling T, de Oliveira Mann CC, Ablasser A, Moldt M, Witte G, et al. Structural mechanism of cytosolic DNA sensing by cGAS. Nature. 2013 Jun 20;498(7454):332–7.

110. Gao P, Ascano M, Wu Y, Barchet W, Gaffney BL, Zillinger T, et al. Cyclic [G(2',5')pA(3“,5”)p] is the metazoan second messenger produced by DNA-activated cyclic GMP-AMP synthase. Cell. 2013 May 23;153(5):1094–107.

111. Wu J, Sun L, Chen X, Du F, Shi H, Chen C, et al. Cyclic GMP-AMP Is an Endogenous Second Messenger in Innate Immune Signaling by Cytosolic DNA. Science. 2013 Feb 14;339(6121):826–30.

112. Ablasser A, Schmid-Burgk JL, Hemmerling I, Horvath GL, Schmidt T, Latz E, et al. Cell intrinsic immunity spreads to bystander cells via the intercellular transfer of cGAMP. Nature. 2013 Nov 28;503(7477):530–4.

113. Ablasser A, Goldeck M, Cavlar T, Deimling T, Witte G, Röhl I, et al. cGAS produces a 2′-5′-linked cyclic dinucleotide second messenger that activates STING. Nature. 2013 May 30.

114. Li XD, Wu J, Gao D, Wang H, Sun L, Chen ZJ. Pivotal Roles of cGAS-cGAMP Signaling in Antiviral Defense and Immune Adjuvant Effects. Science. 2013 Sep 19;341(6152):1390–4.

115. Abe T, Barber GN. Cytosolic-DNA-mediated, STING-dependent proinflammatory gene induction necessitates canonical NF-κB activation through TBK1. J Virol. 2014 May;88(10):5328–41.

116. Lehtinen DA, Harvey S, Mulcahy MJ, Hollis T, Perrino FW. The TREX1 double-stranded DNA degradation activity is defective in dominant mutations associated with autoimmune disease. J Biol Chem. 2008 Nov 14;283(46):31649–56.

117. Crow YJ, Hayward BE, Parmar R, Robins P, Leitch A, Ali M, et al. Mutations in the gene encoding the 3′-5′ DNA exonuclease TREX1 cause Aicardi-Goutières syndrome at the AGS1 locus. Nat Genet. 2006 Jul 16;38(8):917–20.

118. Napirei M, Karsunky H, Zevnik B, Stephan H, Mannherz HG, Möröy T. Features of systemic lupus erythematosus in Dnase1-deficient mice. Nat Genet. 2000 Jun;25(2):177–81.

119. Okabe Y, Kawane K, Akira S, Taniguchi T, Nagata S. Toll-like receptor-independent gene induction program activated by mammalian DNA escaped from apoptotic DNA degradation. J Exp Med. 2005 Nov 21;202(10):1333–9.

120. Okabe Y, Kawane K, Nagata S. IFN regulatory factor (IRF) 3/7-dependent and -independent gene induction by mammalian DNA that escapes degradation. Eur J Immunol. 2008 Nov;38(11):3150–8.

121. Yoshida H, Okabe Y, Kawane K, Fukuyama H, Nagata S. Lethal anemia caused by interferon-beta produced in mouse embryos carrying undigested DNA. Nat Immunol. 2005 Jan;6(1):49–56.

122. Stetson DB, Ko JS, Heidmann T, Medzhitov R. Trex1 Prevents Cell-Intrinsic Initiation of Autoimmunity. Cell. 2008 Aug;134(4):587–98.

123. Ahn J, Gutman D, Saijo S, Barber GN. STING manifests self DNA-dependent inflammatory disease. Proc Natl Acad Sci USA. 2012 Nov 20;109(47):19386–91.

124. Gao D, Li T, Li X-D, Chen X, Li Q-Z, Wight-Carter M, et al. Activation of cyclic GMP-AMP synthase by self-DNA causes autoimmune diseases. Proc Natl Acad Sci USA. 2015 Oct 20;112(42):E5699–705.

125. Hasan M, Koch J, Rakheja D, Pattnaik AK, Brugarolas J, Dozmorov I, et al. Trex1 regulates lysosomal biogenesis and interferon-independent activation of antiviral genes. Nat Immunol. 2012 Nov 18;14(1):61–71.

126. Ablasser A, Hemmerling I, Schmid-Burgk JL, Behrendt R, Roers A, Hornung V. TREX1 Deficiency Triggers Cell-Autonomous Immunity in a cGAS-Dependent Manner. J Immunol. 2014 Jun 6;192(12):5993–7.

127. Gray EE, Treuting PM, Woodward JJ, Stetson DB. Cutting Edge: cGAS Is Required for Lethal Autoimmune Disease in the Trex1-Deficient Mouse Model of Aicardi-Goutières

Syndrome. J Immunol. 2015 Sep 1;195(5):1939–43.

128. Horan KA, Hansen K, Jakobsen MR, Holm CK, Soby S, Unterholzner L, et al. Proteasomal Degradation of Herpes Simplex Virus Capsids in Macrophages Releases DNA to the Cytosol for Recognition by DNA Sensors. J Immunol. 2013 Feb 15;190(5):2311–9.

129. Rasmussen SB, Horan KA, Holm CK, Stranks AJ, Mettenleiter TC, Simon AK, et al. Activation of autophagy by α-herpesviruses in myeloid cells is mediated by cytoplasmic viral DNA through a mechanism dependent on stimulator of IFN genes. J Immunol. 2011 Nov 15;187(10):5268–76.

130. Lio C-WJ, McDonald B, Takahashi M, Dhanwani R, Sharma N, Huang J, et al. cGAS-STING Signaling Regulates Initial Innate Control of Cytomegalovirus Infection. J Virol. 2016 Sep 1;90(17):7789–97.

131. Ma Z, Jacobs SR, West JA, Stopford C, Zhang Z, Davis Z, et al. Modulation of the cGAS-STING DNA sensing pathway by gammaherpesviruses. Proc Natl Acad Sci USA. 2015 Aug 4;112(31):E4306–15.

132. Yoh SM, Schneider M, Seifried J, Soonthornvacharin S, Akleh RE, Olivieri KC, et al. PQBP1 Is a Proximal Sensor of the cGAS-Dependent Innate Response to HIV-1. Cell. 2015 Jun 4;161(6):1293–305.

133. Guo H, König R, Deng M, Riess M, Mo J, Zhang L, et al. NLRX1 Sequesters STING to Negatively Regulate the Interferon Response, Thereby Facilitating the Replication of HIV-1 and DNA Viruses. Cell Host and Microbe. 2016 Apr 13;19(4):515–28.

134. Ma Z, Damania B. The cGAS-STING Defense Pathway and Its Counteraction by Viruses. Cell Host and Microbe. 2016 Feb 10;19(2):150–8.

135. Schoggins JW, MacDuff DA, Imanaka N, Gainey MD, Shrestha B, Eitson JL, et al. Pan-viral specificity of IFN-induced genes reveals new roles for cGAS in innate immunity. Nature. 2014 Jan 30;505(7485):691–5.

136. Watson RO, Bell SL, MacDuff DA, Kimmey JM, Diner EJ, Olivas J, et al. The Cytosolic Sensor cGAS Detects Mycobacterium tuberculosis DNA to Induce Type I Interferons and Activate Autophagy. Cell Host and Microbe. 2015 Jun 10;17(6):811–9.

137. Collins AC, Cai H, Li T, Franco LH, Li X-D, Nair VR, et al. Cyclic GMP-AMP Synthase Is an Innate Immune DNA Sensor for Mycobacterium tuberculosis. Cell Host and Microbe. 2015 Jun 10;17(6):820–8.

138. Watson RO, Manzanillo PS, Cox JS. Extracellular M. tuberculosis DNA Targets Bacteria for Autophagy by Activating the Host DNA-Sensing Pathway. Cell. 2012 Aug 17;150(4):803–15.

139. Lippmann J, Müller HC, Naujoks J, Tabeling C, Shin S, Witzenrath M, et al. Dissection of

a type I interferon pathway in controlling bacterial intracellular infection in mice. Cellular Microbiology. 2011 Aug 24;13(11):1668–82.

140. Storek KM, Gertsvolf NA, Ohlson MB, Monack DM. cGAS and Ifi204 cooperate to produce type I IFNs in response to Francisella infection. J Immunol. 2015 Apr 1;194(7):3236–45.

141. Hansen K, Prabakaran T, Laustsen A, Jørgensen SE, Rahbæk SH, Jensen SB, et al. Listeria monocytogenes induces IFNβ expression through an IFI16-, cGAS- and STING-dependent pathway. EMBO J. 2014 Aug 1;33(15):1654–66.

142. Chen H, Sun H, You F, Sun W, Zhou X, Chen L, et al. Activation of STAT6 by STING is critical for antiviral innate immunity. Cell. 2011 Oct 14;147(2):436–46.

143. Tenoever BR, Ng S-L, Chua MA, McWhirter SM, García-Sastre A, Maniatis T. Multiple functions of the IKK-related kinase IKKepsilon in interferon-mediated antiviral immunity. Science. 2007 Mar 2;315(5816):1274–8.

144. Ng S-L, Friedman BA, Schmid S, Gertz J, Myers RM, Tenoever BR, et al. IκB kinase epsilon (IKK(epsilon)) regulates the balance between type I and type II interferon responses. Proc Natl Acad Sci USA. 2011 Dec 27;108(52):21170–5.

145. Sharma S, Campbell AM, Chan J, Schattgen SA, Orlowski GM, Nayar R, et al. Suppression of systemic autoimmunity by the innate immune adaptor STING. Proc Natl Acad Sci USA. 2015 Feb 2;:201420217.

146. Dong G, You M, Ding L, Fan H, Liu F, Ren D, et al. STING Negatively Regulates Double-Stranded DNA-Activated JAK1-STAT1 Signaling via SHP-1/2 in B Cells. Mol Cells. 2015 May 7.

CHAPTER 2: STAT3 REGULATES HOST DEFENSE AND PROTECTS MICE AGAINST HERPES SIMPLEX VIRUS-1 INFECTION[1]

2.1 Summary

Signal transducer and activator of transcription 3 (STAT3) mediates cellular responses to multiple cytokines, governs gene expression, and regulates the development and activation of immune cells. STAT3 also modulates reactivation of latent herpes simplex virus-1 (HSV-1) in ganglia. However, it is unclear how STAT3 regulates the innate immune response during the early phase of HSV-1 lytic infection. Many cell types critical for the innate immunity are derived from the myeloid lineage. Therefore, here we used myeloid-specific STAT3 knockout mice to investigate the role of STAT3 in the innate immune response against HSV-1. Our results demonstrated that STAT3 knockout bone marrow-derived macrophages (BMMs) expressed decreased levels of Interferon α (IFNα) and interferon-stimulated genes (ISGs) upon HSV-1 infection. In vivo, knockout mice were more susceptible to HSV-1, as marked by higher viral loads and more significant weight loss. Splenic expression of IFNα and ISGs was reduced in the absence of STAT3, indicating that STAT3 is required for optimal type I interferon response to HSV-1. Expression of TNFα and IL-12, cytokines that have been shown to limit HSV-1 replication and pathogenesis, was also significantly lower in knockout mice. Interestingly, STAT3 knockout mice failed to expand $CD8^+$ conventional DC (cDC) population upon HSV-1

[1] This chapter has been accepted by the Journal of Leukocyte Biology and is placed into this dissertation after additional editing by the author. The original citation is as follows: Hsia H-C, Stopford CM, Zhang Z, Damania B, Baldwin AS. Signal transducer and activator of transcription 3 (Stat3) regulates host defense and protects mice against herpes simplex virus-1 (HSV-1) infection. *Journal of Leukocyte Biology*. 2016 Dec 13 (In press)

infection, and this was accompanied by impaired NK and CD8 T cell activation. Collectively, our data demonstrated that myeloid-specific STAT3 deletion causes defects in multiple aspects of the immune system, and that STAT3 has a protective role at the early stage of systemic HSV-1 infection.

2.2 Introduction

Herpes simplex virus 1 (HSV-1) is estimated to infect more than two thirds of the population worldwide. Common symptoms of HSV-1 infection, including local skin or mucosa membrane lesions, usually resolve in a few days to several weeks (1). Localized HSV-1 infections are also often accompanied by viremia (2,3). Following lytic infection, the virus retreats to neurons where it establishes latency. Latency is lifelong and may be asymptomatic with occasional relapses (1). HSV-1 infection seldom causes severe disease in healthy individuals. However, newborns, the elderly, and immunocompromised individuals are prone to HSV-1-induced diseases, such as herpes simplex keratitis (HSK) and life-threatening herpes simplex encephalitis (HSE) (1). These susceptible populations also are more likely to exhibit HSV-1 viremia in the blood (2), and it is now becoming more apparent that primary HSV-1 infection and reactivation can occur beyond the mucocutaneous areas in both immunocompetent and immunocompromised individuals (2). It is therefore important to understand the mechanism by which the immune system controls HSV-1 infection.

Both innate and adaptive immunity are critical in controlling HSV-1 infection. Several major cellular mediators of the innate immunity implicated in limiting HSV-1 pathogenesis are of the myeloid lineage, including macrophages, dendritic cells (DCs), and neutrophils. Macrophages are intrinsically resistant to productive HSV-1 infection (4,5). Depletion of

macrophages in mice leads to higher viral replication and exaggerated pathology (6,7), while adoptive transfer of adult macrophages protects susceptible neonates from lethal HSV-1 infection (8). Macrophages also limit the replication and dissemination of HSV-1 in the peripheral nervous system (9). The protective effects of macrophages are partially mediated through secreted factors, including IL-12, TNFα, and nitric oxide (NO). These factors inhibit viral replication, recruit leukocytes to the site of infection, promote the cellular immune response, and further activate macrophages to protect mice from HSV-1 and other herpesvirus infections (9-13). Specialized macrophages such as marginal zone macrophages (MZMΦs) and marginal metallophilic macrophages (MMMΦs) produce substantial amount of type I interferons to elicit antiviral response during HSV-1 viremia (14). In addition to macrophages, dendritic cells (DCs) also play a pivotal role in the immunity against herpesvirus infections. Mice depleted of DCs have shortened survival and higher viral loads in the nervous system during HSV-1 infection, and the susceptibility is attributed to impaired NK and T cell activation in the absence of DCs (15). Major subsets of DCs include $CD11b^+$ conventional DC (cDC), $CD8^+$ cDC, and plasmacytoid DC (pDC). Both $CD8^+$ cDC and pDC are involved in promoting NK cell activation and anti-HSV cytotoxic T lymphocyte (CTL) immunity (16-18), but only $CD8^+$ cDC is able to cross present and directly activate CD8 T cells (19,20). Importantly, pDCs are capable of producing large quantities of type I interferons during HSV-1 infection (17). Finally, neutrophils have dual roles in HSV-1 infection. It has been suggested that neutrophils inhibit HSV-1 replication (21), but further examination revealed that neutrophils mediate HSV-1-induced tissue injury and immunopathology (22,23).

Signal transducer and activator of transcription 3 (STAT3) is a transcription factor that mediates the cellular responses to multiple cytokines by promoting the expression of genes

implicated in survival, inflammation, proliferation, and migration (24). STAT3 modulates HSV-1 reactivation in the ganglia (25) and governs various aspects of myeloid cell proliferation, differentiation, and responses to infections (26-29). For example, STAT3-null macrophages display heightened immune responses in response to lipopolysaccharide (LPS) and bacterial infections, as marked by the overproduction of pro-inflammatory cytokines (26,30). Additionally, STAT3-null neutrophils are defective in their bactericidal capacity (30). Nonetheless, the role of STAT3 in the myeloid lineage during viral infections has not been fully investigated.

Given the critical role of macrophages and DCs in limiting HSV-1 pathogenesis at the early phase of infection, we set out to investigate if STAT3 in the myeloid lineage modulates the innate immune response to HSV-1. Here we show that the type I interferon response was partially defective in STAT3-null bone marrow-derived macrophages (BMMs) during HSV-1 infection. In vivo, myeloid STAT3 knockout mice exhibited higher viral loads and more significant weight loss during HSV-1 infection compared to wild-type mice. Importantly, knockout mice had decreased splenic expression of IFNα and interferon-stimulated genes (ISGs), as well as decreased expression of IL-12 and TNFα, cytokines known to be protective against HSV-1 infection. Finally, STAT3 knockout mice failed to expand $CD8^+$ cDC during HSV-1 infection, and activation of natural killer (NK) and CD8 T cells was also impaired. In summary, our results indicate that STAT3 in the myeloid lineage contributes to the resistance to HSV-1 infection at the early stage by modulating multiple aspects of innate immunity.

2.3 Results

2.3.1 Characterization of Stat3$^{fl/fl}$ LysM-Cre$^{+/+}$ mice

To investigate if STAT3 in the myeloid lineage affects the innate immune response to HSV-1, we crossed *Stat3*$^{fl/fl}$ mice to LysM-Cre mice to generate myeloid-specific STAT3 knockout mice. Cre recombinase driven by the lysozyme (LysM) promoter is specifically expressed in the myeloid lineage, leading to conditional deletion of loxP-flanked target gene in granulocytes, monocytes, and macrophages (31). In agreement with the literature, bone marrow-derived macrophages (BMMs) from *Stat3*$^{fl/fl}$ LysM-Cre$^{+/+}$ mice (hereafter referred as knockout mice) showed more than 90% reduction of STAT3 protein comparing to BMMs from *Stat3*$^{wt/wt}$ LysM-Cre$^{+/+}$ mice (hereafter referred as wild-type mice). No noticeable reduction of STAT3 protein levels were observed in the brain, liver, or muscle as determined by immunoblotting (Supplemental Figure 2.1).

The *Stat3*$^{fl/fl}$ used in this study (see Materials and Methods) differs from the strain used in the previous LysM-Cre/*Stat3* mouse study (26). Thus, to determine the effect of myeloid *Stat3* deletion with regard to this specific strain, we examined the composition of lymphocytes and myeloid cells in the knockout mice. Lack of STAT3 in the myeloid lineage did not affect the composition of major cell populations in the spleen. Specifically, the percentage of B cells, T cells, neutrophils, monocytes, red pulp macrophages (RpMΦ), marginal metallophilic macrophages (MMMΦ), and marginal zone macrophages (MZMΦ) in the spleen were similar between wild-type and knockout mice (Table 2.1). In the bone marrow, *Stat3* knockout mice had more SSC^{hi} granulocytes and CD11b^{+} myeloid cells owing to a significant expansion of CD11b^{+} Ly6G^{+} neutrophils within the granulocyte compartment (Table 2.2). An increase of the CD11b^{+} Ly6C^{hi} monocytes was also observed (Table 2.2). The expansion of neutrophils was

accompanied by a mild decrease in B cell and T cell populations in the bone marrow. Neutrophilia has been reported by other groups using hematopoietic-specific or inducible *Stat3* knockout mice (28,29). Our results suggest that myeloid-specific deletion of *Stat3* is sufficient to cause the neutrophil expansion phenotype. The number of $CD11b^{lo}$ $F4/80^{+}$ macrophages in the bone marrow did not differ between wild-type and knockout mice (Table 2.2). Similar to the previous study (26), we did not observe a differentiation block of STAT3-null BMMs cultured *in vitro* (data not shown), suggesting that STAT3 is not crucial in normal macrophage differentiation. Taken together, our data agreed with the previous studies and independently verified that myeloid *Stat3* deletion leads to neutrophil expansion in the bone marrow but has minimal effects on splenic cells or BMM differentiation by using a different $Stat3^{fl/fl}$ strain.

2.3.2 Stat3 knockout BMMs show attenuated type I interferon response to HSV-1 infection

HSV-1 is able to enter and infect BMMs and peritoneal macrophages, but few infectious viral particles are produced following virus entry, indicating that macrophages are non-permissive to productive HSV-1 infection (4,5). To determine if STAT3 plays a role in the intrinsic resistance of macrophages to HSV-1, BMMs from wild-type or knockout mice were infected with HSV-1 at a multiplicity of infection (MOI) of 3, and infectious viral particles in the supernatant were measured at 12 and 24 hours post infection (hpi) by plaque assay. Similar to wild-type BMMs, STAT3 knockout BMMs produced limited amount of infectious viral particles, and the viral titer reduced over time (Figure 2.1A), indicating that knockout BMMs are capable of restricting HSV-1 replication. No statistical difference was observed between wild-type and knockout BMMs in their susceptibility to HSV-1 as measured by infectious viral

particles produced (Figure 2.1A). Thus, *Stat3* deletion in the macrophages does not impair their intrinsic resistance to HSV-1.

To further investigate the response of BMMs to HSV-1, we examined the signaling events and host gene expression following HSV-1 infection. HSV-1 induced robust tyrosine phosphorylation and activation of STAT1 and STAT3 in wild-type BMMs, and STAT1 activation appeared to be normal in the absence of STAT3 (Figure 2.1B). Phosphorylation of IκBα (p-IκBα) was induced, and phospho-p65 (p-p65) was induced to a lesser extent, indicating activation of the NF-κB pathway by HSV-1 infection (Figure 2.1B). Importantly, p-IκBα level was higher in knockout BMMs, indicating enhanced NF-κB activity, while the induction of ISG15, an interferon-stimulated gene (ISG), was reduced in knockout BMMs (Figure 2.1B). HSV-1 also induced the expression of several genes involved in signaling and immune regulation (Figure 2.1C-M). Of note, induction of SOCS3, a STAT3 inhibitor highly upregulated by active STAT3 (32), was blunted in knockout macrophages (Figure 2.1C), confirming the lack of STAT3 functionality in knockout BMMs.

It has been reported that STAT3-null macrophages express higher levels of pro-inflammatory genes in response to LPS and bacterial infection (26,30). Similarly, we found that during HSV-1 infection, knockout BMMs expressed more TNFα, inducible nitric oxide synthase (iNOS), and IL-12b than wild-type BMMs (Figure 2.1D-F), but not other inflammatory cytokines such as IL-1β and IL-6 (Figure 2.1G-H). Knockout BMMs also expressed more CXCL2 (Figure 2.1I), a neutrophil chemoattractant responsible for neutrophil mobilization to the site of HSV-1 infection (33). On the contrary, induction of CCL2, a monocyte chemoattractant and a STAT3 target gene, was decreased in knockout BMMs (Figure 2.1J). These data show that *Stat3* knockout BMMs induce higher expression of a subset of pro-inflammatory cytokines upon

viral infection. We also examined the expression of type I interferons and ISGs. While expression of IFNβ was unaffected (Figure 2.1K), HSV-1-induced IFNα expression was severely diminished in the absence of STAT3 (Figure 2.1L). Moreover, expression of two ISGs, namely ISG15 and USP18, was decreased in the knockout BMMs (Figure 2.1B, 2.1M), indicating that while STAT3 is dispensable for IFNβ expression, it is required for IFNα expression and optimal expression of ISGs in response to HSV-1 infection.

Taken together, our data showed that in vitro HSV-1 infection activates STAT1 and STAT3 in BMMs. Loss of STAT3 did not impair STAT1 activation or the intrinsic ability of BMMs to limit HSV-1 replication. However, *Stat3* knockout BMMs had significantly lower expression of IFNα and ISGs, suggesting that effective induction of IFNα and ISGs in BMMs during HSV-1 infection is dependent on STAT3.

2.3.3 Myeloid Stat3 knockout mice are more susceptible to HSV-1 infection

Type I interferons, including IFNα and IFNβ, are critical in mounting antiviral defense at the early stage of viral infection by inducing the expression of ISGs (34). The attenuated type I interferon response in STAT3 knockout macrophages may have profound effects on the outcome of systemic HSV-1 infection. Thus, we set out to investigate if *Stat3* knockout mice are more susceptible to systemic HSV-1 infection. Wild-type or knockout mice were infected with $2x10^8$ pfu of HSV-1 via tail vein injection. Most mice succumbed to death within two days, but the wild-type mice survived longer (Figure 2.2A). Viral loads, as determined by HSV-1 genome copy number relative to mouse β-Actin copy number, showed a trend of increase in the brain, liver, and spleen of knockout mice, but the difference was not statistical significant

(Supplemental Figure 2.2). These results suggest that STAT3 in myeloid cells have a protective role during lethal systemic HSV-1 infections and prompted further investigation.

Next, we challenged the mice with a lower dose of HSV-1. Mice were infected with $1x10^7$ pfu of HSV-1 by tail vein injection. Both groups of mice displayed symptoms including hunched posture, signs of hind limb weakness, and significant weight loss starting at 2 days post infection (dpi). No statistical difference in survival was observed (Figure 2.2B). However, *Stat3* knockout mice experienced significantly worse weight loss over the course of infection (Figure 2.2C). To determine the impact of myeloid-specific *Stat3* deletion on the innate immunity against HSV-1 at the early stage of infection, we examined the viral loads in the brain and the spleen at 2 dpi. *Stat3* knockout mice had significantly higher viral loads in the brain at 2 dpi (Figure 2.2D). Viral loads were also marginally higher in the spleens of knockout mice at 2 dpi (Figure 2.2E). These data showed that *Stat3* knockout mice are more susceptible to HSV-1 infection, and the differences are discernible at the earlier stages of infection.

2.3.4 Susceptibility of Stat3 knockout mice is not caused by immunopathology in the brain

To investigate the mechanisms contributing to the higher brain viral loads in knockout mice, we examined the expression of immunoregulatory genes in the brain. Factors including IFNα, IFNβ, IFNγ, IL-12, TNFα, and NO are known to be critical in inhibiting HSV-1 replication in various settings in vitro and in vivo (10-13,35,36). While IFNγ expression in the brain was below the detection threshold (data not shown), iNOS, TNFα, IFNα, IFNβ, and IL-12 were not differentially expressed in the brains of wild-type and knockout mice (Figure 2.3A-E), and thus cannot account for the higher viral loads in the brains of STAT3 knockout mice. Microglia, a macrophage-like cell type in the brain, are intrinsically resistant to HSV-1 infection

(37) and elicit significant immune responses in the brain during HSV-1 infection (23,38,39). Given that LysM-Cre has been reported to result in partial deletion of the loxP-flanked gene in microglia (40), it is possible that LysM-Cre causes *Stat3* deletion in microglia, thereby altering their responses to HSV-1 infection and undermining their ability of restricting HSV-1 replication in the brain. However, we found that wild-type microglia expressed low levels of STAT3, and the expression was not noticeably reduced in the microglia of *Stat3* knockout animals (Figure 3F). Previous studies also suggested that immune cell infiltrates are the major cause of herpes simplex encephalitis (HSE) immunopathology (23,41). In this setting, CCL2 and CXCL2 produced by microglia are the primary macrophage and neutrophil chemoattractants (38,42). To probe the possibility of immunopathology in STAT3 knockout mice, we further examined the expression of CCL2 and CXCL2. We found that CCL2 and CXCL2 were not differentially expressed between wild-type and knockout mice (Figure 3G-3H). Moreover, there was no evidence of $CD45^+$ hematopoietic-origin infiltrating cells or $Ly6G^+$ neutrophils in the brains of both wild-type and knockout mice (Figure 2.3F). Taken together, our data showed that the higher viral loads in the brain and exaggerated symptoms of *Stat3* knockout mice are not due to immune cell infiltration or microglia defects in the brain. Rather, it is more likely caused by failure of the immune system in *Stat3* knockout mice to restrain the replication and spread of HSV-1 to the central nervous system.

2.3.5 Stat3 knockout mice express reduced levels of antiviral cytokines in the spleen

Next, we examine the immune responses in the spleens of infected mice. Intravenous infection of HSV-1 in mice is known to elicit robust immune responses in the spleen, and splenic MMMΦs and MZMΦs are the major producer of type I interferons in this setting (14). Myeloid

STAT3 deletion did not affect the percentage of MMMΦ and MZMΦ in the spleen (Table 2.1). However, similar to the findings with STAT3 knockout BMMs (Figure 2.1), splenic expression of IFNα and USP18 at 2 dpi was significantly lower in the knockout mice, while expression of IFNβ and IFNγ was unaffected (Figure 2.4A-D), indicating a partially defective type I interferon response. On the contrary, splenic expression of iNOS was not affected by myeloid STAT3 deletion (Figure 4E), and splenic expression of TNFα and IL-12β was lower in knockout mice (Figure 2.4F-G). These data showed that type I interferon response in the spleens of STAT3 knockout mice is also impaired during systemic HSV-1 infection, while expression of type II interferon, namely IFNγ, is not dependent on STAT3. Because TNFα signaling is important in promoting DC survival during differentiation and upon activation (43), and DC is a major producer of IL-12 in the spleen (44-46), reduced expression of TNFα and IL-12 in *Stat3* knockout mice prompted us to investigate the possibility of defective DC functionality in the knockout mice during HSV-1 infection.

2.3.6 Stat3 knockout mice have decreased CD8$^+$ cDC frequency during HSV-1 infection

STAT3 is critical for DC differentiation from hematopoietic stem cells (47), and it has been reported that LysM-Cre can lead to partial deletion of target genes in a small fraction of splenic DCs (31). Therefore, we asked if LysM-Cre-mediated *Stat3* deletion affects splenic DC at steady-state and during HSV-1 infection. We found that myeloid STAT3 deletion did not affect the percentage of total splenic DC or CD11b$^+$ conventional DC (cDC) subset at steady-state. Additionally, knockout mice were able to expand the total splenic DC and CD11b$^+$ cDC population to a level comparable to that of wild-type mice in response to HSV-1 infection (Figure 2.5A-C). Wild-type and knockout mice also had similar numbers of CD8$^+$ cDCs at

steady-state. However, a mild reduction in $CD8^+$ cDC population was observed in the knockout mice during HSV-1 infection (Figure 2.5D). Knockout mice also had more steady-state pDCs, although similar levels of pDC were observed in wild-type and knockout mice during HSV-1 infection (Figure 2.5E). These data suggest that STAT3 may have a minor role in pDC differentiation at steady-state. Importantly, the reduction of $CD8^+$ cDC population in *Stat3* knockout mice during HSV-1 infection demonstrates that STAT3 contributes to $CD8^+$ cDC differentiation, proliferation, or survival in response to HSV-1 infection.

2.3.7 Stat3 knockout mice have impaired NK and T cell activation during HSV-1 infection

Splenic $CD8^+$ cDCs are specialized to cross-present viral antigens to CD8 T cells to elicit virus-specific CTL immunity (20,48). During HSV-1 infection, DCs also have a critical role in promoting natural killer (NK) cell and CTL activation (15). Given that *Stat3* knockout mice failed to expand $CD8^+$ cDC population during HSV-1 infection, we asked if activation of NK and $CD8^+$ T cells in *Stat3* knockout mice was affected. We found that mock-infected the knockout mice had less steady-state splenic NK cells (identified as $CD3^-$ $NK1.1^+$), but HSV-1 infection increased the number of NK cells to a level comparable to that of wild-type mice (Figure 2.6A-B). NK cells in wild-type mice upregulated the activation marker CD69 at 2 dpi (Figure 2.6C). However, NK cell activation was diminished in *Stat3* knockout mice (Figure 6C). Activation of CD8 T cells was mostly unaffected by *Stat3* deletion (Figure 2.6D), although the degree of activation was marginally lower in knockout mice (Figure 2.6E). These data demonstrated that myeloid *Stat3* deletion leads to impaired NK cell activation and minor defects in CD8 T cell activation, and both may contribute to HSV-1 susceptibility of STAT3 knockout mice.

2.4 Discussion

In this study, we investigated the role of STAT3 in myeloid cells during HSV-1 infection. In vivo, *Stat3* knockout mice were more susceptible to HSV-1, as marked by shortened survival, higher viral loads in the brain and the spleen, and significant weight loss (Figure 2.2). Myeloid *Stat3* knockout mice are predisposed to develop chronic colitis at later ages (26), and this may complicate our interpretation of the significant weight loss in *Stat3* knockout mice. In agreement with the previous study, we found that knockout mice usually do not manifest symptoms of colitis until 16 weeks old or later. Using healthy mice at around 10 weeks old allowed us to avoid mice with pre-existing conditions, although we cannot rule out the possibility of HSV-1 infection triggering the onset of colitis and impeding the weight gain and recovery from acute HSV-1 infection. However, the fact that *Stat3* knockout mice also had significantly higher viral loads argues that the weight loss is associated with an aggravated disease resulting from impaired immune system that fails to restrain the virus from replicating and spreading.

Viral infections induce the production of type I interferons, namely IFNα and IFNβ. Type I interferons promote the expression of ISGs to establish an antiviral state by activating the transcription factors STAT1 and interferon-stimulated gene factor 3 (ISGF3), which is comprised of STAT1, STAT2, and interferon regulatory factor 9 (IRF9) (34). It has been shown that STAT3 negatively regulates type I interferon-induced ISGs by inhibiting STAT1 (49,50). Surprisingly, our data showed that STAT3 is required for optimal IFNα and ISG expression in the BMMs during HSV-1 infection (Figure 2.1B, 2.1L-M). While it is possible that STAT3 directly regulates the expression of ISGs in a positive manner during HSV-1 infection, it is more likely that reduced expression of ISGs is a result of diminished expression of IFNα. Type I interferon production usually occurs in two phases. In the first phase, viral infection activates IRF3 to

promote IFNβ expression. In the second phase, IFNβ induces the expression of IRF7, which in turn promotes IFNα expression and sustains IFNβ expression (34). We speculate that STAT3 primarily affects the second phase of interferon production, such as the activation of IRF7, since the production of IFNβ was normal in *Stat3* knockout BMMs (Figure 2.1K). Additionally, HSV-1-induced production of type I interferons is mediated by several different cellular sensing mechanisms (45,51-53). It is also possible that these sensing mechanisms are impaired in the absence of STAT3, resulting in diminished IFNα production. Apart from the impaired type I interferon response, *Stat3* knockout BMMs also highly express a subset of pro-inflammatory genes upon HSV-1 infection (Figure 2.1D-F). It has been shown that *Stat3* knockout BMMs have prolonged and heightened inflammatory response due to defective IL-10 signaling (26). Elevated expression of pro-inflammatory genes in *Stat3* knockout BMMs is presumably driven by hyper-activation of NF-κB. It has been shown that STAT3 keeps the activity of NF-κB in check by inhibiting the expression of a positive regulator of NF-κB (54) and by promoting the expression of a microRNA that suppresses NF-κB (55). Our data corroborated with previous studies by showing that the phosphorylation of IκBα and the expression of the classic NF-κB target gene TNFα were significantly increased in *Stat3* knockout BMMs (Figure 2.1B, 2.1D), suggesting an elevated NF-κB activity.

During systemic infection of HSV-1, *Stat3* knockout mice expressed less IFNα, IL-12 and TNFα in the spleen (Figure 2.4A, 2.4F-G). The antiviral effect of IFNα is well established (36). TNFα also inhibits HSV-1 replication in vitro (9). In vivo, TNFα protects mice from lethal herpes encephalitis (12), and IL-12 promotes the protective Th1 response against herpesvirus (11). Thus, dampened expression of IFNα, IL-12, and TNFα in the spleen may collectively contribute to the susceptibility of STAT3 knockout mice. The source of these cytokines,

however, remains to be determined. It has been shown that MMMΦ and MZMΦ are the major source of IFNα in the spleen during HSV-1 infection (14), and pDC, cDC, and other cell types are also capable of producing ample amount of IFNα when exposed to HSV-1 (45,51). Reduced expression of IL-12 in knockout mice may be due to reduced $CD8^+$ cDC population during HSV-1 infection, since $CD8^+$ cDCs are efficient IL-12 producers (44).

The role of neutrophils in viral infections ranges from protective to immunopathological (56). Early studies using Gr-1 antibody for neutrophil depletion suggested that infiltrating neutrophils suppress HSV-1 replication in cornea (21). However, Gr-1 is expressed by other groups of immune cells, and it was later revealed that non-neutrophil $Gr\text{-}1^+$ cells are primarily responsible for HSV-1 inhibition (57). Moreover, infiltrating neutrophils are a major mediator of HSV-1-induced immunopathology in the brain and the cornea (22,23), and CXCL2 promotes neutrophil chemotaxis to the site of infection during HSV-1 infection (58). Given that myeloid *Stat3* knockout mice have a significant expansion in neutrophil population, we originally speculated that increased neutrophil infiltration in the brain leads to aggravated symptoms. Nonetheless, both wild-type and *Stat3* knockout mice were devoid of $Ly6G^+$ neutrophil or $CD45^+$ hematopoietic cell infiltrates in the brain (Figure 2.3F), and CXCL2 expression level was indistinguishable between wild-type and knockout mice (Figure 2.3H), indicating that neutrophil-mediated immunopathology is not implicated in the susceptibility of *Stat3* knockout mice to HSV-1. The role of neutrophils in the spleen and the blood during systemic HSV-1 infection will require further investigation.

The effect of myeloid STAT3 knockout on DC differentiation (Figure 2.5) is minimal comparing to hematopoietic STAT3 knockout, which results in a drastic reduction in DC population (47). The majority of splenic DCs are from common myeloid progenitors (CMPs)

(59,60). Given that LysM-Cre is only moderately expressed in CMPs (61), the minor impacts of myeloid STAT3 deletion on DC differentiation can be explained by an incomplete deletion of STAT3 in CMPs. The reason for increased steady-state pDC population in our model is unclear. In fact, CD11c-Cre-mediated STAT3 knockout causes a reduction in pDC population (62). It has been shown that the immediate DC progenitors express high level of STAT3 but are CD11c negative, and they upregulate CD11c just prior to differentiating into distinct DC subsets (63). Thus, CD11c-Cre-mediated *Stat3* deletion would have occurred at the final stage of DC differentiation. In order to understand how STAT3 affects pDC differentiation, it will be of interest to compare how LysM-Cre and CD11c-Cre affect STAT3 expression in these immediate DC progenitors and the consequences of such perturbations. On the other hand, myeloid *Stat3* knockout mice have a reduction in $CD8^+$ cDC population during HSV-1 infection. It is possible that STAT3 facilitates the differentiation or proliferation of $CD8^+$ cDC in response to acute HSV-1 infection. However, given that myeloid STAT3 knockout does not affect the differentiation of steady-state $CD8^+$ cDCs, we speculate that STAT3 regulates the survival of $CD8^+$ cDCs during HSV-1 infection. Activated DCs are known to undergo apoptosis unless protected by TNFα (43) and HSV-1 also induces apoptosis in infected DCs (64). The reduction of splenic $CD8^+$ cDCs in *Stat3* knockout mice during HSV-1 infection is likely a result of reduced splenic TNFα and enhanced apoptosis.

DCs play a critical role in controlling HSV-1 pathogenesis by mediating NK and T cell activation, and mice depleted of DCs show higher mortality and higher viral loads in the nervous system (15). $CD8^+$ cDCs are unique in their ability to cross present viral antigens to CD8 T cells and promote CTL response against HSV-1 infection (20,48). We found that activation of NK cells was dampened in STAT3 knockout mice (Figure 2.6C). Impaired activation of NK cells

may be due to the combinatory effect of reduced $CD8^+$ cDCs and diminished IL-12 and IFNα expression, since IL-12 secreted by $CD8^+$ cDCs and IFNα both mediate NK cell activation during viral infection (18,65). Because we did not observe a difference in NK cytotoxicity in vitro (data not shown), it will be of interest to determine if NK cells from *Stat3* knockout mice are deficient in other aspects, such as cytokine production. We also noticed a minor decrease in CD8 T cell activation altitude at 2 dpi (Figure 2.6E). Whether this observation translates to compromised adaptive immunity to HSV-1 at the later stage of infection awaits further investigation. Interestingly, knockout mice also showed a moderate reduction in the steady-state NK cell population (Figure 2.6B). It is unclear why myeloid *Stat3* deletion leads to reduction of NK cells, since NK cells are generally believed to arise from the lymphoid lineage (66). However, it has been recently reported that myeloid precursors are capable of differentiating into NK cells (67,68), thereby raising possible implications of myeloid STAT3 in NK cell development.

In conclusion, our data showed that myeloid-specific *Stat3* deletion causes defects in multiple aspects of the innate immune system in response to HSV-1. While individual defects may not change the outcome of infection, collectively they result in higher susceptibility of *Stat3* knockout mice to HSV-1. Future studies will be focusing on the mechanisms with respect to each defect, such as the mechanism by which STAT3 modulates IFNα production. The impact of impaired innate immunity on adaptive immunity-mediated control of HSV-1 infection and reactivation will be another interesting area for investigation.

2.5 Materials and Methods

Animals. This study was performed under protocols approved by Institutional Animal Care and Use Committee guidelines of the University of North Carolina Chapel Hill. Mice were kept and bred in sterile facilities under conditions in accordance with NIH Guide for the Care and Use of Laboratory Animals and UNC IACUC guidelines. *Stat3*$^{fl/fl}$ and LysM-Cre C57BL/6 mice were obtained from the Jackson laboratory. Mice were bred to each other to generate myeloid-specific STAT3 knockout mice. Eight to 12-week old animals were used for HSV-1 infection studies. For infections, mice were intravenously injected via the tail vein with HSV-1 (KOS strain) and monitored one to three times daily after injection. To collect tissues for molecular studies, mice were euthanized by CO_2 followed by cervical dislocation. For survival studies, mice lost more than 20% of original weight were immediately euthanized, while all other mice were euthanized at the end of the study.

Virus, cells, and plaque assay. Vero cells (ATCC) were propagated in DMEM with 10% FBS. HSV-1 (KOS strain) was amplified on Vero cells. Three days post-infection, supernatants were harvested and centrifuged at 2500 rpm to remove cell debris. The supernatants were then ultracentrifuged at 25,000 rpm to concentrate the virus. Virus pellets were resuspended in plain DMEM. To isolate bone marrow-derived macrophages (BMMs), bone marrows were collected from the femur and tibia of age- and sex-matched 8-10 weeks old mice. The cells were cultured in RPMI 1640 with 10% FBS and 10% L929-conditioned media. After 5-6 days of culture, the adherent cells contained about 95% F4/80-positive macrophages as determined by flow cytometry. BMMs were infected with HSV-1 at a multiplicity of infection (MOI) = 3, incubated at 37°C for 30 min, washed with DMEM twice, and cultured in DMEM with 2% FBS. Infectious viral titer was determined by plaque assay using Vero cells. Supernatants from

infected macrophages were serial-diluted in DMEM before infecting confluent Vero cells for 1 hour at 37°C, after which the supernatants were replaced with DMEM with 1% of methylcellulose and 2% of serum. Three technical replicates were prepared for each dilution. Infected Vero cells were kept at 37°C with 5% CO_2 for 72 hours before staining with 0.5% crystal violet in 50% ethanol to reveal the plaques. Titers were shown as plaque-forming unit (pfu) per ml.

Quantitative real-time PCR. Total RNA from the cultured macrophages or mouse tissues were purified using QIAGEN RNeasy Plus kit according to manufacturer's protocol. One to 2 μg of RNA was used to synthesize cDNA using M-MLV reverse transcriptase (Life Technologies, Carlsbad, CA, USA). For gene expression assay, standard TaqMan probes, primers, and reagents were used (Thermo Fisher, Walthem, MA, USA). To determine the relative genomic copy number of HSV-1 in mouse tissues, real-time PCR was performed using Maxima SYBR green master mix (Thermo Fisher) with the following primers: *Actb* forward: 5'-GGCTGTATTCCCCTCCATCG-3'; *Actb* reverse: 5'-CCAGTTGGTAACAATGCCATGT-3'; HSV-1 *pol* forward: 5'-CATCACCGACCCGGAGAGGGAC-3'; HSV-1 *pol* reverse: 5'-GGGCCAGGCGCTTGTTGGTGTA-3'.

Immunoblotting. Cells or tissues were lysed in RIPA buffer (10 mM Tris pH 8.0, 1 mM EDTA, 1 mM EGTA, 1% Triton X-100, 0.1% sodium deoxycholate, 0.1% SDS, 140 mM NaCl) with a protease inhibitor cocktail (Promega, Madison, WI, USA) and a phosphatase inhibitor cocktail (Sigma, St. Louis, MO, USA). Lysates were centrifuged to remove cell debris, and the supernatant were mixed with LDS loading buffer (Life Technologies) containing 100 mM DTT and heated before running SDS-PAGE with bis-tris NuPAGE gel and MOPS buffer (Life Technologies). Proteins were transferred onto 0.45 μm PVDF membrane, blocked with 5% milk

in TBST, and incubated in primary antibodies at the dilution of 1:500 to 1:2000 in 5% milk in TBST overnight. Blots were then washed and incubated in the appropriate HRP-conjugated secondary antibodies (Promega). Chemiluminescence substrate (Thermo Fisher) was used for film exposure. STAT1 (#9172), p-STAT1 (#9167), STAT3 (#9139), p-STAT3 (#9145), ISG15 (#2758), p-p65 (#3033), p65 (#3034), p-IκBα (#9246), and IκBα (#4812) antibodies were from Cell Signaling Technology (Danvers, MA, USA).

Flow cytometry. Mice were euthanized to collect the spleens and bone marrows. Spleens were mashed using syringe plungers and 100 μm cell strainers. The cells were resuspended in FACS buffer (3% FBS, 1mM EDTA in PBS), passed through 40 μm cell strainer, and red blood cells were lysed by ACK buffer (150 mM NH_4Cl, 10 mM $KHCO_3$, 0.1 mM EDTA). The white blood cell suspensions were blocked with anti-mouse CD16/CD32 antibody (eBioscience14-0161-86) at 1:100 dilution for 30 minutes before being stained with the appropriate primary and secondary antibodies for 1 hour each at 1:100 dilution in FACS buffer. CD8-FITC (11-0081-81), CD4-PE (12-0042-81), CD19-PE-Cy7 (250193-81), CD3-APC (17-0032-82), F4/80-Alexa488 (53-4801-82), CD11b-PE-Cy7 (250112-82), CD11c-APC (17-0114-82), CD209-PE (12-2091-82), and streptavidin-eF450 (48-4317-82) antibodies were from eBioscience (San Diego, CA, USA). Ly6G-PE (108407), Ly6C-APC (128015), B220-biotin (103204), CD169-PE-Cy7 (142412), CD69-APC (104513), and NK1.1-PE-Cy7 (108713) antibodies were from BioLegend (San Diego, CA, USA). Flow cytometry was carried out on a CyAn machine and analyzed by FlowJo.

Immunohistochemistry. Mouse tissues were fixed in 10% buffered formalin for 24 hours, washed with PBS three times, and incubated in 30%, 50%, and 70% ethanol for 30 minutes each. Fixed tissues were embedded in paraffin and sectioned into slices.

Immunohistochemistry was carried out with Bond immunostainer (Leica Biosystems Inc. Norwell, MA). Slides were dewaxed in Bond dewax solution (AR9222) and hydrated in Bond wash solution (AR9590). Antigen retrieval was performed for 30 min at 100ºC in Bond-Epitope Retrieval solution1 pH-6.0 (AR9961) followed by a 10-minute protein block (#X0909, DAKO, Carpineria, CA). Rodent block M reagent (# RB961G, Biocare Medical, Concord, CA) was applied for 20 min only to STAT3 slides. After pretreatment, slides were incubated for 30 min with CD45 and Ly-6G (Abcam #25386, #25337) antibodies at 1:100 and 1:200 dilution respectively, and for 1h with STAT3 (Cell Signaling #9139) antibody at 1:750 dilution. Detection of all antibodies was performed using Bond™ Polymer Refine Detection (DS9900), and for CD45 and Ly-6G the secondary antibody from the kit was replaced with ImmPRESS HRP Anti-Rat Ig (#MP-7444-15, Vector Labs, Burlingame, CA). Stained slides were dehydrated and coverslipped. Positive and negative controls (no primary antibody) were also performed for each antibody to ensure the specificity of staining.

Statistical analyses. Three to five technical replicates were used for each data point. Data points were shown as mean with standard deviation, and two-tailed Student's t-test was used to calculate p-value and significance unless otherwise noted.

Table 2.1 Cellular composition of the spleen[a]

	WT (n=3)	KO (n=3)
Myeloid cells[b]	12.3 ± 4.7	11.8 ± 2.6
Neutrophils[c] (% myeloid)	16.9 ± 5.9	19.6 ± 7.4
Ly6C^{hi} monocytes[d] (% myeloid)	28.7 ± 2.0	32.6 ± 10.5
Ly6C^{lo} monocytes[e] (% myeloid)	51.9 ± 7.6	45.3 ± 17.9
Red pulp macrophages[f]	2.42 ± 0.40	2.77 ± 0.12
Marginal zone macrophages[g]	0.24 ± 0.03	0.28 ± 0.08
Marginal metallophilic macrophages[h]	0.40 ± 0.11	0.51± 0.18
B cells[i]	56.7 ± 4.2	51.6 ± 3.2
T cells[j]	26.4 ± 1.0	27.4 ± 5.7
CD4$^+$ T cells[k] (% T cells)	50.6 ± 3.5	52.7 ± 3.4
CD8$^+$ T cells[l] (% T cells)	41.3 ± 1.7	39.0 ± 1.7

[a] All numbers are expressed as percent of total cells except where noted.
[b] CD11b$^+$
[c] CD11b$^+$ Ly6G$^+$ Ly6C$^+$
[d] CD11b$^+$ Ly6G$^-$ Ly6C$^+$
[e] CD11b$^+$ Ly6G$^-$ Ly6C^{lo}
[f] CD11b^{lo} F4/80$^+$
[g] CD11c$^-$ CD209$^+$
[h] CD11c$^-$ CD169$^+$
[i] CD19$^+$
[j] CD3$^+$
[k] CD3$^+$ CD4$^+$
[l] CD3$^+$ CD8$^+$

Table 2.2 Cellular composition of the bone marrow[a].

	WT (n=3)	KO (n=2)
Granulocytes[b]	54.8 ± 1.2	68.2 ± 4.5 *
Myeloid cells[c]	45.7 ± 0.8	58.9 ± 6.2 *
Neutrophils[d]	27.9 ± 0.3	40.4 ± 5.0 *
Neutrophils (% Myeloid cells)	61.3 ± 1.2	68.6 ± 1.3 **
Macrophages[e]	1.3 ± 0.2	1.1 ± 0.5
$Ly6C^{hi}$ monocytes[f]	5.3 ± 0.4	6.4 ± 0.3 *
$Ly6C^{lo}$ monocytes[g]	10.2 ± 0.8	10.2 ± 0.9

[a] All numbers are expressed as percent of total cells except where noted.
[b] SSC^{hi}
[c] $CD11b^{+}$
[d] $CD11b^{+}$ $Ly6G^{+}$ $Ly6C^{+}$
[e] $CD11b^{lo}$ $F4/80^{+}$
[f] $CD11b^{+}$ $Ly6G^{-}$ $Ly6C^{hi}$
[g] $CD11b^{+}$ $Ly6G^{-}$ $Ly6C^{lo}$
*$p<0.05$; **$p<0.01$

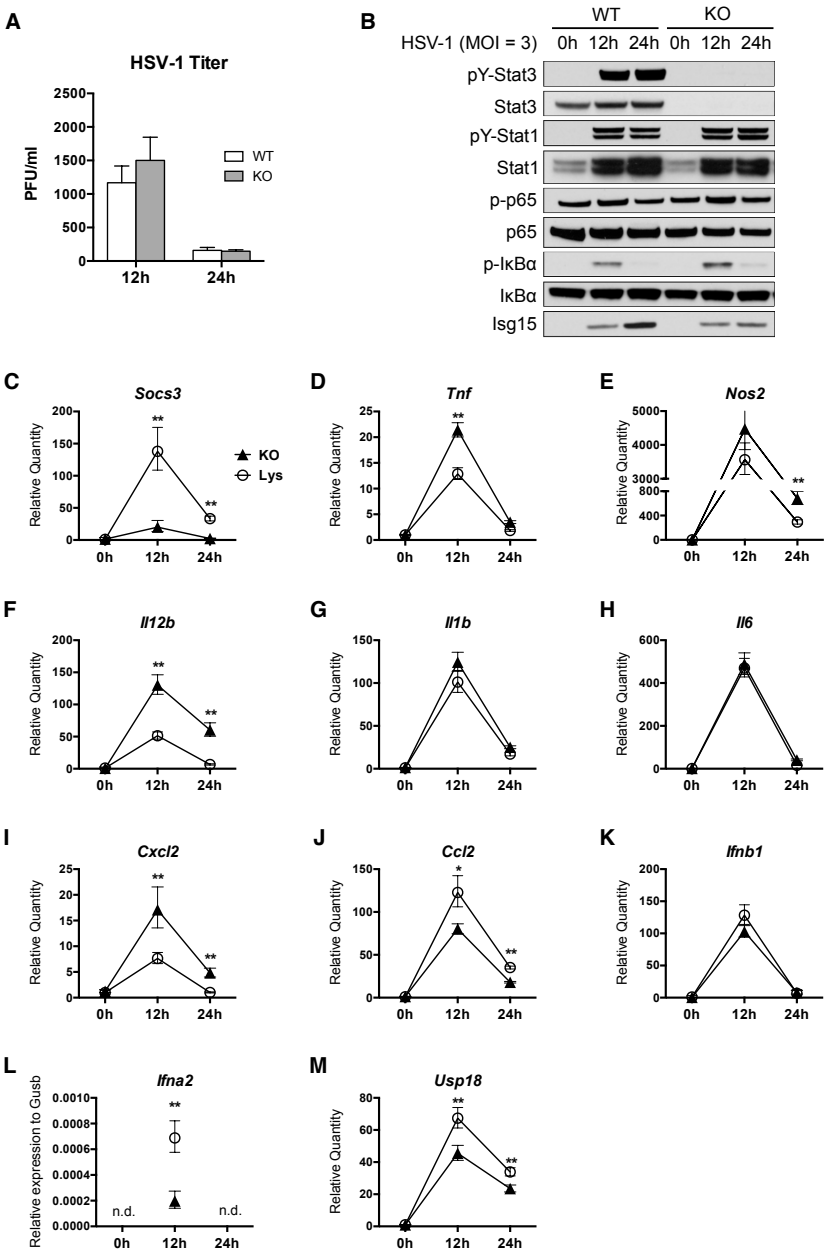

Figure 2.1 STAT3 knockout BMMs show attenuated type I interferon response to HSV-1 infection

WT or STAT3 KO BMMs were infected with HSV-1 at MOI=3. (A) Viral titer in the supernatants at 12 and 24 hpi was determined by plaque assay on Vero cells with three technical replicates. (B) Western blotting of lysates from HSV-1 infected BMMs at the indicated time-points. (C-M) Gene expression of HSV-1 infected BMMs was determined by qRT-PCR with three technical replicates for each sample. All values were normalized to *Gusb* and compared to the expression of WT BMMs at 0h except for IFNα, which was shown as relative expression to *Gusb*. All values were shown as mean with 95% confidence intervals. Statistical significance was determined by Student's t-test. *p<0.05. **p<0.01. N.d.= not determined (below detection threshold).

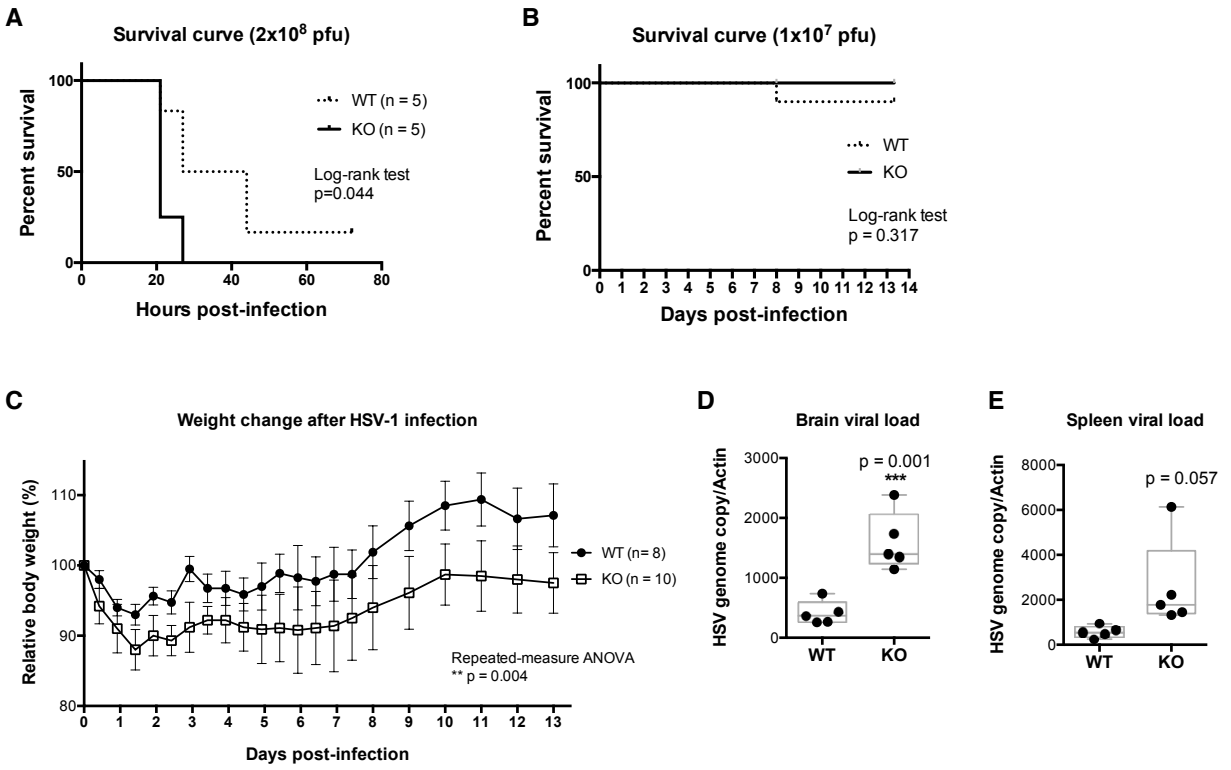

Figure 2.2 Myeloid STAT3 knockout mice are more susceptible to HSV-1 infection
(A) Five sex- and age-matched WT or KO mice were intravenously injected with $2x10^8$ pfu of HSV-1. Survival of infected mice was monitored three times daily. Statistical analysis was done by log-rank test. (B) Ten sex- and age-matched WT or KO mice were intravenously injected with $1x10^7$ pfu of HSV-1. Survival of infected mice was monitored and analyzed as described in (A). (C) Sex- and age-matched WT or KO mice were intravenously injected with $1x10^7$ pfu of HSV-1. Each mouse was weighted immediately before infection and twice daily after infection. All measurements were normalized to the starting weight of each mouse and expressed as a percentage of the starting weight. Statistical analysis was done by repeated measurement ANOVA using PRISM (GraphPad). (D-E) Five mice of each genotype were infected as described in (C) and sacrificed at 2 dpi. HSV-1 viral loads in the brain or the spleen were determined by qRT-PCR with three technical replicates for each mouse. Data were shown as HSV-1 copy number relative to mouse *Actb* expression. Statistical significance was determined by Student's t-test. **p<0.01

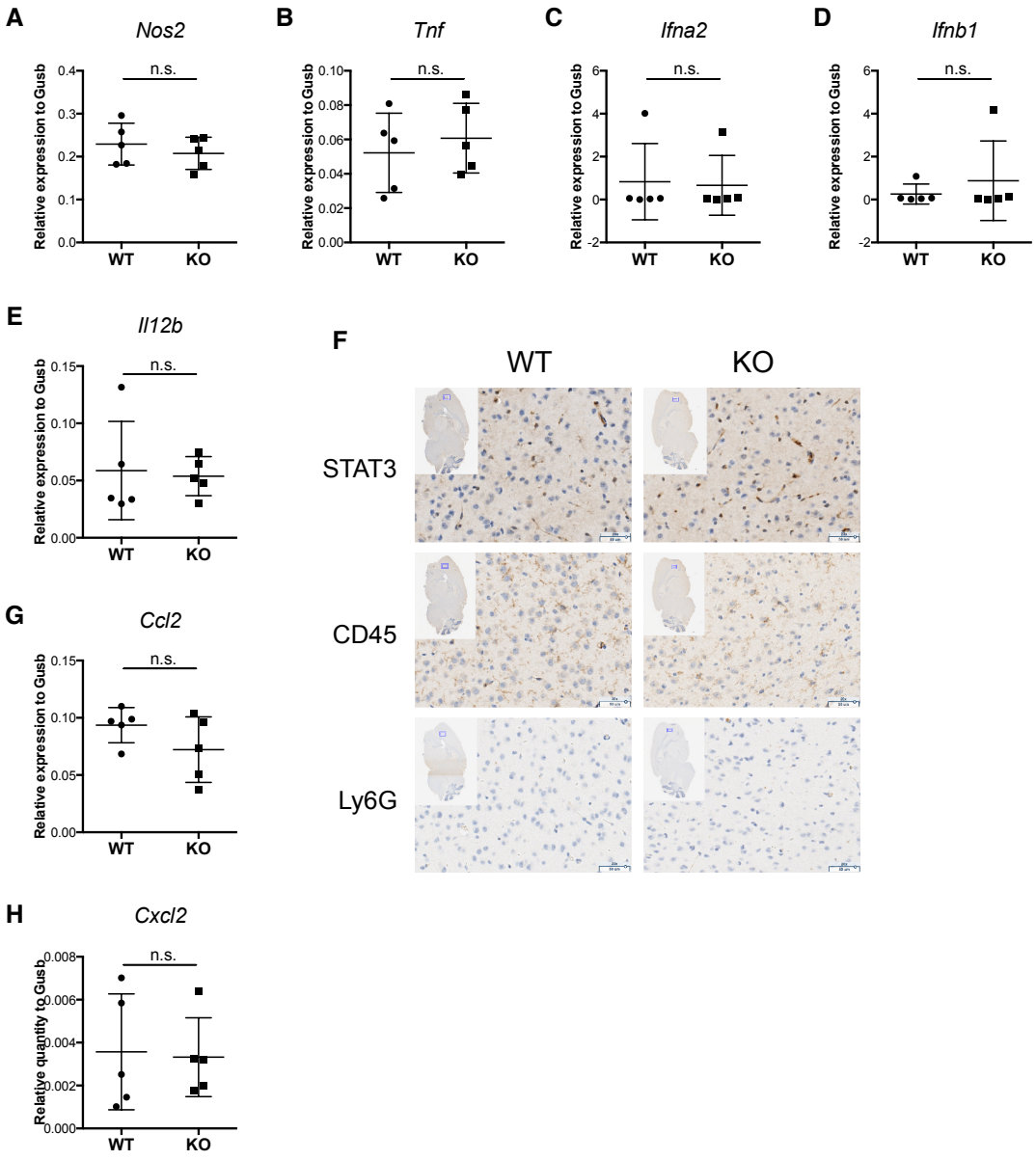

Figure 2.3 Susceptibility of STAT3 knockout mice is not caused by immunopathology in the brain

WT or KO mice were intravenously injected with $1x10^7$ pfu of HSV-1 as described in Figure 3. Five mice of each genotype were sacrificed at 2 dpi to collect the brains. (A-E) Relative expression of iNOS, TNFα, IFNα, IFNβ, IL-12 in the brain was determined by qRT-PCR with three technical replicates for each mouse. All values were normalized to *Gusb* expression and shown as mean with 95% confidence intervals. Statistical analysis was done by Student's t-test. N.s. = not significant (F) Brain hemispheres from WT or KO mice sacrificed at 2 dpi were fixed and stained with STAT3, CD45, or Ly6G antibodies as described in Materials and Methods. Microglia showed low levels of CD45 staining. Representative figures from each genotype were shown. (G-H) Relative expression of CCL2 and CXCL2 in the brain was determined by qRT-PCR as mentioned above.

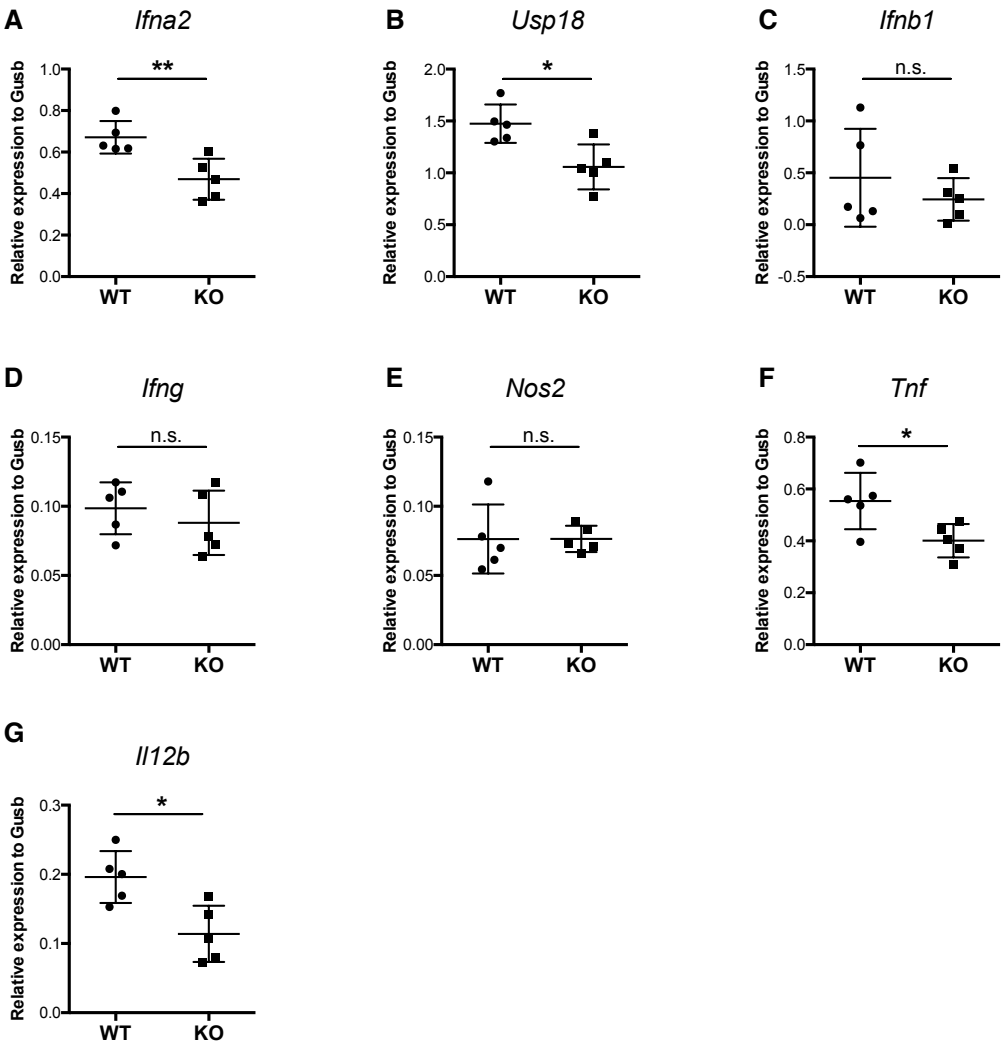

Figure 2.4 STAT3 knockout mice express reduced levels of antiviral cytokines in the spleen
WT or KO mice were infected as described in Figure 3. Five mice of each genotype were sacrificed at 2 dpi to collect the spleens. (A-H) Expression of IFNα, USP18, IFNβ, IFNγ, iNOS, TNFα, and IL-12 in the spleen was determined by qRT-PCR with three technical replicates for each mouse. All values were normalized to *Gusb* expression and shown as mean with 95% confidence intervals. Statistical analysis was done by t-test. **$p<0.01$. *$p<0.05$. N.s. = not significant.

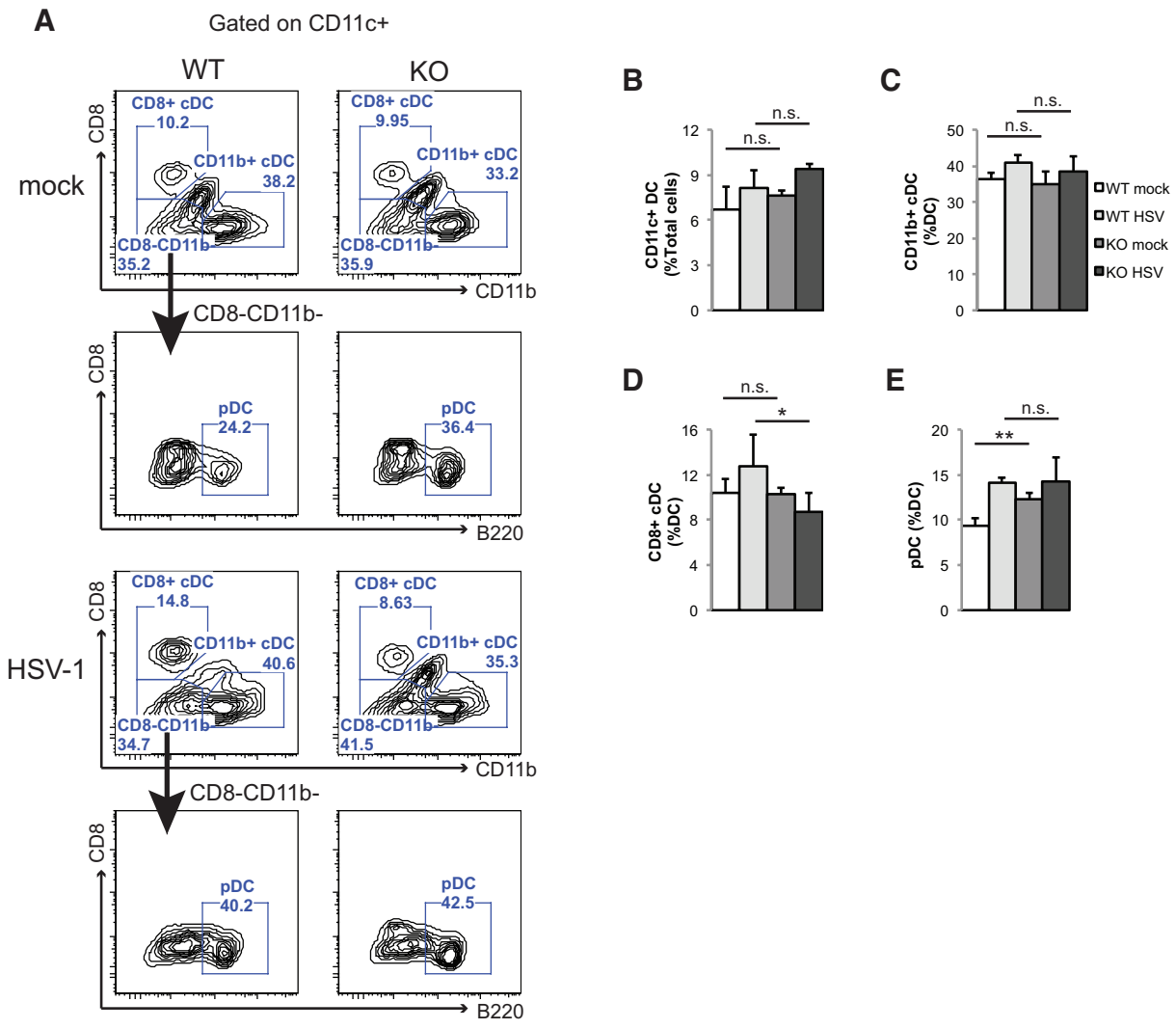

Figure 2.5 STAT3 knockout mice have decreased CD8$^+$ cDC frequency during HSV-1 infection

Sex- and age-mached WT or KO mice were infected with 1x10^7 pfu of HSV-1 by tail vein injection. Mock-infected WT (N=3) and KO mice (N=3), and infected WT (N=5) and KO mice (N=4) were sacrificed at 2 dpi, and splenic cells were collect for flow cytometry analysis. (A) Splenic cells were gated on CD11c$^+$ followed by CD8, CD11b, and B220 analyses to determine the percentage of CD8$^+$ cDC (CD11c$^+$ CD8$^+$ CD11b$^-$), CD11b$^+$ cDC (CD11c$^+$ CD8$^-$ CD11b$^+$), and pDC (CD11c$^+$ CD8$^-$ CD11b$^-$ B220$^+$) populations. Representative figures from one mouse of each group were shown here. (B-E) Results summarized the percentage of total DC, CD11b$^+$ cDC, CD8$^+$ cDC, and pDC from flow analysis. Data were shown as mean with standard deviation. Statistical analysis was done by Student's t-test. *p<0.05. **p<0.01.

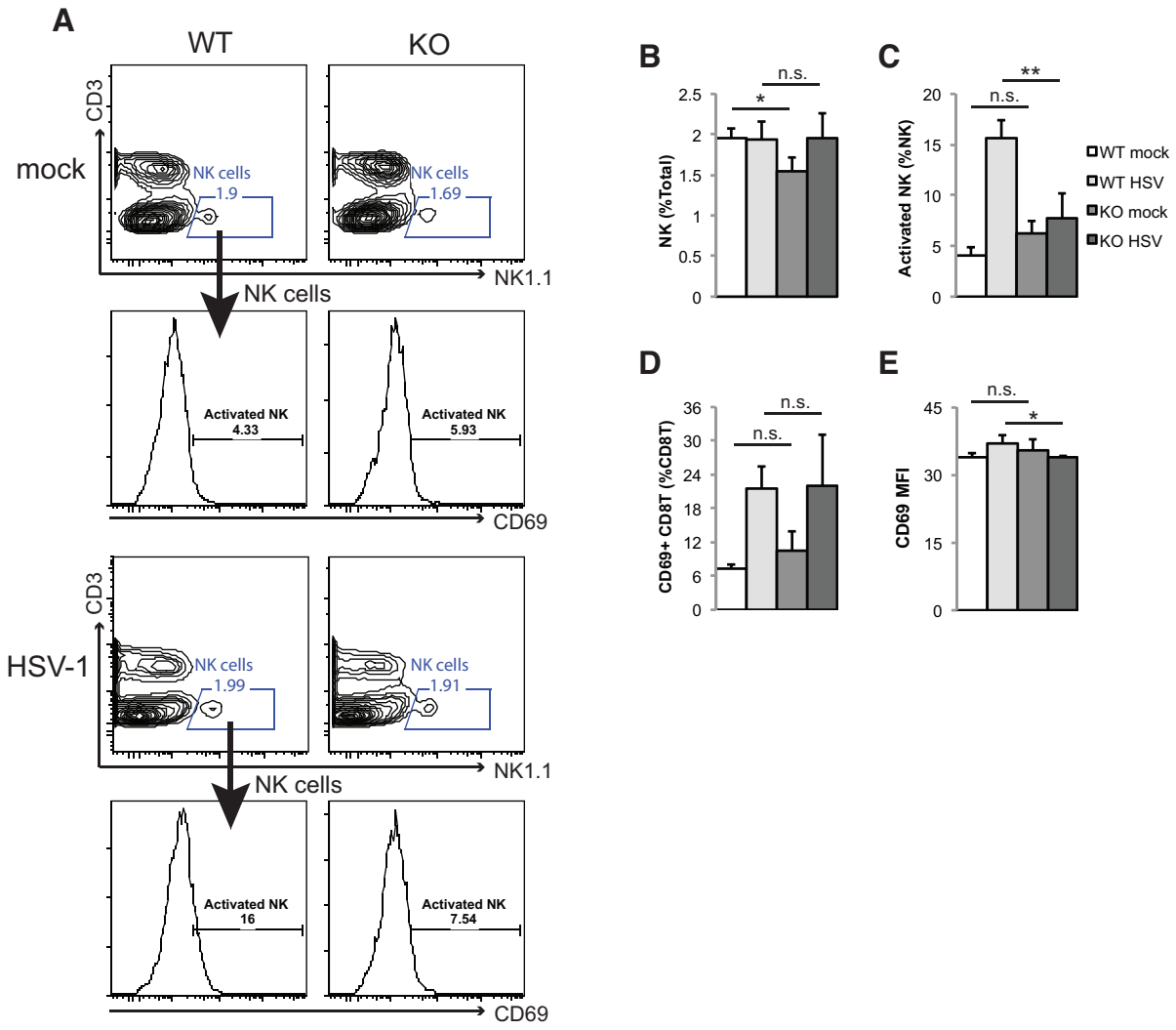

Figure 2.6 STAT3 knockout mice have impaired NK and T cell activation during HSV-1 infection

WT and KO mice were infected and sacrificed for flow cytometry analysis as described in Figure 6. (A) Representative figures of one mouse from each group were shown. NK cells in the spleen were defined by $CD3^{-}$ $NK1.1^{+}$ gate. Activated NK cells were further gated by $CD69^{+}$ staining. (B-C) Results summarized the percentage of total NK and activated NK cells. (D) Results summarized the percentage of activated CD8 T cells ($CD3^{+}$ $CD8^{+}$ $CD69^{+}$) in the spleen. (E) The mean fluorescence intensity (MFI) of CD69 was calculated from activated CD8 T cells defined in (D). Data were shown as mean with standard deviation. Statistical analysis was done by Student's t-test. * $p<0.05$. ** $p<0.01$.

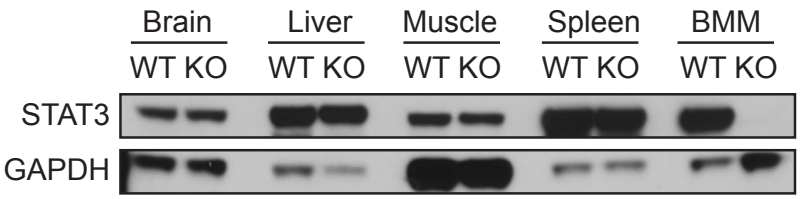

Supplemental Figure 2.1 Myeloid-specific deletion of STAT3
Tissues from WT and KO mice were homogenized in RIPA buffer, while BMMs were lysed in RIPA buffer. The lysates were subjected to western blotting to determine the levels of STAT3

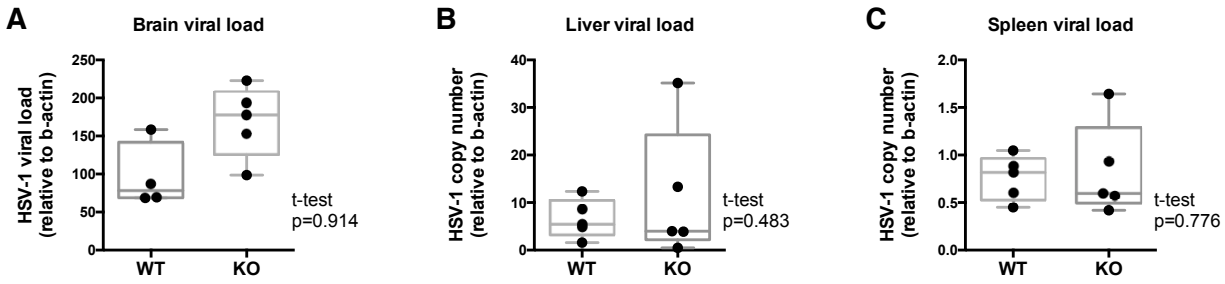

Supplemental Figure 2.2 KO mice showed marginally higher viral loads in the brain
Five sex- and age-matched WT and KO mice were intravenously injected with $2x10^8$ pfu of HSV-1. The brains (A), livers (B), and spleencs (C) were collected postmortem to determine HSV-1 viral loads by qRT-PCR with three technical replicates per mouse. Data were shown as HSV-1 copy number relative to mouse *Actb* expression. Statistical significance was determined by Student's t-test.

REFERENCES

1. Whitley RJ, Roizman B. Herpes simplex virus infections. The Lancet. 2001 May;357(9267):1513–8.

2. Zuckerman RA. The Clinical Spectrum of Herpes Simplex Viremia. Clin Infect Dis. 2009 Nov;49(9):1302–4.

3. Youssef R, Shaker O, Sobeih S, Mashaly H, Mostafa WZ. Detection of herpes simplex virus DNA in serum and oral secretions during acute recurrent herpes labialis. J Dermatol. 2002 Jul;29(7):404–10.

4. Howie S, Norval M, Maingay J, McBride WH. Interactions between herpes simplex virus and murine bone marrow macrophages. Arch Virol. 1986;87(3-4):229–39.

5. Morahan PS, Mama S, Anaraki F, Leary K. Molecular localization of abortive infection of resident peritoneal macrophages by herpes simplex virus type 1. J Virol. 1989 May;63(5):2300–7.

6. Zisman B, Hirsch MS, Allison AC. Selective effects of anti-macrophage serum, silica and anti-lymphocyte serum on pathogenesis of herpes virus infection of young adult mice. J Immunol. 1970 May;104(5):1155–9.

7. Mott K, Brick DJ, van Rooijen N, Ghiasi H. Macrophages are important determinants of acute ocular HSV-1 infection in immunized mice. Invest Ophthalmol Vis Sci. 2007 Dec;48(12):5605–15.

8. Hirsch MS, Zisman B, Allison AC. Macrophages and age-dependent resistance to Herpes simplex virus in mice. J Immunol. 1970 May;104(5):1160–5.

9. Kodukula P, Liu T, Rooijen NV, Jager MJ, Hendricks RL. Macrophage control of herpes simplex virus type 1 replication in the peripheral nervous system. J Immunol. 1999 Mar 1;162(5):2895–905.

10. Croen KD. Evidence for antiviral effect of nitric oxide. Inhibition of herpes simplex virus type 1 replication. J Clin Invest. 1993 Jun;91(6):2446–52.

11. Sin JI, Kim JJ, Arnold RL, Shroff KE, McCallus D, Pachuk C, et al. IL-12 gene as a DNA vaccine adjuvant in a herpes mouse model: IL-12 enhances Th1-type CD4+ T cell-mediated protective immunity against herpes simplex virus-2 challenge. J Immunol. 1999 Mar 1;162(5):2912–21.

12. Lundberg P, Welander PV, Edwards CK, van Rooijen N, Cantin E. Tumor necrosis factor (TNF) protects resistant C57BL/6 mice against herpes simplex virus-induced encephalitis independently of signaling via TNF receptor 1 or 2. J Virol. 2007 Feb;81(3):1451–60.

13. MacLean A, Wei XQ, Huang FP, Al-Alem UA, Chan WL, Liew FY. Mice lacking inducible nitric-oxide synthase are more susceptible to herpes simplex virus infection

despite enhanced Th1 cell responses. J Gen Virol. 1998 Apr;79:825–30.

14. Eloranta ML, Alm GV. Splenic marginal metallophilic macrophages and marginal zone macrophages are the major interferon-alpha/beta producers in mice upon intravenous challenge with herpes simplex virus. Scand J Immunol. 1999 Apr;49(4):391–4.

15. Kassim SH, Rajasagi NK, Zhao X, Chervenak R, Jennings SR. In vivo ablation of CD11c-positive dendritic cells increases susceptibility to herpes simplex virus type 1 infection and diminishes NK and T-cell responses. J Virol. 2006 Apr;80(8):3985–93.

16. Yoneyama H, Matsuno K, Toda E, Nishiwaki T, Matsuo N, Nakano A, et al. Plasmacytoid DCs help lymph node DCs to induce anti-HSV CTLs. J Exp Med. 2005 Aug 1;202(3):425–35.

17. Swiecki M, Wang Y, Gilfillan S, Colonna M. Plasmacytoid dendritic cells contribute to systemic but not local antiviral responses to HSV infections. PLoS Pathog. 2013 Oct;9(10):e1003728.

18. Andrews DM, Scalzo AA, Yokoyama WM, Smyth MJ, Degli-Esposti MA. Functional interactions between dendritic cells and NK cells during viral infection. Nat Immunol. 2002 Dec 23;4(2):175–81.

19. Hildner K, Edelson BT, Purtha WE, Diamond M, Matsushita H, Kohyama M, et al. Batf3 deficiency reveals a critical role for CD8alpha+ dendritic cells in cytotoxic T cell immunity. Science. 2008 Nov 14;322(5904):1097–100.

20. Belz GT, Smith CM, Eichner D, Shortman K, Karupiah G, Carbone FR, et al. Cutting Edge: Conventional CD8 + Dendritic Cells Are Generally Involved in Priming CTL Immunity to Viruses. J Immunol. 2004 Feb 5;172(4):1996–2000.

21. Tumpey TM, Chen SH, Oakes JE, Lausch RN. Neutrophil-mediated suppression of virus replication after herpes simplex virus type 1 infection of the murine cornea. J Virol. 1996 Feb;70(2):898–904.

22. Yan XT, Tumpey TM, Kunkel SL, Oakes JE, Lausch RN. Role of MIP-2 in neutrophil migration and tissue injury in the herpes simplex virus-1-infected cornea. Invest Ophthalmol Vis Sci. 1998 Sep;39(10):1854–62.

23. Marques CP, Cheeran MC-J, Palmquist JM, Hu S, Urban SL, Lokensgard JR. Prolonged microglial cell activation and lymphocyte infiltration following experimental herpes encephalitis. J Immunol. 2008 Nov 1;181(9):6417–26.

24. Yu H, Pardoll D, Jove R. STATs in cancer inflammation and immunity: a leading role for STAT3. Nat Rev Cancer. 2009 Nov;9(11):798–809.

25. Du T, Zhou G, Roizman B. Modulation of reactivation of latent herpes simplex virus 1 in ganglionic organ cultures by p300/CBP and STAT3. Proc Natl Acad Sci USA. 2013 Jul 9;110(28):E2621–8.

26. Takeda K, Clausen BE, Kaisho T, Tsujimura T, Terada N, Förster I, et al. Enhanced Th1 activity and development of chronic enterocolitis in mice devoid of Stat3 in macrophages and neutrophils. Immunity. 1999 Jan;10(1):39–49.

27. Matsukawa A, Kudo S, Maeda T, Numata K, Watanabe H, Takeda K, et al. Stat3 in resident macrophages as a repressor protein of inflammatory response. J Immunol. 2005 Sep 1;175(5):3354–9.

28. Lee C-K, Raz R, Gimeno R, Gertner R, Wistinghausen B, Takeshita K, et al. STAT3 is a negative regulator of granulopoiesis but is not required for G-CSF-dependent differentiation. Immunity. 2002 Jul;17(1):63–72.

29. Panopoulos AD, Zhang L, Snow JW, Jones DM, Smith AM, Kasmi El KC, et al. STAT3 governs distinct pathways in emergency granulopoiesis and mature neutrophils. Blood. 2006 Dec 1;108(12):3682–90.

30. Matsukawa A, Takeda K, Kudo S, Maeda T, Kagayama M, Akira S. Aberrant inflammation and lethality to septic peritonitis in mice lacking STAT3 in macrophages and neutrophils. J Immunol. 2003 Dec 1;171(11):6198–205.

31. Clausen BE, Burkhardt C, Reith W, Renkawitz R, Förster I. Conditional gene targeting in macrophages and granulocytes using LysMcre mice. Transgenic Res. 1999 Aug;8(4):265–77.

32. Suzuki A, Hanada T, Mitsuyama K, Yoshida T, Kamizono S, Hoshino T, et al. CIS3/SOCS3/SSI3 plays a negative regulatory role in STAT3 activation and intestinal inflammation. J Exp Med. 2001 Feb 19;193(4):471–81.

33. Nguyen-Jackson H, Panopoulos AD, Zhang H, Li HS, Watowich SS. STAT3 controls the neutrophil migratory response to CXCR2 ligands by direct activation of G-CSF-induced CXCR2 expression and via modulation of CXCR2 signal transduction. Blood. 2010 Apr 22;115(16):3354–63.

34. Ivashkiv LB, Donlin LT. Regulation of type I interferon responses. Nat Rev Immunol. 2014 Jan;14(1):36–49.

35. Heise MT, Virgin HW. The T-cell-independent role of gamma interferon and tumor necrosis factor alpha in macrophage activation during murine cytomegalovirus and herpes simplex virus infections. J Virol. 1995 Feb;69(2):904–9.

36. Sainz B, Halford WP. Alpha/Beta interferon and gamma interferon synergize to inhibit the replication of herpes simplex virus type 1. J Virol. 2002 Nov;76(22):11541–50.

37. Lokensgard JR, Hu S, Sheng W, vanOijen M, Cox D, Cheeran MC, et al. Robust expression of TNF-alpha, IL-1beta, RANTES, and IP-10 by human microglial cells during nonproductive infection with herpes simplex virus. J Neurovirol. 2001 Jun;7(3):208–19.

38. Aravalli RN, Hu S, Rowen TN, Palmquist JM, Lokensgard JR. Cutting Edge: TLR2-

Mediated Proinflammatory Cytokine and Chemokine Production by Microglial Cells in Response to Herpes Simplex Virus. J Immunol. 2005 Sep 21;175(7):4189–93.

39. Marques CP, Hu S, Sheng W, Lokensgard JR. Microglial cells initiate vigorous yet non-protective immune responses during HSV-1 brain infection. Virus Research. 2006 Oct;121(1):1–10.

40. Cho I-H, Hong J, Suh EC, Kim JH, Lee H, Lee JE, et al. Role of microglial IKKbeta in kainic acid-induced hippocampal neuronal cell death. Brain. 2008 Nov;131(Pt 11):3019–33.

41. Lundberg P, Ramakrishna C, Brown J, Tyszka JM, Hamamura M, Hinton DR, et al. The Immune Response to Herpes Simplex Virus Type 1 Infection in Susceptible Mice Is a Major Cause of Central Nervous System Pathology Resulting in Fatal Encephalitis. J Virol. 2008 Jun 26;82(14):7078–88.

42. Kurt-Jones EA, Chan M, Zhou S, Wang J, Reed G, Bronson R, et al. Herpes simplex virus 1 interaction with Toll-like receptor 2 contributes to lethal encephalitis. Proc Natl Acad Sci USA. 2004 Feb 3;101(5):1315–20.

43. Lehner M, Kellert B, Proff J, Schmid MA, Diessenbacher P, Ensser A, et al. Autocrine TNF Is Critical for the Survival of Human Dendritic Cells by Regulating BAK, BCL-2, and FLIPL. J Immunol. 2012 May 3;188(10):4810–8.

44. Hochrein H, Shortman K, Vremec D, Scott B, Hertzog P, O'Keeffe M. Differential production of IL-12, IFN-alpha, and IFN-gamma by mouse dendritic cell subsets. J Immunol. 2001 May 1;166(9):5448–55.

45. Krug A, Luker GD, Barchet W, Leib DA, Akira S, Colonna M. Herpes simplex virus type 1 activates murine natural interferon-producing cells through toll-like receptor 9. Blood. 2004 Feb 15;103(4):1433–7.

46. Farrand KJ, Dickgreber N, Stoitzner P, Ronchese F, Petersen TR, Hermans IF. Langerin+CD8 + Dendritic Cells Are Critical for Cross-Priming and IL-12 Production in Response to Systemic Antigens. J Immunol. 2009 Dec 9;183(12):7732–42.

47. Laouar Y, Welte T, Fu X-Y, Flavell RA. STAT3 is required for Flt3L-dependent dendritic cell differentiation. Immunity. 2003 Dec;19(6):903–12.

48. Smith CM, Belz GT, Wilson NS, Villadangos JA, Shortman K, Carbone FR, et al. Cutting Edge: Conventional CD8 + Dendritic Cells Are Preferentially Involved in CTL Priming After Footpad Infection with Herpes Simplex Virus-1. J Immunol. 2003 May 1;170(9):4437–40.

49. Ho HH, Ivashkiv LB. Role of STAT3 in type I interferon responses. Negative regulation of STAT1-dependent inflammatory gene activation. J Biol Chem. 2006 May 19;281(20):14111–8.

50. Wang WB, Levy DE, Lee CK. STAT3 Negatively Regulates Type I IFN-Mediated Antiviral Response. J Immunol. 2011 Aug 19;187(5):2578–85.

51. Hochrein H, Schlatter B, O'Keeffe M, Wagner C, Schmitz F, Schiemann M, et al. Herpes simplex virus type-1 induces IFN-alpha production via Toll-like receptor 9-dependent and -independent pathways. Proc Natl Acad Sci USA. 2004 Aug 3;101(31):11416–21.

52. Thompson MR, Sharma S, Atianand M, Jensen SB, Carpenter S, Knipe DM, et al. Interferon γ-inducible protein (IFI) 16 transcriptionally regulates type i interferons and other interferon-stimulated genes and controls the interferon response to both DNA and RNA viruses. J Biol Chem. 2014 Aug 22;289(34):23568–81.

53. Horan KA, Hansen K, Jakobsen MR, Holm CK, Soby S, Unterholzner L, et al. Proteasomal Degradation of Herpes Simplex Virus Capsids in Macrophages Releases DNA to the Cytosol for Recognition by DNA Sensors. J Immunol. 2013 Feb 15;190(5):2311–9.

54. Zhang H, Hu H, Greeley N, Jin J, Matthews AJ, Ohashi E, et al. STAT3 restrains RANK- and TLR4-mediated signalling by suppressing expression of the E2 ubiquitin-conjugating enzyme Ubc13. Nat Commun. 2014;5:5798.

55. Xiang M, Birkbak NJ, Vafaizadeh V, Walker SR, Yeh JE, Liu S, et al. STAT3 induction of miR-146b forms a feedback loop to inhibit the NF-κB to IL-6 signaling axis and STAT3-driven cancer phenotypes. Sci Signal. 2014;7(310):ra11.

56. Drescher B, Bai F. Neutrophil in viral infections, friend or foe? Virus Research. 2013 Jan;171(1):1–7.

57. Wojtasiak M, Pickett DL, Tate MD, Bedoui S, Job ER, Whitney PG, et al. Gr-1+ cells, but not neutrophils, limit virus replication and lesion development following flank infection of mice with herpes simplex virus type-1. Virology. 2010 Nov 10;407(1):143–51.

58. Tumpey TM, Fenton R, Molesworth-Kenyon S, Oakes JE, Lausch RN. Role for macrophage inflammatory protein 2 (MIP-2), MIP-1alpha, and interleukin-1alpha in the delayed-type hypersensitivity response to viral antigen. J Virol. 2002 Aug;76(16):8050–7.

59. Manz MG, Traver D, Miyamoto T, Weissman IL, Akashi K. Dendritic cell potentials of early lymphoid and myeloid progenitors. Blood. 2001 Jun 1;97(11):3333–41.

60. Traver D, Akashi K, Manz M, Merad M, Miyamoto T, Engleman EG, et al. Development of CD8alpha-positive dendritic cells from a common myeloid progenitor. Science. 2000 Dec 15;290(5499):2152–4.

61. Ye M, Iwasaki H, Laiosa CV, Stadtfeld M, Xie H, Heck S, et al. Hematopoietic stem cells expressing the myeloid lysozyme gene retain long-term, multilineage repopulation potential. Immunity. 2003 Nov;19(5):689–99.

62. Melillo JA, Song L, Bhagat G, Blazquez AB, Plumlee CR, Lee C, et al. Dendritic Cell

(DC)-Specific Targeting Reveals Stat3 as a Negative Regulator of DC Function. J Immunol. 2010 Feb 17;184(5):2638–45.

63. Onai N, Obata-Onai A, Schmid MA, Ohteki T, Jarrossay D, Manz MG. Identification of clonogenic common Flt3+M-CSFR+ plasmacytoid and conventional dendritic cell progenitors in mouse bone marrow. Nat Immunol. 2007 Oct 7;8(11):1207–16.

64. Bosnjak L, Miranda-Saksena M, Koelle DM, Boadle RA, Jones CA, Cunningham AL. Herpes Simplex Virus Infection of Human Dendritic Cells Induces Apoptosis and Allows Cross-Presentation via Uninfected Dendritic Cells. J Immunol. 2005 Feb 7;174(4):2220–7.

65. Madera S, Rapp M, Firth MA, Beilke JN, Lanier LL, Sun JC. Type I IFN promotes NK cell expansion during viral infection by protecting NK cells against fratricide. J Exp Med. 2016 Feb 8;213(2):225–33.

66. Kondo M, Weissman IL, Akashi K. Identification of clonogenic common lymphoid progenitors in mouse bone marrow. Cell. 1997 Nov 28;91(5):661–72.

67. Grzywacz B, Kataria N, Kataria N, Blazar BR, Miller JS, Verneris MR. Natural killer-cell differentiation by myeloid progenitors. Blood. 2011 Mar 31;117(13):3548–58.

68. Chen Q, Ye W, Jian Tan W, Mei Yong KS, Liu M, Qi Tan S, et al. Delineation of Natural Killer Cell Differentiation from Myeloid Progenitors in Human. Sci Rep. 2015;5:15118.

CHAPTER 3: CYTOSOLIC DNA PROMOTES STAT3 PHOSPHORYLATION BY TBK1 TO RESTRAIN STAT3 ACTIVITY[2]

3.1 Summary

Cytosolic DNA can elicit beneficial as well as undesirable immune responses. For example, viral or microbial DNA triggers cell-intrinsic immune responses to defend against infections, whereas aberrant cytosolic accumulation of self-DNA results in pathological conditions, such as autoimmunity. Given the importance of these DNA-provoked responses, a better understanding of their molecular mechanisms is needed. Cytosolic DNA engages stimulator of interferon genes (STING) to activate TANK-binding kinase 1 (TBK1), which subsequently phosphorylates the transcription factor interferon regulatory factor 3 (IRF3) to promote interferon expression. Recent studies have reported that additional transcription factors, including nuclear factor kappa-B (NF-κB) and signal transducer and activator of transcription 6 (STAT6), are also activated by cytosolic DNA, suggesting that cytosolic DNA-induced gene expression is orchestrated by multiple factors. Here we show that cytosolic DNA activates STAT3, another member of the STAT family, via an autocrine mechanism involving interferon β (IFNβ) and IL-6. Additionally, we observed a novel cytosolic DNA-induced phosphorylation at serine 754 in the transactivation domain of STAT3. Upon cytosolic DNA stimulation, S754 is directly phosphorylated by TBK1 in a STING-dependent manner. Moreover, S754

[2] This chapter has been accepted by Journal of Biological Chemistry and is placed in this dissertation after additional editing by the author. The original citation is as follows: H-C Hsia, JE Hutti, AS Baldwin. Cytosolic DNA Promotes Signal Transducer and Activator of Transcription 3 (STAT3) Phosphorylation by TANK-binding kinase 1 (TBK1) to Restrain STAT3 Activity. *Journal of Biological Chemistry*. 2017 Feb 10. (In press)

phosphorylation inhibits cytosolic DNA-induced STAT3 transcriptional activity, and selectively reduces STAT3 target genes that are upregulated in response to cytosolic DNA. Taken together, our results suggest that cytosolic DNA-induced STAT3 activation *via* IFNβ and IL-6 is restrained by S754 phosphorylation of STAT3. Our findings reveal a new signaling axis downstream of the cytosolic DNA pathway and suggest potential interactions between innate immune responses and STAT3-driven oncogenic pathways.

3.2 Introduction

Double-stranded DNA (dsDNA) in the cytosol is a danger-associated molecular pattern (DAMP) that triggers inflammation and immune responses. Cytosolic DNA can be derived from viral or intracellular microbial infections, undigested phagocytosed materials, and activated self retroelements (1). The presence of cytosolic DNA is detected by several cellular sensors, which in turn initiate signaling cascades to induce inflammatory response and type I interferon production (2). Despite the redundancy between these cytosolic DNA sensors, cyclic GMP-AMP synthase (cGAS) is the predominant sensor relaying the presence of cytosolic DNA to downstream signaling cascades (3). Upon binding to dsDNA, cGAS produces cyclic 2'-3' GMP-AMP (cGAMP), which serves as a second messenger to activate the endoplasmic reticulum adaptor protein stimulator of interferon genes (STING) (3-6). Activation of STING by cGAMP leads to STING oligomerization, followed by recruitment and activation of TANK-binding kinase 1 (TBK1) (7,8). Subsequently, TBK1 phosphorylates interferon regulatory factor 3 (IRF3) to promote expression of interferons (IFNs), thereby initiating immune responses to establish an antiviral state (7,9,10). In addition to IRFs, other transcription factors, including

nuclear factor κB (NF-κB) and signal transducer and activator of transcription 6 (STAT6), are also activated by STING and TBK1 downstream of cytosolic DNA (11-14).

The transcription factor STAT3 is activated by tyrosine 705 phosphorylation downstream of a variety of cytokines, such as epidermal growth factor (EGF) and IL-6 (15). Phosphorylation at tyrosine 705 leads to nuclear accumulation of STAT3 homodimers and expression of target genes containing a gamma-activated site (GAS) in their promoters (16). STAT3 drives the expression of pro-survival and inflammatory genes, and sustained activation of STAT3 has been shown to promote proliferation, enhance survival of neoplastic cells, and facilitate inflammation-driven tumorigenesis (17-19). In addition to its role in promoting tumorigenesis, STAT3 also represses the anti-tumor activity of hematopoietic cells, making it a key candidate for targeted cancer therapy and immunotherapy (20,21). STAT1, another STAT family member, predominantly functions downstream of interferons. STAT1 homodimers induced by IFNγ recognize almost identical GAS sites as STAT3 dimers do *in vitro*, but STAT1 and STAT3 have different, albeit overlapping, target genes *in vivo* (22). On the other hand, type I IFNs, including IFNα and IFNβ, induce the formation of not only STAT1 homodimer but interferon-stimulated gene factor 3 (ISGF3) complex comprising of STAT1, STAT2, and IRF9. The ISGF3 complex promotes the expression of genes containing an IFN-stimulated response element (ISRE) in their promoters (23). Reciprocal antagonizing effects between STAT1 and STAT3 can be observed in certain scenarios (24). For example, STAT3 inhibits STAT1-dependent induction of ISRE genes in response to type I IFN stimulation presumably through STAT1:STAT3 heterodimerization (25).

While dimerization and activity of STAT proteins are controlled by tyrosine phosphorylation, recent studies demonstrated that the function of STATs can also be modulated

by TBK1 and the closely related kinase IκB kinase epsilon (IKKε). Phosphorylation of STAT1 at S708 by IKKε disrupts STAT1 homodimerization and favors ISGF3 formation, thereby shifting the type I IFN-induced gene expression profile from GAS-driven genes to ISRE-driven genes (26). Cytosolic nucleic acids and viral infections engage the STING-TBK1 pathway, leading to TBK1-mediated phosphorylation of STAT6 at S407 and STAT6 activation (14). Interestingly, functional loss of cGAS or STING has been observed in colorectal cancer and melanoma and correlates with disease progression and elevated STAT3 activation (27-29), suggesting a role of STING in restricting STAT3 activity and tumor progression. Thus, we sought to determine if activity of STAT3 can be regulated by the STING-TBK1 pathway downstream of cytosolic DNA. Here we show that STAT3 is activated by cytosolic DNA through an autocrine mechanism involving IFNβ and IL-6. At the same time, cytosolic DNA activates TBK1 in a cGAS and STING dependent manner to directly phosphorylate STAT3 at serine 754 in the transactivation domain (TAD). This TBK1-mediated phosphorylation at S754 is inhibitory and restrains cytosolic DNA, IL-6, and IFNβ-induced activation of STAT3. Our finding provides a possible explanation to the role of STING in limiting STAT3 activation, and further emphasizes the complex signaling cascades and gene expression initiated by cytosolic DNA.

3.3 Results

3.3.1 TBK1 directly phosphorylates STAT3 at serine 754

Previous studies demonstrated that TBK1 and IKKε, respectively, regulate the function of STAT6 and STAT1 by direct phosphorylation (14,26). To determine if TBK1 and IKKε also phosphorylate other STATs, we examined the sequences of STATs against the optimal substrate motif for TBK1 and IKKε (30,31), and identified serine 754 in the TAD of STAT3 as a potential

TBK1/IKKε phosphorylation site (Figure 3.1A). In order to test if STAT3 is a substrate of TBK1 or IKKε, IKKε and STAT3 were overexpressed in HEK293T cells, and immunoprecipitated STAT3 was blotted with an IKK family phospho-substrate motif antibody (see Materials and Methods). Overexpression of wild-type IKKε strongly induced phosphorylation of STAT3 at Y705 as well as a site recognized by the IKK phospho-substrate motif antibody (Figure 3.1B). We then generated an antibody specific for phospho-S754-STAT3 and repeated the experiment with TBK1. Similarly, overexpression of wild-type, but not kinase-dead, TBK1 induced STAT3 phosphorylation at multiple sites, and S754A mutation of STAT3 abolished the signal of pS754-STAT3 specific antibody (Figure 3.1C), suggesting that TBK1 kinase activity is critical for the phosphorylation of STAT3 at S754. Overexpression of TBK1 and IKKε in HEK293T may lead to activation of other kinases, which in turn phosphorylate STAT3. To determine if TBK1 is capable of phosphorylating STAT3 directly, we performed an *in vitro* kinase assay with purified TBK1 and recombinant GST-STAT3 from bacteria. Autoradiography showed that incubation with wild-type but not kinase-dead TBK1 led to strong phosphorylation on wild-type STAT3, and that S754A mutation of STAT3 abolished the phosphorylation (Figure 3.1D). This TBK1-mediated phosphorylation on STAT3 was also recognized by the pS754-STAT3-specific antibody (Figure 3.1D). These data show that TBK1 is capable of directly phosphorylating STAT3 at S754.

3.3.2 STAT3 is phosphorylated at S754 in response to cytosolic dsDNA

TBK1 is activated downstream of toll-like receptors (TLRs) and several other TLR-independent pathways (32). To determine if S754 phosphorylation of STAT3 occurs under these conditions, we asked if these TBK1-activating agonists promote STAT3 phosphorylation at

S754. L929 cells were treated with lipopolysaccharide (LPS), or transfected with poly(I:C), poly(dA:dT), or a 70-bp long double-stranded DNA (VACV70mer) (33), to engage TLR4, MDA5/RIG-I, or the cytosolic DNA pathway, respectively. Transfection with poly(I:C) or DNA resulted in varying degrees of TBK1, IRF3, and STAT1 activation, but only transfection with dsDNA, including poly(dA:dT) and VACV70mer, led to strong phosphorylation of STAT3 at S754 (Figure 3.2A). Induction of STAT3 S754 phosphorylation correlated with robust TBK1 activation (as marked by S172 phosphorylation) and phosphorylation of IRF3, a major substrate of TBK1 (Figure 3.2A). STAT3 was also activated by cytosolic dsDNA transfection, as marked by Y705 phosphorylation, which was accompanied by a modest induction of S727 phosphorylation (Figure 3.2A). This demonstrates that cytosolic dsDNA leads to TBK1 activation, STAT3 activation, and S754 phosphorylation of STAT3. To determine if similar responses can be observed in human cell lines, we tested the human monocytic cell line THP-1 with these stimuli as well as flagellin, which signals through TLR5. Similarly, cytosolic DNA, especially poly(dA:dT), induced the most robust S754 and Y705 phosphorylation of STAT3. This was accompanied by slight STAT3 S727 phosphorylation and robust activation of STAT1 (Figure 3.2B). Poly(dA:dT) transfection induced association of STAT3 with TBK1 and IKKε, while VACV70mer induced association of STAT3 with TBK1 but not IKKε (Figure 3.2B). These stimuli also induced various degrees of IKKα/IKKβ activation and p65 phosphorylation, indicative of NF-κB activation (Figure 3.2B). Finally, a time-course experiment revealed that association between TBK1 and STAT3 was induced as early as 1.5 hours after dsDNA transfection, coinciding with the timing of S754 phosphorylation, while Y705 phosphorylation of STAT3 was detected at a later time-point (Figure 3.2C). Taken together, these data show that

among different TBK1 activators, cytosolic DNA induces the most robust STAT3 activation and phosphorylation at S754.

3.3.3 TBK1 is required for cytosolic DNA-induced STAT3 phosphorylation at S754

Given that cytosolic DNA induces robust TBK1 activation, STAT3 phosphorylation, and association between TBK1 and STAT3, we asked if TBK1 is required for cytosolic DNA-induced S754 phosphorylation of STAT3. We found that STAT3 S754 phosphorylation and IRF3 phosphorylation were abrogated with genetic ablation of TBK1 or siRNA-mediated TBK1 knockdown (Figure 3.3A-B). On the other hand, IKKε knockdown had negligible effects on STAT3 S754 or IRF3 phosphorylation (Figure 3.3C), indicating that TBK1 but not IKKε is required for cytosolic DNA-induced STAT3 phosphorylation. It has been shown that cytosolic DNA also activates IKKα and IKKβ (Figure 3.2B and (13), and that the optimal substrate motif of IKKα and IKKβ shares a partial homology to that of TBK1 and IKKε (30,31,34,35). To further investigate the role of individual IKKs in promoting STAT3 phosphorylation upon cytosolic DNA challenge, we used an IKKα/IKKβ-specific inhibitor compound A (36) and two TBK1/IKKε-specific inhibitors AZ-5C and AZ-5E (37). The TBK1/IKKε inhibitors blocked the induction of p-IRF3 and pS754-STAT3, while p-p65 was mostly unaffected (Figure 3.3D). Y705 phosphorylation of STAT3 was also dependent on TBK1 and/or IKKε (Figure 3.3D). In contrast, the IKKα/IKKβ inhibitor potently blocked the induction of p-p65 but had minimal effect on p-IRF3, pS754-STAT3, or pY705-STAT3 in THP-1 cells (Figure 3.3D). This indicates that phosphorylation of STAT3 S754 is mediated by TBK1 and is independent of IKKα and IKKβ, while activation of NF-κB p65 is mediated by IKKα and/or IKKβ. Taken together, our data

demonstrate that TBK1, rather than IKKα, IKKβ, or IKKε, is the principle kinase that mediates S754 phosphorylation of STAT3 upon cytosolic DNA challenge.

3.3.4 The cGAS-STING-TBK1 pathway induces STAT3 S754 phosphorylation in response to cytosolic DNA

Because the ER membrane protein STING is indispensible for cytosolic DNA-induced TBK1 activation (10,38), we tested if STING is also required for STAT3 S754 phosphorylation in response to cytosolic DNA. Indeed, knockdown of STING significantly reduced cytosolic DNA-induced pS754-STAT3 (Figure 3.4A). Moreover, pS754-STAT3 can be induced by ectopic expression of STING in HEK293T cells in a dose-dependent manner, suggesting that S754 phosphorylation occurs downstream of STING activation (Figure 3.4B). We also tested if the cytosolic dsDNA sensor cGAS is required in this setting. Knockdown of cGAS led to reduced activation of TBK1 and phosphorylation of IRF3, and a moderate reduction in the levels of pS754-STAT3 (Figure 3.4C). The moderate reduction of pS754-STAT3 may be due to incomplete knockdown of cGAS or the redundancy of other cytosolic DNA sensors. Activation of cGAS by cytosolic DNA leads to production of cGAMP, which subsequently promotes STING activation and activation of the TBK1-IRF3 signaling axis. We found that transfection of cGAMP is sufficient to induce S754 phosphorylation of STAT3 (Figure 3.4D), further supporting the model in which S754 phosphorylation of STAT3 occurs downstream of STING. These data demonstrate that cytosolic DNA engages cGAS and STING to activate TBK1 and induce STAT3 S754 phosphorylation.

3.3.5 Secreted cytokines induce activation of STAT3 in response to cytosolic DNA

We next set out to determine the mechanism of STAT3 activation (as marked by Y705 phosphorylation) in response to cytosolic DNA. In THP-1 cells, activation of STAT3 was suppressed by TBK1/IKKε inhibitors (Figure 3.3D), suggesting that TBK1 kinase activity is required for STAT3 activation. Since TBK1 is not a tyrosine kinase, activation of STAT3 is likely mediated by tyrosine kinases that are directly or indirectly activated by TBK1. It is well established that Janus kinases (JAKs) activate STAT3 by phosphorylating Y705. We thus asked if JAKs are involved in STAT3 activation in response to cytosolic DNA. Treating the cells with a pan-Janus kinases (JAKs) inhibitor pyridine 6 (39) effectively blocked STAT3 phosphorylation at Y705, but TBK1 activation and phosphorylation of STAT3 at S754 was unaffected (Figure 3.5A). These data and the TBK1 inhibitor data (Figure 3.3D) suggest that cytosolic DNA-induced STAT3 activation is primarily mediated by JAKs, of which the activation is dependent on TBK1. Because JAKs usually function downstream of cytokine receptors, we hypothesized that cytosolic DNA induces production of cytokines, leading to activation of the JAKs and STAT3 through an autocrine mechanism. An alternative hypothesis would be that TBK1 activates JAKs directly or through a cascade of kinase activation in a cell-autonomous manner. To test these hypotheses, we asked if conditioned media from dsDNA-transfected cells are able to activate STAT3 in naive recipient cells. We found that conditioned media from dsDNA transfected THP-1 strongly induced pY705-STAT3 but not pS754-STAT3 in the recipient cells (Figure 3.5B, lanes 10-14). When cells were treated with cycloheximide immediately before dsDNA transfection to block protein synthesis, the ability of conditioned media to induce pY705-STAT3 in the recipient cells was abrogated (Figure 3.5B, lanes 15-18). Although the possibility of cell-autonomous TBK1-mediated JAKs activation cannot be completely ruled out

because a weak STAT3 activation was still observed in cycloheximide-treated cells (Figure 3.5B, lanes 6-9), these results argue that STAT3 activation is primarily mediated by *de novo* synthesized secreted factors. We noticed that expression of several STAT3 activating cytokines, including IL-6 and IFNβ, was induced by cytosolic DNA, and the induction of IFNβ was blunted by TBK1 inhibitor (Supplemental Figure 3.1). Therefore, we tested the involvement of IL-6 and IFNβ in STAT3 activation. Indeed, an IFNβ neutralizing antibody reduced the ability of conditioned media to activate STAT3 in the recipient cells, and the IL-6 neutralizing antibody also had a modest effect (Figure 3.5C). Taken together, our data show that cytosolic DNA-induced S754 phosphorylation of STAT3 is strictly cell-autonomous, whereas Y705 phosphorylation, and thus activation of STAT3, is primarily mediated by secreted factors such as IFNβ through an autocrine mechanism.

3.3.6 S754 phosphorylation of STAT3 restricts cytosolic DNA-induced STAT3 target gene expression

Next, we sought to determine the effect of cytosolic DNA-induced S754 phosphorylation on STAT3 activation and target gene expression. THP-1 cells reconstituted with wild-type or mutant STAT3 following CRISPR-mediated knockout (Supplemental Figure 3.2) were transfected with dsDNA to induce STAT3 activation and S754 phosphorylation. Activation of wild-type and S754D STAT3 by cytosolic DNA was significantly lower than that of the S754A mutant, suggesting that S754 phosphorylation inhibits STAT3 activation (Figure 3.6A). STAT1 and p65 were also activated by cytosolic DNA, but their activation was not affected by the status of STAT3, and p65 showed constitutive association with STAT3 (Figure 3.6A). We also examined the gene expression induced by cytosolic DNA. STAT3 target gene *SOCS3* was

upregulated in the presence of STAT3 (Figure 3.6B), and its expression was further elevated in the S754A cells, consistent with increased activation of the S754A mutant (Figure 3.6A). The NF-κB target gene *IL6* was also upregulated in the presence of STAT3, but S754 phosphorylation did not have any measurable effect on its expression (Figure 3.6C). This suggests that there may be cooperative binding and transcriptional activation between STAT3 and NF-κB in regulating IL-6 transcription, but S754 phosphorylation of STAT3 does not affect the gene expression mediated by this complex. In agreement with this hypothesis, the interaction between p65 and STAT3 was not affected by cytosolic DNA or the status of S754 phosphorylation (Figure 3.6A). We also asked if S754 phosphorylation of STAT3 modulates the inhibitory effect of STAT3 on ISGF3 target genes (25), and found that *CXCL10* was downregulated by wild-type and mutant STAT3 to similar levels (Figure 3.6D), suggesting that S754 phosphorylation is not involved in the inhibition of ISGF3 target genes by STAT3. Finally, chromatin-immunoprecipitation demonstrates that upon cytosolic DNA challenge, STAT3 was recruited to the predicted binding sites in *SOCS3* promoter (Figure 3.6E), and that the increased abundance of S754A STAT3 at the *SOCS3* promoter correlated with gene expression levels (Figure 3.6B). These data demonstrate that cytosolic DNA-induced S754 phosphorylation of STAT3 dampens the expression of STAT3 target gene without affecting the expression of NF-κB or ISGF3 genes.

3.3.7 S754 phosphorylation suppresses the transcriptional activity of STAT3

Because S754 is located in the transactivation domain of STAT3, we hypothesized that phosphorylation at S754 modulates the transcriptional activity of STAT3 in response to IL-6 and IFNβ. We asked if S754 phosphorylation of STAT3 affects the expression of a STAT reporter

containing tandem GAS sites in response to IFNβ and IL-6 by using a phosphomimetic mutant (S754D), since S754 phosphorylation is not induced by IFNβ or IL-6 alone. To avoid interference from endogenous STAT3, the reporter assay was carried out using CRISPR-mediated STAT3 knockout HEK293T cells (Supplemental Figure 3.2) or STAT3-null MEFs stably expressing wild-type or mutant STAT3. We found that IFNβ induced a much higher expression of the STAT reporter in the presence of wild-type STAT3, but the transcriptional inactive Y705F mutant inhibited reporter expression (Figure 3.7A), indicating that STAT3 contributes to GAS-driven gene expression in response to IFNβ. The reporter expression was reduced with the S754D mutant, suggesting an inhibitory role for S754 phosphorylation in the transcriptional activity of STAT3 (Figure 3.7A). In contrast, STAT3 did not affect GAS-driven gene expression in response to IFNγ (Figure 3.7A), which predominantly activates STAT1 but not STAT3 (15). The S754D mutant also showed decreased activation upon IFNβ stimulation (Figure 3.7B), consistent with the results from reporter assays. We then asked if TBK1-induced S754 phosphorylation affects STAT3 activation in response to IFNβ. Because overexpression of TBK1 leads to significant production of cytokines, resulting in elevated basal STAT3 activation (40) (Figure 3.1C), here we expressed a moderate amount of TBK1 before treating the cells with IFNβ. We found that TBK1 expression suppressed IFNβ-induced STAT3 activation, but the S754A mutant was more refractory to this TBK1-mediated inhibition (Figure 3.7C, lanes 5 and 7). These data show that S754 phosphorylation inhibits IFNβ-induced activation of STAT3. We also probed the possibility that S754 phosphorylation of STAT3 may affect STAT3-mediated inhibition on ISGF3 target genes. Consistent with *CXCL10* expression in THP-1 cells (Figure 3.6D), wild-type and mutant STAT3 inhibited IFNβ-induced ISRE reporter expression to comparable levels (Supplemental Figure 3.3), indicating that S754 phosphorylation of STAT3

does not affect ISGF3 activity. Similar to the IFNβ reporter assays, S754D mutant was also less active in response to IL-6 as measured by STAT reporter assays and by the levels of Y705 phosphorylation, which inversely correlated with the levels of S754 phosphorylation or phosphomimetic mutation (Figure 3.7D-E). Collectively, these data demonstrate that S754 phosphorylation suppresses the transcriptional activity of STAT3 induced by IL-6 and IFNβ.

3.4 Discussion

In this study, we identified STAT3 as a novel substrate of TBK1 downstream of the cytosolic DNA pathway. In the presence of cytosolic DNA, TBK1 phosphorylates STAT3 at S754 to limit STAT3 activity induced by cytokines such as IL-6 and IFNβ. Previously, it has been shown that IKKε regulates STAT1 dimerization and that TBK1 regulates STAT6 activity by direct phosphorylation (14,26). Our finding places a third STAT member under the control of IKKε/TBK1. Interestingly, the IKKε/TBK1-mediated phosphorylation sites in STAT1, STAT3, and STAT6 differ in their location within the proteins (Figure 3.1A). In the case of STAT1, phosphorylation of S708, which resides in between the SH2 domain and the TAD, disrupts SH2 domain-mediated STAT1 homodimerization by steric hindrance (26). How TBK1-mediated S407 phosphorylation regulates the activity of STAT6 is less clear. S407 resides within a highly conserved region of STAT DNA binding domain, and structural analysis demonstrated that mutations in this region abolish the DNA binding ability of STATs (41). Thus, it is plausible that S407 phosphorylation affects the DNA binding affinity of STAT6. It is also worth noting that TBK1 induces a reduced but still significant phosphorylation on STAT6 S407A mutant (14), suggesting the existence of additional TBK1 phosphorylation sites in STAT6. In fact, we identified another IKKε/TBK1 substrate motif in STAT6 TAD, in which S733 is the residue that

corresponds to S754 of STAT3. Our preliminary data suggest that TBK1 overexpression also leads to STAT6 phosphorylation at S733 (H-.C. Hsia, unpublished data). For future investigations, it would be of interest to determine if this phosphorylation serves as an additional mechanism by which TBK1 regulates STAT6 activity in a manner similar to what we discovered with STAT3.

The two IKK-related kinases TBK1 and IKKε are structurally similar and prefer almost identical substrate sequences *in vitro* (30,31). However, they appear to have distinct yet partially overlapping roles *in vivo* (42). Studies using TBK1 or IKKε knockout cells showed that TBK1 is the principle kinase that phosphorylates IRF3 to initiate interferon production in response to innate immune stimuli and pathogens, while IKKε has a minor or negligible role on activating IRF3 and interferon production (11,43,44). Similarly, in our model, although overexpression of TBK1 and IKKε both induced S754 phosphorylation of STAT3 (Figure 3.1B, 3.1C), endogenous IKKε did not have a measurable impact on STAT3 phosphorylation in response to VACV70mer (dsDNA with 33% GC content) transfection (Figure 3.3C). However, it is worth noting that while VACV70mer only induced interaction between STAT3 and TBK1, poly(dA:dT) transfection induced interaction of STAT3 with TBK1 and IKKε (Figure 3.2B), suggesting that IKKε may contribute to the signaling cascades and STAT3 phosphorylation downstream of AT-rich cytosolic DNA. AT-rich cytosolic DNA not only activates the STING/TBK1 pathway but also engages the cytosolic dsRNA sensor RIG-I by a polymerase III-dependent mechanism (45). Thus, the differential interactions between STAT3 and IKKε/TBK1 in response to VACV70mer and poly(dA:dT) may be due to the activation of cytosolic dsRNA pathway specifically downstream of poly(dA:dT). It is also conceivable that IKKε will play a more dominant role in

scenarios where its expression is highly induced (46). Whether IKKε contributes to STAT3 S754 phosphorylation and regulation under these conditions remains to be tested.

The NF-κB pathway is also activated by cytosolic DNA, but the roles of different IKKs in this context remain controversial (11-13). Ishii *et al.* suggested that TBK1 is dispensable for cytosolic DNA-induced NF-κB activation (11), while Abe and colleagues demonstrated a significant dependence of NF-κB activation on TBK1 (12,13). In MEFs and THP-1 cells, we observed that IKKα/IKKβ and TBK1 are each responsible for cytosolic DNA-induced p65 NF-κB activation or IRF3 activation (Figure 3.3A, 3.3D), indicating that the signaling events dictating NF-κB and IRF3 activation diverge at or above the level of these kinases. Intriguingly, p65 activation in L929 is mostly dependent on TBK1 (Figure 3.3B), consistent with the observation made by Abe *et al.* (13). It is unclear why such differences exist. One possible explanation may be the availability of different signaling molecules and the formation of different complexes. For instance, depending on the cell type, TBK1 may localize to the mitochondria or the ER in response to cytosolic DNA (47). Therefore, it is likely that signaling pathways downstream of cytosolic DNA and STING may be influenced by the availability of cell type-specific machinery and platforms as well as the subcellular localization of TBK1.

While it is unclear why S754 phosphorylation dampens the activity of STAT3, studies on a natural occurring STAT3 isoform STAT3β provide a plausible hypothesis. Alternative splicing of the STAT3 transcript results in the truncated STAT3β isoform that is 48 amino acids shorter than the full-length STAT3 (48). STAT3β shows strong Y705 phosphorylation and DNA binding activity even in the absence of stimulation, but it lacks intrinsic transcriptional activity due to the lack of TAD (48,49). Interestingly, STAT3β dimers are more stable than dimers formed by full-length STAT3, and deletion of 19 residues at the C-terminus (amino acids 752-770) of full-

length STAT3 is sufficient to significantly enhance Y705 phosphorylation, DNA binding activity, and dimer stability (50). Because the C-terminus of STAT3 is rich in acidic amino acids that are negatively charged, it was therefore proposed that the cluster of negative charges in the TAD interferes STAT3 dimerization and makes phosphorylated Y705 more accessible to phosphatases (50). Given this mechanism, phosphorylation or phosphomimetic mutation of S754 will introduce more negative charges to the region and may destabilize STAT3 dimers, thereby reducing its transcriptional activity. Alternatively, it is also possible that S754 phosphorylation affects the interaction between STAT3 and its co-activators to modulate STAT3 activity. Future studies will be focusing on testing these hypotheses.

There is mounting evidence of the critical role of cytosolic DNA in tumorigenesis and anti-tumor immune responses. Functional loss of the cGAS/STING cytosolic DNA pathway has been observed in some commonly used cell-lines and high-passage immortalized MEFs (5) as well as colorectal cancer and melanoma, in which loss of the cytosolic DNA pathway correlates with tumor progression (27,28). In a mouse model of colitis-associated colorectal cancer, STING deficient mice showed elevated NF-κB and STAT3 activity and developed advanced disease, suggesting a role of STING in controlling inflammatory responses and tumorigenesis (29). According to our model, loss of the cytosolic DNA sensing pathway will predict loss of the TBK1-mediated restraint on STAT3 activity, allowing the tumor cells to have elevated STAT3 activation in response to cytokines such as IL-6. Given the well-established role of STAT3 in promoting tumorigenesis, our finding suggests a possible mechanism in which tumor cells without the cytosolic DNA pathway may have a survival advantage due to unchecked STAT3 activation. On the other hand, activation of dendritic cells (DC) in the tumor microenvironment by engaging the cGAS/STING pathway leads to significant T cell recruitment and anti-tumor

immunity (51,52). Since STAT3 negatively regulates DC activity and the anti-tumor response of hematopoietic cells (20,53), cytosolic DNA-mediated restraint on STAT3 activity may serve as an additional mechanism to strengthen the anti-tumor immunity of hematopoetic cells in the tumor microenvironment.

In summary, we identified a novel signaling axis in which TBK1 modulates STAT3 activity in response to cytosolic DNA. Our findings reveal a new mechanism by which the activity of STAT3 can be fine-tuned by a single phosphorylation, and shed lights on the possible crosstalks between innate immune responses and STAT3-driven oncogenic pathways.

3.5 Materials and Methods

Plasmids and viruses. Mouse STAT3 was cloned into pBabe-puro (Addgene #1764)(54) using BamHI and EcoRI. N-terminal HA-tagged STAT3 was cloned into 3XHA-pEBB vector using BamHI and NotI. N-terminal FLAG-tagged STAT3 was cloned into pENTR-3C plasmid using BamHI and EcoRI, followed by Gateway recombination into pLenti6/UbC/V5 destination vector (Thermo Fisher). The C terminus of STAT3 (amino acids 700-770) was cloned into pGEX-4T-1 in frame with N-terminal GST using BamHI and EcoRI. STAT3 mutant plasmids were generated by site-directed mutagenesis and confirmed by sequencing. STAT3 CRISPR plasmid was constructed using lentiCRISPRv2 (Addgene #52961) (55) with an sgRNA targeting 5' UTR of human STAT3 (Supplemental Figure 3.2). The primer sequences for sgRNA cloning are as follows: 5'-CAC CGT GCC GGA GAA ACA GGT GAA G-3', 5'-AAA CCT TCA CCT GTT TCT CCG GCA C-3'.

Protein purification and in vitro assays. Rosetta cells (Novagen) harboring pGEX-4T-1-STAT3 plasmid were grown to log-phase and treated with 0.5 mM of IPTG at 30°C for 16

hours. The cells were lysed (50 mM Tris pH 7.6, 150 mM NaCl, 1 mM EDTA, 5 mM DTT, 25 μg/ml lysozyme, protease inhibitor cocktail (Promega)) at room temperature, followed by addition of 1.25 μg/ml of sodium deoxycholate, 1.25 μM of $MgCl_2$, and 62.5 μg/ml of DNase I. Cleared lysates (13000 rpm, 15 min, 4°C) were incubated with glutathione agarose beads (Amersham) at 4°C for 2 hours. The beads were washed twice with modified RIPA (150 mM NaCl, 1% NP-40, 0.25% sodium deoxycholate, 50 mM Tris pH 7.6, 1 mM β-glycerol phosphate), twice with high salt (500 mM NaCl) modified RIPA, and twice with kinase buffer (1 mM β-glycerol phosphate, 20 mM Tris pH 7.4, 12 mM $MgCl_2$). Purified protein was eluted by incubating the beads with 30 mM glutathione in kinase buffer with 0.1% Tween 20 for 20 minutes at room temperature with shaking. Wild-type and K38A GST-TBK1 were purified from HEK293T transfected with pEBG-GST-TBK1 plasmids as previously described (31). For *in vitro* kinase assays, 1 to 2 μl of purified GST-STAT3 was incubated with 2 to 4 μl of wild-type GST-TBK1 or K38A GST-TBK1 in kinase buffer with 1 mM ATP and 10 μCi of ^{32}P-γ-ATP at room temperature for 2 hours. The reaction was resolved by SDS-PAGE followed by immunoblotting or autoradiography.

Cells. THP-1 cells were maintained in RPMI1640 with 10% FBS, while HEK293T, L929, and MEFs were maintained in DMEM with 10% FBS and kept at 37°C with 5% CO_2. STAT3-null MEFs were a gift from Dr. Hua Yu (City of Hope), and TBK1 null MEFs were a gift from Amgen. Retroviruses were produced by co-transfection of pBabe-puro-STAT3 and pCL10A1 plasmids into HEK293T cells, and lentiviruses were produced by co-transfection of pLenti6-STAT3 with psPAX2 and pMD2.G into HEK293T cells. The supernatants containing viruses were 0.45 um-filtered before being used for transduction. To reconstitute STAT3 expression in STAT3-null MEFs, MEFs were transduced with pBabe-puro-STAT3 retroviruses

and selected for puromycin resistance. To generate STAT3 CRISPR knockout cells, THP-1 or HEK293T cells were transduced with STAT3 CRISPR virus and selected for puromycin resistance, and single clones were analyzed for STAT3 knockout efficiency (Supplemental Figure 3.2). To reconstitute STAT3 in THP-1, deltaSTAT3-THP-1 cells were transduced with pLenti6-STAT3 viruses and selected for blasticidin resistance. To activate TBK1, cells were transfected with poly (I:C), poly (dA:dT), VACV70mer, or 2'-3' cGAMP using lipofectamine 2000 (Thermo Fisher) at 1:1 ratio (μg/μl), and the final concentration of nucleic acids was 2 μg/ml unless otherwise noted. THP-1 cells were treated with 25 ng/ml of PMA (Sigma #P1585) overnight to induce adherence before cytosolic DNA transfection. Poly(I:C) (#tlrl-pic) poly(dA:dT) (#tlrl-patn), cGAMP (#tlrl-cga23), and LPS (#tlrl-eblps) were from Invivogen. VACV70mer was prepared by annealing complimentary 70-nt primers as previously described (33). For conditioned media experiments, supernatants from nucleic acid transfected cells were collected and 0.2 μm-filtered, mixed with 20 μg/ml of normal mouse IgG (Millipore, 12-371), 20 μg/ml of human IL-6 neutralizing antibody (R&D Systems #MAB206), or 40 μg/ml of human IFNβ neutralizing antibody (BioLegend #514004), and incubated at room temperature for 20 minutes before being added to recipient cells.

Transfection of siRNA. Transfection of siRNA was carried out using lipofectamine 2000 according to manufacturer's protocol. Mouse *Tbk1* (#M-063162-01-0005), mouse *Ikbke* (IKKε) (#M-040798-01-0005), mouse *Tmem173* (STING) (#M-055528-01-0005), and control siRNAs (#D-001210-03-05) were from Dharmacon. Mouse *Mb21d1* (cGAS) siRNA was from Sigma (#SASI_Mm01_00129826)

Reporter assays. The STAT reporter 4xM67 pTATA TK-firefly luciferase plasmid (Addgene #8688) (56) and pRL-TK-renilla luciferase plasmid (Promega) were co-transfected at

15:1 to 20:1 ratios into deltaSTAT3 293T cells together with 4xHA-STAT3 plasmids. Twenty-four hours after transfection, cells were treated with 25 pg/ml of mouse IFNβ (R&D Systems, 8499-IF-010) or 200 pg/ml of mouse IFNγ (R&D Systems, 285-IF-100). Cells were lysed with passive lysis buffer (Promega) for dual-luciferase assay (Promega) at 16-24 hours after treatment. The relative luciferase unit (RLU) was calculated by normalizing the reading of firefly luciferase to that of renilla luciferase, and RLU of the control cells was set to one. For IL-6 reporter assays, STAT3 reconstituted MEFs were transfected with reporters in the same manner and treated with 100 ng/ml of mouse IL-6 (BioLegend, 575704) for 24 hours.

Immunoblotting and immunoprecipitation. For immunoblotting, cells were lysed in RIPA buffer with protease inhibitor cocktail (Promega), phosphatase inhibitor cocktail (Sigma), and 1 mM Na_3VO_4. Cleared lysates were resolved by SDS-PAGE (NuPAGE bis-tris gels, Thermo Fisher), transferred to PVDF membranes (Millipore #IPVH00010), and blocked in 5% non-fat milk in TBST. The membranes were incubated in primary antibodies (1:1000-1:5000) in TBST at 4°C overnight, washed with TBST, and incubated in appropriate HRP-conjugated secondary antibodies (Promega) (1:10000). Pierce ECL (Thermo Fisher) was added to the blots, which were then exposed to films and developed, or imaged using ChemiDoc (BioRad). For immunoprecipitation, cells were lysed in 0.5% NP-40 buffer (0.5% NP-40, 150 mM NaCl, 20 mM Tris pH 7.6, 1 mM EGTA, 1 mM EDTA, 1 mM β-glycerol phosphate, and 0.5% glycerol) with protease and phosphatase inhibitors and Na_3VO_4. Cleared lysates were incubated with M2 Flag (Sigma) or STAT3 antibodies at 4°C overnight, followed by incubation with dynabeads protein G (Thermo Fisher) for 1 hour at 4°C and washing with 0.5% NP-40 buffer, and resolved by SDS-PAGE and immunoblotting. The following antibodies were from Cell Signaling Technology: GST (#2624, #2625), p-IKKα/IKKβ (S176/S180) (#2697), IKKβ (#2684), IKKε

(#3416), p-IRF3 (S396) (#4947), IRF3 (#4302), p-TBK1 (S172) (#5483), TBK1 (#3013), p-STAT3 (Y705) (#9145, #9132), p-STAT3 (S727) (#9134), p-p65 (S536) (#3033), p65 (#8242), STING (#13647), p-STAT3 (S754) (BL14578: 5163), and IKK phospho-substrate motif (G9108). The IKK p-substrate motif antibody was generated against the phosphorylated IKK consensus sequence x-(Y/F)-x-pS-L-x, where pS is the phospho-serine targeted by IKKs (30,31,34,35). GAPDH (sc-25778) and β-tubulin (sc-9104) antibodies were from Santa Cruz. Densitometry analyses were carried out using the gel analysis function of ImageJ.

Chromatin immunoprecipitation (ChIP). ChIP was performed as previously described (57). Briefly, cells were fixed by formaldehyde, lysed, and sonicated to yield DNA fragments of 200-500 bp. Lysates were diluted to 0.1% of SDS and precleared by incubating with BSA and salmon sperm DNA-blocked Dynabead magnetic protein G beads (Thermo Fisher). Lysates corresponding to $5x10^6$ cells were used for each ChIP with 5 μg of rabbit IgG (Cell Signaling Technology #2729) or rabbit anti-STAT3 antibody (Cell Signaling Technology #12640), followed by capture with Dynabead magnetic protein G beads. DNA-protein-antibody complexes were eluted, and DNA was un-crosslinked and purified by phenol-chloroform. The quantity of input DNA was determined by Nanodrop. The quantity of DNA corresponding to the STAT3 binding site in SOCS3 promoter in immunoprecipitated chromatin was determined by qRT-PCR with three technical repeats using SYBR green (Thermo Fisher) and the following primers: 5'-TAA GAA GGC TGA TTT CTG GCA GAG G-3', 5'-CCA GGT CGG CCT CCT AGA ACT-3'. Data are shown as mean with standard deviation, and are representative of two independent experiments.

Quantitative real-time PCR. Total RNA from cells were purified using QIAGEN RNeasy Plus kit according to manufacturer's protocol. One to 2 μg of RNA was used to

synthesize cDNA using M-MLV reverse transcriptase (Thermo Fisher). Quantitative real-time PCR (qRT-PCR) was carried out using synthesized cDNA, and tandard TaqMan probes, primers, and reagents (Thermo Fisher). The expression level of target genes was calculated by ddCt method relative to the level of *GUSB*. Data shown were the relative quantity (RQ), with RQ of the control cells set to one.

Statistical analysis. For reporter assays and qRT-PCR, data were shown as mean with standard deviation or mean with 95% confidence intervals, respectively. Each data point was from three technical replicates. Analyses were done by Prism (Graphpad) using t-test with FDR controlled at 1%.

Inhibitors and reagents. The IKKα/IKKβ-specific inhibitor Compound A was a generous gift from Dr. Karl Ziegelbauer (Bayer). The TBK1/IKKε-specific inhibitors AZ-5C and AZ-5E were synthesized by Dr. Stephen Frye's group at UNC-Chapel Hill. The pan-JAK inhibitor pyridone 6 was from Millipore (#420099), and cycloheximide was from Sigma (#C7698).

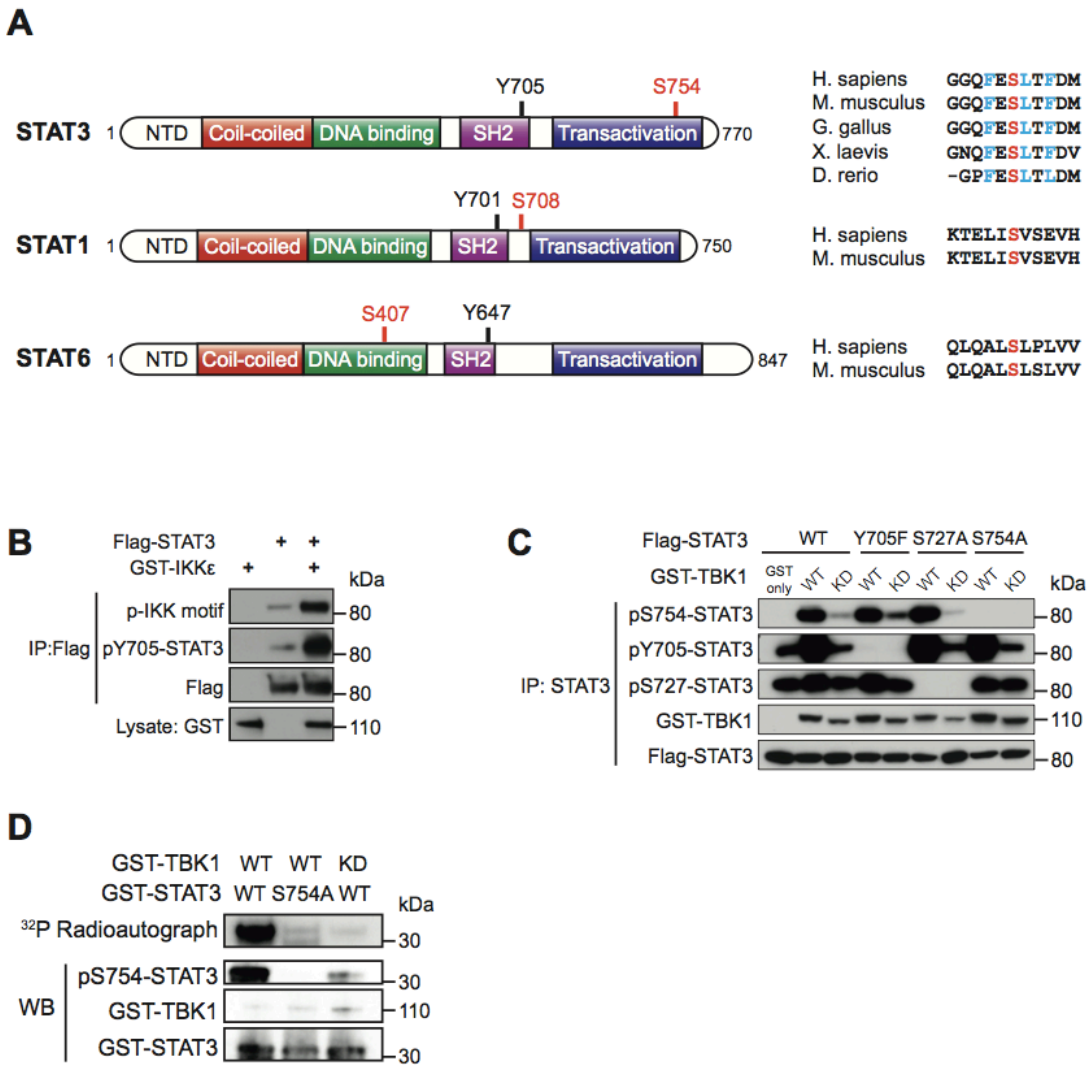

Figure 3.1 IKKε and TBK1 induce STAT3 phosphorylation at S754
(A) A schematic figure showing the domain structure of STAT3 and the location of S754. Sequences of STAT3 from several vertebrates were aligned to compare the homology, with residues critical for TBK/IKKε substrate recognition marked in blue, and S754 marked in red. Also shown are the domain structure of STAT1 and STAT6, with previously identified IKKε/TBK1 target serine residues marked in red and the sequence alignments shown on the right. NTD: N-Terminal domain; SH2: Src homology 2. (B) Flag-tagged STAT3 (3 μg) was co-transfected with GST-IKKε (3 μg) into HEK293T cells. STAT3 was immunoprecipitated and blotted with an IKK substrate motif antibody. (C) Flag-tagged wild-type, Y705F, S727A, or S754A STAT3 (3 μg) were co-transfected with wild-type or K38A (kinase dead, KD) GST-TBK1 (3 μg) into HEK293T cells. STAT3 was immunoprecipitated and blotted with phosphorylation-specific antibodies to detect S754, Y705, and S727 phosphorylation. (D) *In vitro* kinase assay using GST-tagged C-terminus of STAT3 and GST-TBK1 purified from HEK293T as described in Experimental Procedures. The mixture was resolved by SDS-PAGE and blotted with GST and pS754-STAT3 antibodies. Phosphorylation of STAT3 was also detected by autoradiography. Data in (B-D) are representative of 4, 3, and 2 independent experiments.

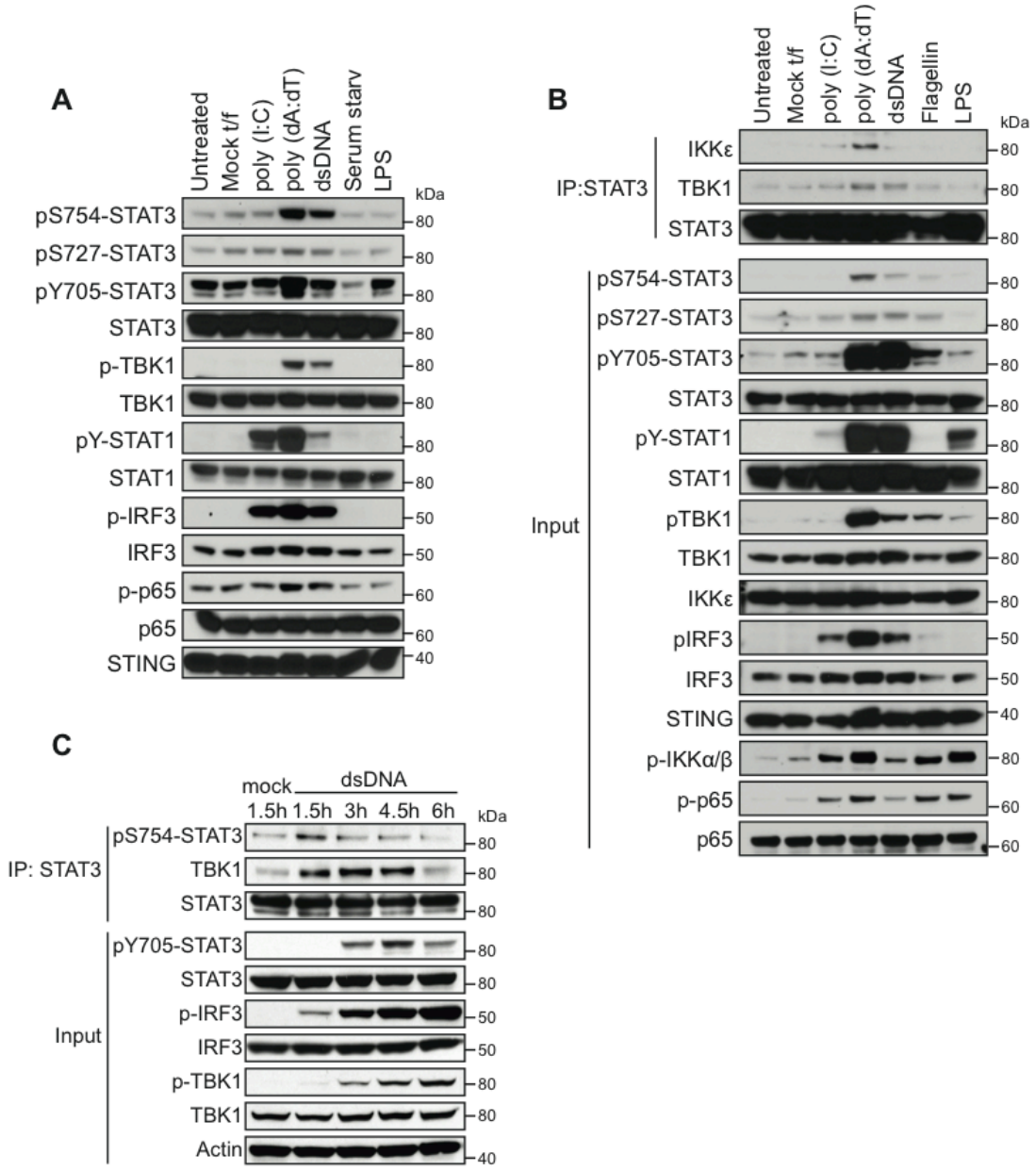

Figure 3.2 Cytosolic DNA induces STAT3 activation and phosphorylation at S754
(A) L929 cells were transfected with poly (I:C), poly (dA:dT), VACV70mer (hereafter referred to as dsDNA) using lipofectamine 2000, or treated with 1 μg/ml of LPS, or serum starved for 3 hours. Lysates were analyzed by western blotting to determine the levels of TBK1, IRF3, and STAT3 activation. (B) THP-1 cells were treated as described in (A), or treated with 1 μg/ml of flagellin for 3 hours. Lysates were analyzed by western blotting, and STAT3 was immunoprecipitated and blotted for co-precipitated IKKε or TBK1. (C) A time-course analysis of signaling responses to cytosolic DNA. THP-1 cells were mock-transfected or transfected with dsDNA and analyzed by western blotting at indicated times. STAT3 was immunoprecipitated and blotted for p-S754 and co-precipitated TBK1. Data in this figure are representative of 2 independent experiments.

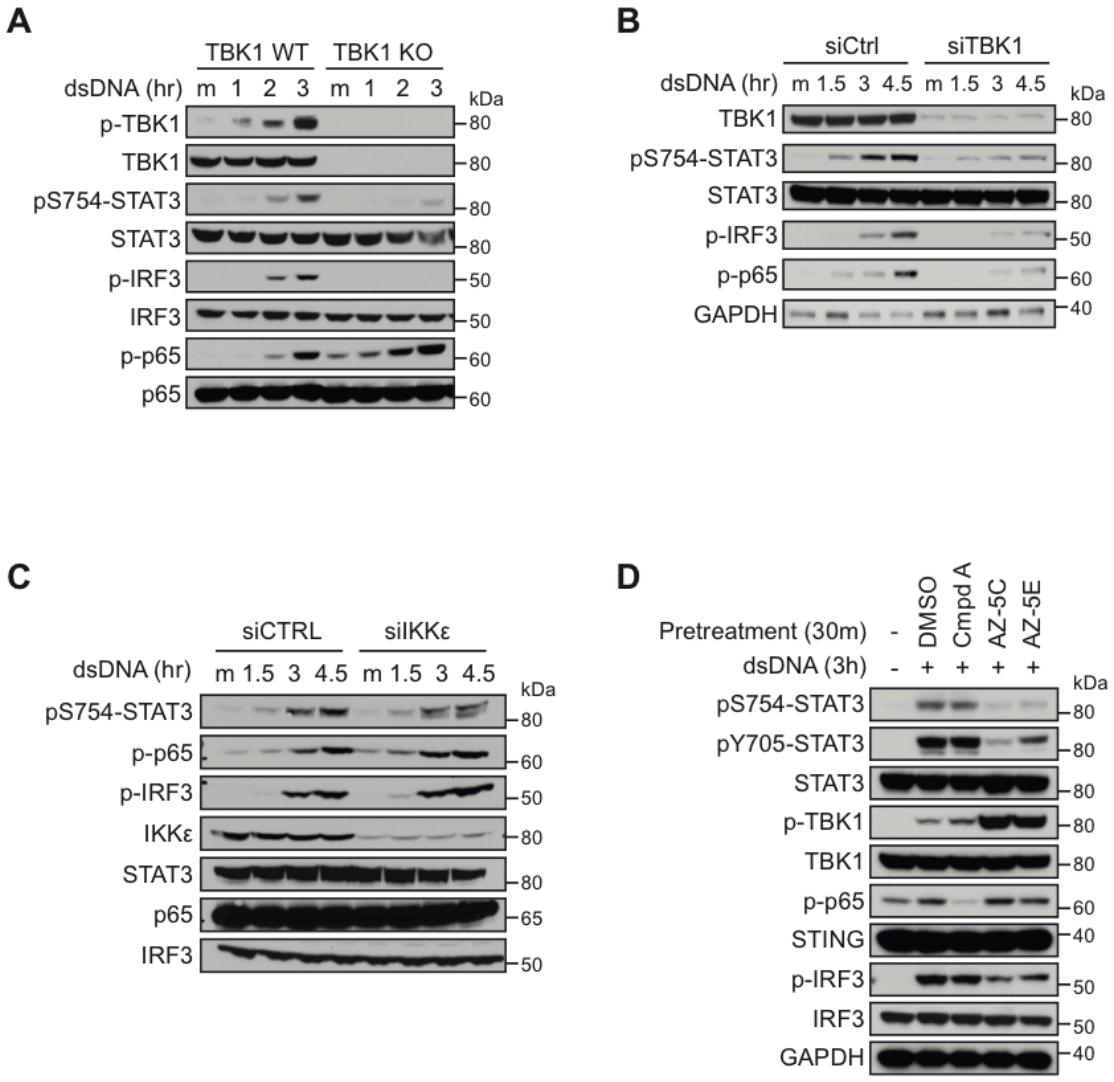

Figure 3.3 TBK1 activity is required for cytosolic DNA-induced S754 phosphorylation of STAT3

(A) Wild-type or TBK1 knockout MEFs were transfected with 5 μg/ml of dsDNA and analyzed by western blotting at indicated time points. (B) L929 cells were transfected with control siRNA or TBK1 siRNA. Forty-eight hours after siRNA transfection, cells were transfected with dsDNA and analyzed by western blotting. (C) L929 cells were transfected with control siRNA or IKKε siRNA. Sixty-eight hours after siRNA transfection, cells were transfected with dsDNA and analyzed by western blotting. (D) THP-1 cells were pretreated with DMSO, 5 μg/ml of compound A (an IKKα/IKKβ inhibitor), or 2 μM of AZ-5C or AZ-5E (IKKε/TBK1 inhibitors) for 30 minutes, followed by transfection with dsDNA for 3 hours. Cells were lysed and blotted for p-TBK1, p-IRF3, p-p65, and p-STAT3 to determine the activation of corresponding pathways. Data in (A-C) and (D) are representative of 2 and 3 independent experiments, respectively.

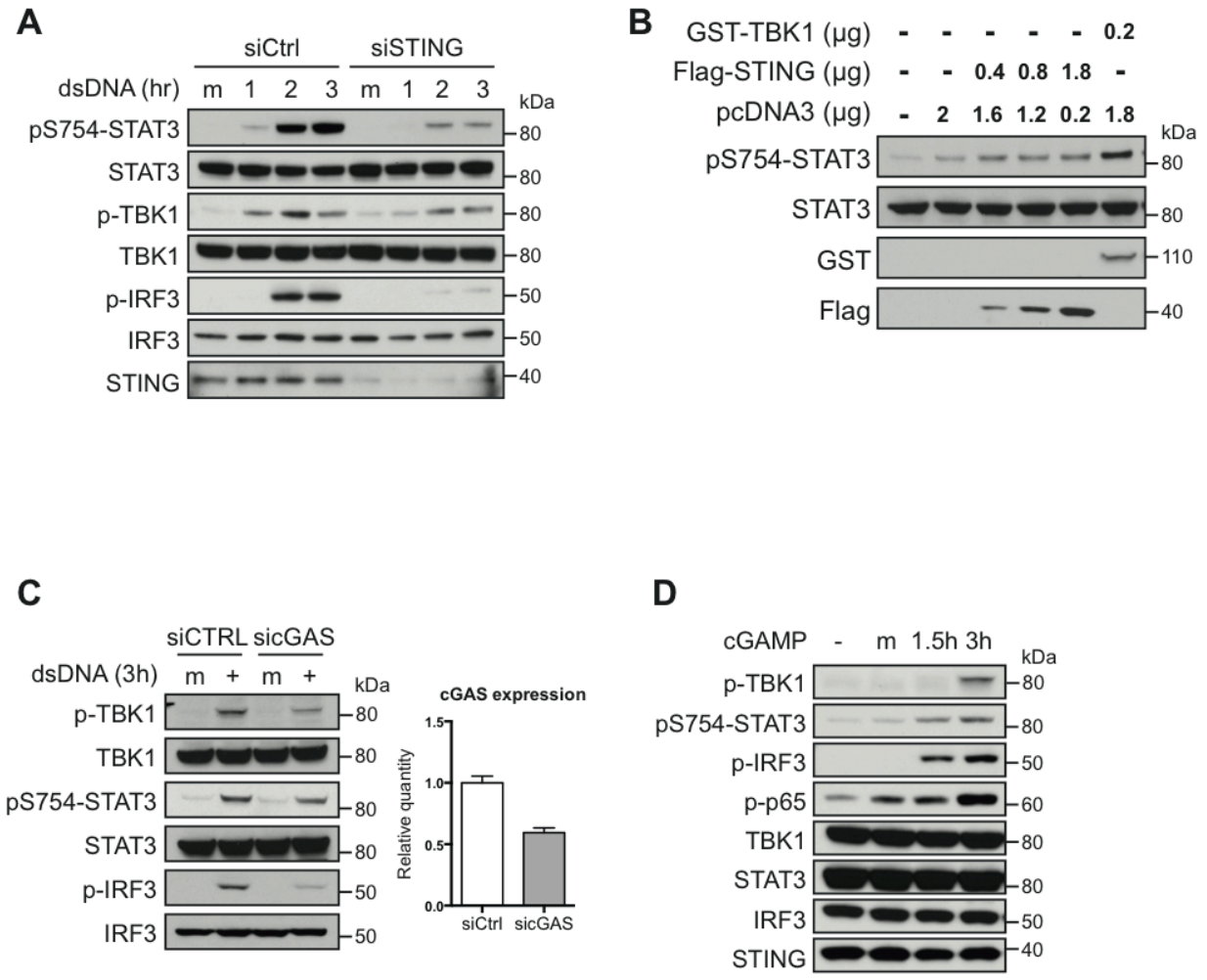

Figure 3.4 Cytosolic DNA induces pS754-STAT3 via the cGAS/STING axis
(A) L929 cells were transfected with control or IKKε siRNA. Forty-eight hours post-transfection, cells were transfected with dsDNA and analyzed by western blotting at indicated time points. (B) Increasing amount of STING expression plasmid was transfected into HEK293T cells with decreasing amount of pcDNA3 empty vector, such that same amount of total DNA was used in every transfection. After 24 hours, cells were lysed and blotted for pS754-STAT3. GST-TBK1 transfected cells were used as a positive control. (C) L929 cells were transfected with control or cGAS siRNA. After 68 hours, cells were harvested for qRT-PCR to measure cGAS expression levels, or transfected with dsDNA for 3 hours and analyzed by western blotting. The expression of cGAS was normalized to *Gusb*. (D) L929 cells were mock-transfected or transfected with cGAMP and analyzed by western blotting. Data in (A) and (B-D) are representative of 3 and 2 independent experiments, respectively.

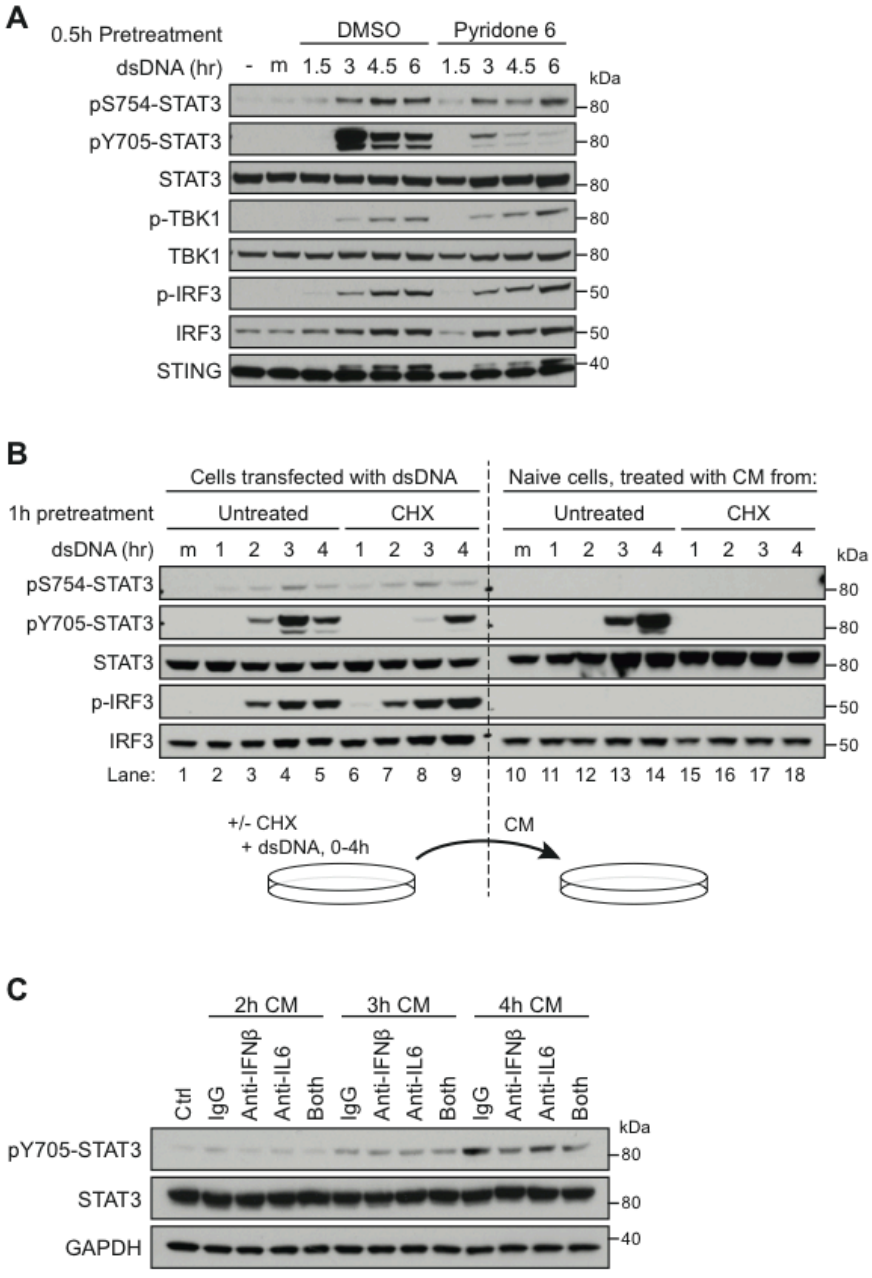

Figure 3.5 Cytosolic DNA-induced STAT3 activation is mediated by *de novo* synthesized secreted factors

(A) THP-1 cells were pre-treated with DMSO or 100 nM of the pan-JAK inhibitor pyridone 6 for 30 minutes, followed by transfection of dsDNA. Cells were analyzed by western blotting at indicated time points. (B) THP-1 cells were left untreated or treated with 30 μg/ml of cycloheximide (CHX) to block protein synthesis. After 1 hour of treatment, cells were transfected with dsDNA and lysed for western blotting at indicated time points, and results are shown in the left half of the blots. Conditioned media (CM) were collected from the dsDNA-transfected cells at the same time points, applied to naïve recipient cells for 20 minutes, and results are shown in the right half of the blots. (C) THP-1 cells were transfected with dsDNA, and conditioned media (CM) were collected at 2, 3, or 4 hours after transfection. Conditioned

media were incubated with 20 μg/ml of control IgG, 20 μg/ml of IL-6 neutralizing antibody, or 40 μg/ml of IFNβ neutralizing antibody for 20 minutes, and applied to naïve recipient cells for 20 minutes before western blotting. Data in this figure are representative of 3 independent experiments.

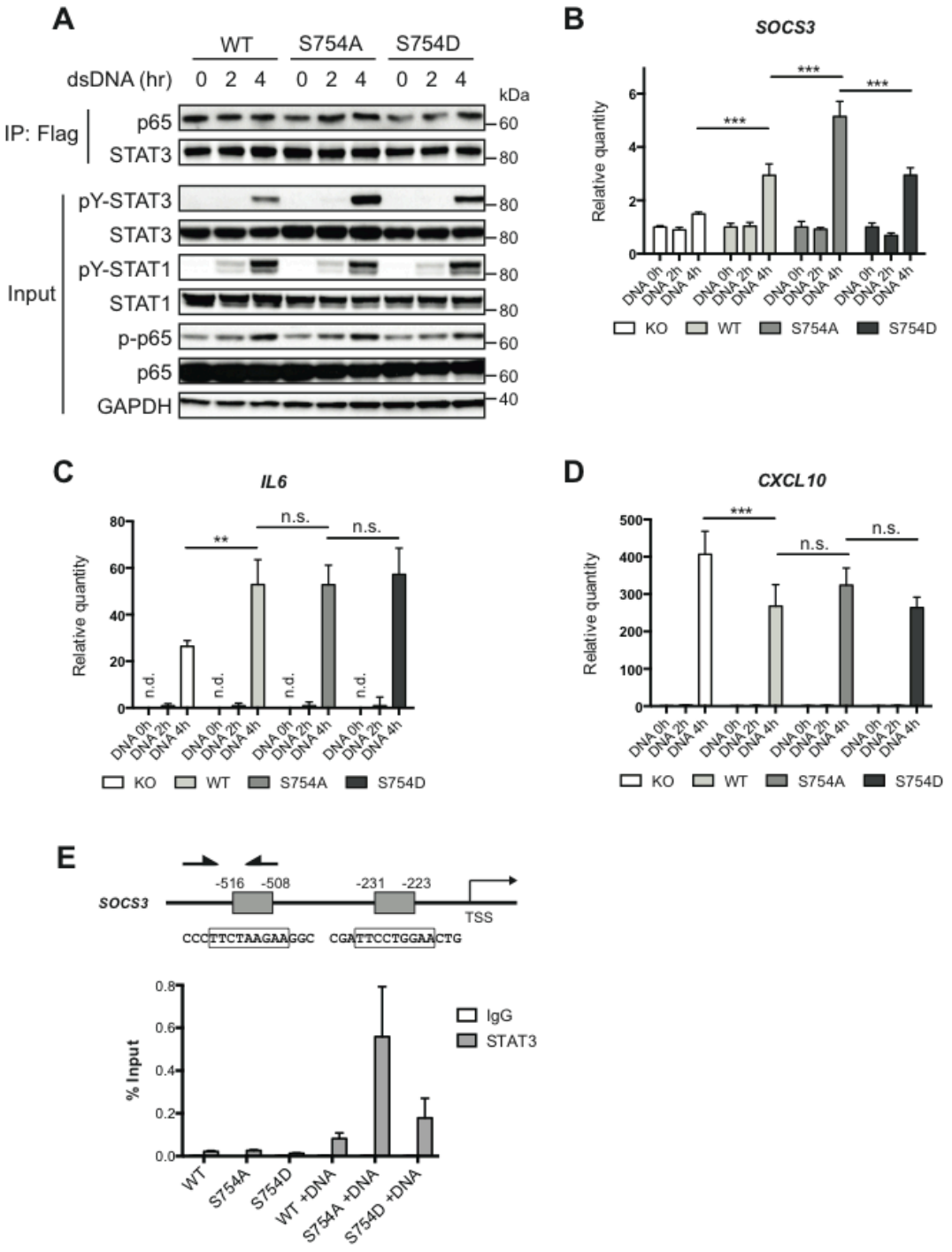

Figure 3.6 . S754 phosphorylation restricts STAT3 activation in response to cytosolic DNA
(A) deltaSTAT3 THP-1 cells reconstituted with wild-type or mutant STAT3 were transfected with dsDNA for 2 or 4 hours. Cells were analyzed by western blotting to assess the activation of STAT1, STAT3, and NF-κB p65. (B-D) deltaSTAT3 and reconstituted THP-1 cells were treated as described in (A), and RNA was collected for qRT-PCR to determine the expression levels of *SOCS3*, *IL6*, and *CXCL10*. *** $p<0.001$, ** $p<0.01$, n.s. not significant, n.d. not determined (below detection threshold). (E) A diagram of the SOCS3 promoter showing predicted STAT3

binding sites (gray boxes), with numbers indicate locations relative to the transcription starting site (TSS). Enrichment of STAT3 at the distal binding site was determined by ChIP as described in Experimental Procedures. Immunoprecipitated DNA from control or dsDNA transfected (3 hours) THP-1 cells was quantified by qRT-PCR using primers corresponding to the arrows in the diagram. The quantities of immunoprecipitated DNA are shown as percentages of input DNA. Data in (A-B) are representative of 4 independent experiments, and data in (C-E) are representative of 2 independent experiments.

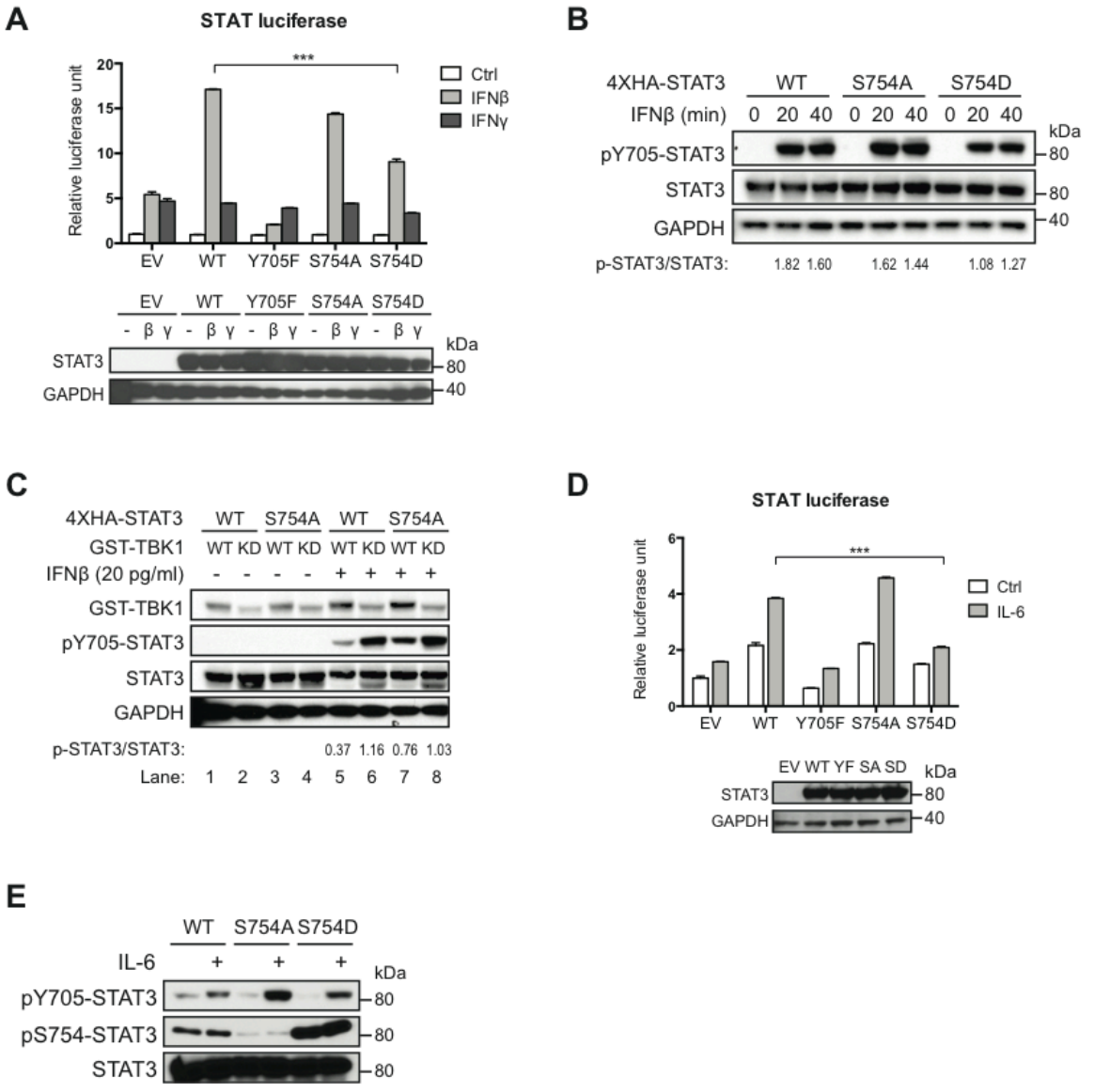

Figure 3.7 S754 phosphorylation inhibits transcriptional activity of STAT3
(A) Dual luciferase assay was used to determine STAT3 activity as described in Experimental Procedures. deltaSTAT3 HEK293T cells in 12-well plates were transfected with 0.5 μg of empty vector (EV) or 4xHA-STAT3 plasmids, 0.5 μg of STAT firefly luciferase plasmid, and 25 ng of TK-renilla luciferase plasmid, followed by treatment with 25 pg/ml of human IFNβ or 200 pg/ml of human IFNγ. Cell lysates were used for western blotting to verify STAT3 expression levels. Data are shown as mean with standard deviation. ***p<0.001 (B) deltaSTAT3 HEK293T cells in 6-cm plates were transfected with 3 μg of 4xHA-STAT3 plasmids. Twenty-four hours after transfection, cells were treated with 20 pg/ml of human IFNβ for 30 minutes, and lysed for western blotting. Densitometric ratios of pY705-STAT3 to STAT3 were shown to evaluate the levels of STAT3 activation. (C) deltaSTAT3 HEK293T cells in 10-cm plates were transfected with 3 μg of 4xHA-STAT3 plasmids and 1 μg of wild-type or kinase-dead GST-TBK1 plasmids. Twenty-four hours after transfection, cells were treated with 20 pg/ml of human IFNβ and lysed for western blotting. Densitometric ratios of pY705-STAT3 to STAT3 were shown to evaluate

the levels of STAT3 activation. (D) STAT3-null MEFs reconstituted with wild-type or mutant STAT3 in 12-well plates were transfected with 0.5 ug of STAT firefly luciferase reporter and 33 ng of tk-renilla luciferase plasmid, followed by treatment of 100 ng/ml of mouse IL-6 before dual luciferase assays. Data were shown as mean with standard deviation. ***$p<0.001$ (E) STAT3-null MEFs reconstituted with wild-type or mutant STAT3 were treated with 30 ng/ml of mouse IL-6 for 30 minutes and analyzed by western blotting to determine the levels of STAT3 activation. Data in (A), (B-C), (D-E) are representative of 3, 2, and 4 independent experiments, respectively.

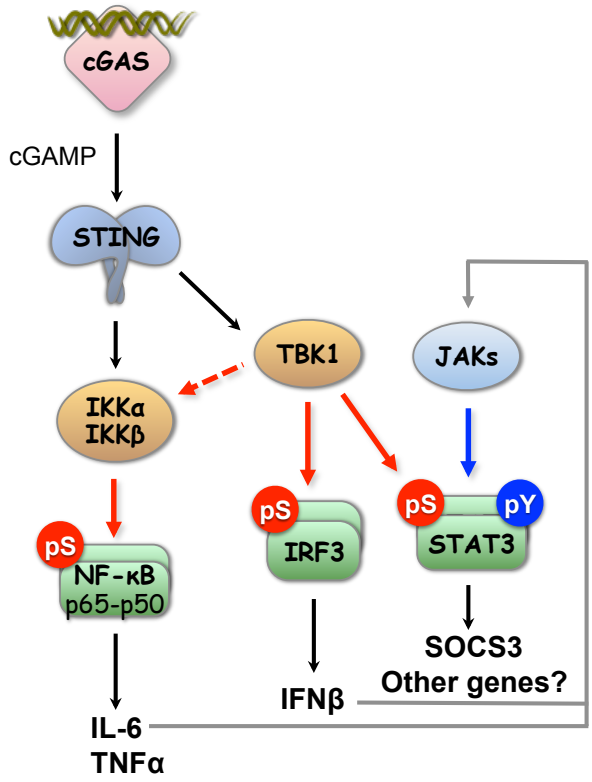

Figure 3.8 Schematic overview of STAT3 activation and regulation downstream of the cytosolic DNA pathway

Works presented in this chapter show that TBK1 directly phosphorylates STAT3 at S754 in response to cytosolic DNA in a cGAS and STING-dependent manner. Meanwhile, activation of IRF3 and NF-κB leads to production of IL-6 and IFNβ, which in turn activate STAT3 via JAKs. TBK1-mediated phosphorylation of S754 dampens STAT3 activity as demonstrated by reduced expression of the STAT3 target gene SOCS3.

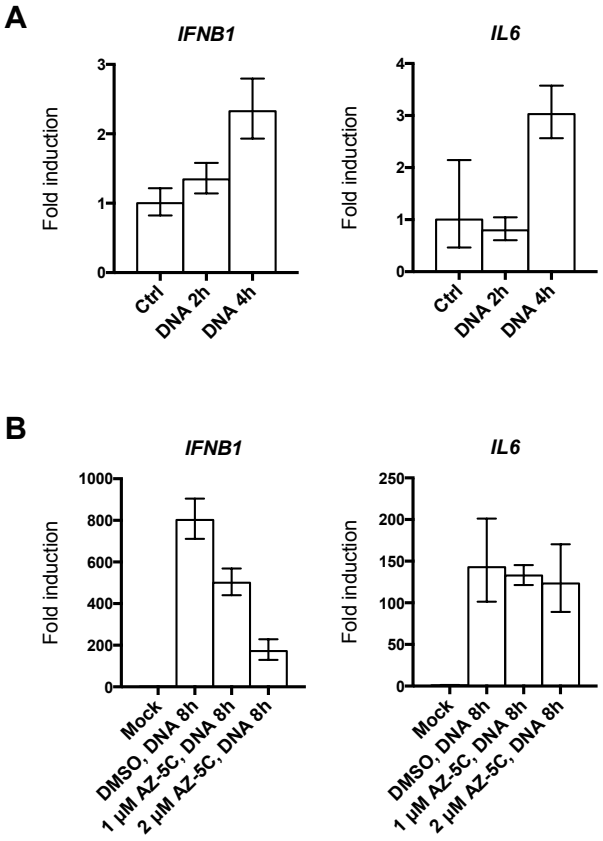

Supplemental Figure 3.1 Cytosolic DNA induces expression of IFNβ and IL-6
(A) THP-1 cells were transfected with dsDNA, and the expression levels of *IFNB1* and *IL6* at 2 and 4 hours post-transfection were determined by qRT-PCR. (B) THP-1 cells were pretreated with 1 or 2 μM of TBK1 inhibitor (AZ-5C) for 30 minutes, and transfected with dsDNA transfection for 8 hours. Expression levels of *IFNB1* and *IL6* were determined by qRT-PCR.

A

Human STAT3 sgRNA #6:

Targeting Exon1/intron junction, 5'UTR of STAT3 transcript

Off-targets		
No off-targets with 0, 1, or 2 mismatches		
Gene	# of mismatches	Sequence
Keratin 20 (intron)	3	CCCCTTCtCCTGTTTCTCCcGCt
TMEM17 (intron); LOC105374764 (intron)	3	TGCCtGtGAAACAGGTGAAtGGG
Mitogen-activated protein kinase 11 (intron)	3	CCCCTTCtCCTGTTTCcCCtGCA

B

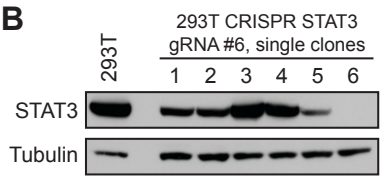

C

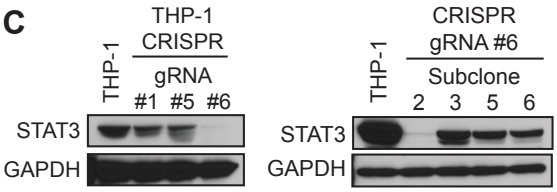

Supplemental Figure 3.2 CRISPR-mediated knockout of STAT3 in HEK293T and THP-1
(A) A schematic figure showing the target site of STAT3 sgRNA #6 at the 5' UTR of human STAT3 transcript. Potential off-targets of STAT3 sgRNA #6 were summarized in the table. (B) HEK293T cells were transduced with plentiCRISPRv2-STAT3-sgRNA6 virus. Puromycin-resistant individual clones were selected and analyzed by western blotting to determine the efficiency of STAT3 kncokout. Subclone #6 was designated as deltaSTAT3 HEK293T and used for the experiments in this paper. (C) THP-1 cells were transduced with three different plenti-CRISPRv2-STAT3 sgRNA viruses. Cells transduced with sgRNA#6 were further selected for puromycin-resistant individual clones. Subclone #2 were designated as deltaSTAT3 THP-1, reconstituted with wild-type or mutant STAT3, and used for experiments shown in Figure 3.6.

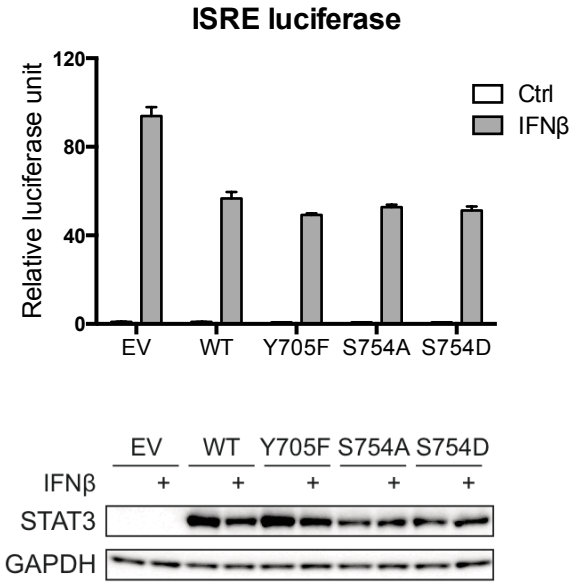

Supplemental Figure 3.3 STAT3 inhibits IFNβ-induced ISRE reporter expression
deltaSTAT3 293T cells were transfected with 167 ng of 4xHA-STAT3 plasmids, 167 ng of ISRE firefly luciferase plasmid, and 9 ng of tk-renilla luciferase plasmid. Twenty-four hours after transfection, cells were treated with 25 pg/ml of human IFNβ for another 24 hours before dual luciferase assay.

REFERENCES

1. Paludan SR, Bowie AG. Immune sensing of DNA. Immunity. 2013 May 23;38(5):870–80.

2. Broz P, Monack DM. Newly described pattern recognition receptors team up against intracellular pathogens. Nat Rev Immunol. 2013 Aug;13(8):551–65.

3. Wu J, Sun L, Chen X, Du F, Shi H, Chen C, et al. Cyclic GMP-AMP Is an Endogenous Second Messenger in Innate Immune Signaling by Cytosolic DNA. Science. 2013 Feb 14;339(6121):826–30.

4. Diner EJ, Burdette DL, Wilson SC, Monroe KM, Kellenberger CA, Hyodo M, et al. The innate immune DNA sensor cGAS produces a noncanonical cyclic dinucleotide that activates human STING. Cell Rep. 2013 May 30;3(5):1355–61.

5. Sun L, Wu J, Du F, Chen X, Chen ZJ. Cyclic GMP-AMP Synthase Is a Cytosolic DNA Sensor That Activates the Type I Interferon Pathway. Science. 2013 Feb 14;339(6121):786–91.

6. Ablasser A, Goldeck M, Cavlar T, Deimling T, Witte G, Röhl I, et al. cGAS produces a 2′-5′-linked cyclic dinucleotide second messenger that activates STING. Nature. 2013 May 30.

7. Tanaka Y, Chen ZJ. STING Specifies IRF3 Phosphorylation by TBK1 in the Cytosolic DNA Signaling Pathway. Sci Signal. 2012 Mar 6;5(214):ra20–0.

8. Liu S, Cai X, Wu J, Cong Q, Chen X, Li T, et al. Phosphorylation of innate immune adaptor proteins MAVS, STING, and TRIF induces IRF3 activation. Science. 2015 Mar 13;347(6227):aaa2630.

9. Zhong B, Yang Y, Li S, Wang Y-Y, Li Y, Diao F, et al. The adaptor protein MITA links virus-sensing receptors to IRF3 transcription factor activation. Immunity. 2008 Oct 17;29(4):538–50.

10. Ishikawa H, Barber GN. STING is an endoplasmic reticulum adaptor that facilitates innate immune signalling. Nature. 2008 Aug 24;455(7213):674–8.

11. Ishii KJ, Coban C, Kato H, Takahashi K, Torii Y, Takeshita F, et al. A Toll-like receptor–independent antiviral response induced by double-stranded B-form DNA. Nat Immunol. 2005 Nov 13;7(1):40–8.

12. Abe T, Harashima A, Xia T, Konno H, Konno K, Morales A, et al. STING recognition of cytoplasmic DNA instigates cellular defense. Mol Cell. 2013 Apr 11;50(1):5–15.

13. Abe T, Barber GN. Cytosolic-DNA-mediated, STING-dependent proinflammatory gene induction necessitates canonical NF-κB activation through TBK1. J Virol. 2014 May;88(10):5328–41.

14. Chen H, Sun H, You F, Sun W, Zhou X, Chen L, et al. Activation of STAT6 by STING is critical for antiviral innate immunity. Cell. 2011 Oct 14;147(2):436–46.

15. Zhong Z, Wen Z, Darnell JE. Stat3: a STAT family member activated by tyrosine phosphorylation in response to epidermal growth factor and interleukin-6. Science. 1994 Apr 1;264(5155):95–8.

16. Reich NC. STATs get their move on. JAK-STAT. 2014 Oct 20;2(4):e27080.

17. Bromberg JF, Wrzeszczynska MH, Devgan G, Zhao Y, Pestell RG, Albanese C, et al. Stat3 as an oncogene. Cell. 1999 Aug 6;98(3):295–303.

18. Yu H, Pardoll D, Jove R. STATs in cancer inflammation and immunity: a leading role for STAT3. Nat Rev Cancer. 2009 Nov;9(11):798–809.

19. Grivennikov SI, Karin M. Dangerous liaisons: STAT3 and NF-kappaB collaboration and crosstalk in cancer. Cytokine and Growth Factor Reviews. 2010 Feb;21(1):11–9.

20. Kortylewski M, Kujawski M, Wang T, Wei S, Zhang S, Pilon-Thomas S, et al. Inhibiting Stat3 signaling in the hematopoietic system elicits multicomponent antitumor immunity. Nat Med. 2005 Nov 20;11(12):1314–21.

21. Kortylewski M, Yu H. Role of Stat3 in suppressing anti-tumor immunity. Current Opinion in Immunology. 2008 Apr;20(2):228–33.

22. Horvath CM, Wen Z, Darnell JE. A STAT protein domain that determines DNA sequence recognition suggests a novel DNA-binding domain. Genes Dev. 1995 Apr 15;9(8):984–94.

23. Ivashkiv LB, Donlin LT. Regulation of type I interferon responses. Nat Rev Immunol. 2014 Jan;14(1):36–49.

24. Regis G, Pensa S, Boselli D, Novelli F, Poli V. Ups and downs: The STAT1:STAT3 seesaw of Interferon and gp130 receptor signalling. Semin Cell Dev Biol. 2008 Aug;19(4):351–9.

25. Wang WB, Levy DE, Lee CK. STAT3 Negatively Regulates Type I IFN-Mediated Antiviral Response. J Immunol. 2011 Aug 19;187(5):2578–85.

26. Ng S-L, Friedman BA, Schmid S, Gertz J, Myers RM, Tenoever BR, et al. IκB kinase epsilon (IKK(epsilon)) regulates the balance between type I and type II interferon responses. Proc Natl Acad Sci USA. 2011 Dec 27;108(52):21170–5.

27. Xia T, Konno H, Ahn J, Barber GN. Deregulation of STING Signaling in Colorectal Carcinoma Constrains DNA Damage Responses and Correlates With Tumorigenesis. Cell Rep. 2016 Jan 12;14(2):282–97.

28. Xia T, Konno H, Barber GN. Recurrent Loss of STING Signaling in Melanoma Correlates

with Susceptibility to Viral Oncolysis. Cancer Res. 2016 Sep 28.

29. Zhu Q, Man SM, Gurung P, Liu Z, Vogel P, Lamkanfi M, et al. Cutting edge: STING mediates protection against colorectal tumorigenesis by governing the magnitude of intestinal inflammation. J Immunol. 2014 Nov 15;193(10):4779–82.

30. Hutti JE, Shen RR, Abbott DW, Zhou AY, Sprott KM, Asara JM, et al. Phosphorylation of the tumor suppressor CYLD by the breast cancer oncogene IKKepsilon promotes cell transformation. Mol Cell. 2009 May 14;34(4):461–72.

31. Hutti JE, Porter MA, Cheely AW, Cantley LC, Wang X, Kireev D, et al. Development of a High-Throughput Assay for Identifying Inhibitors of TBK1 and IKKε. Harhaj E, editor. PLoS ONE. 2012 Jul 30;7(7):e41494.

32. Chau T-L, Gioia R, Gatot J-S, Patrascu F, Carpentier I, Chapelle J-P, et al. Are the IKKs and IKK-related kinases TBK1 and IKK-epsilon similarly activated? Trends Biochem Sci. 2008 Apr 1;33(4):171–80.

33. Unterholzner L, Keating SE, Baran M, Horan KA, Jensen SB, Sharma S, et al. IFI16 is an innate immune sensor for intracellular DNA. Nat Immunol. 2010 Nov;11(11):997–1004.

34. Hutti JE, Turk BE, Asara JM, Ma A, Cantley LC, Abbott DW. IkappaB kinase beta phosphorylates the K63 deubiquitinase A20 to cause feedback inhibition of the NF-kappaB pathway. Mol Cell Biol. 2007 Nov;27(21):7451–61.

35. Marinis JM, Hutti JE, Homer CR, Cobb BA, Cantley LC, McDonald C, et al. IκB kinase α phosphorylation of TRAF4 downregulates innate immune signaling. Mol Cell Biol. 2012 Jul;32(13):2479–89.

36. Ziegelbauer K, Gantner F, Lukacs NW, Berlin A, Fuchikami K, Niki T, et al. A selective novel low-molecular-weight inhibitor of IkappaB kinase-beta (IKK-beta) prevents pulmonary inflammation and shows broad anti-inflammatory activity. Br J Pharmacol. 2005 May;145(2):178–92.

37. Wang T, Block MA, Cowen S, Davies AM, Devereaux E, Gingipalli L, et al. Discovery of azabenzimidazole derivatives as potent, selective inhibitors of TBK1/IKKε kinases. Bioorganic & Medicinal Chemistry Letters. 2012 Mar 1;22(5):2063–9.

38. Ishikawa H, Ma Z, Barber GN. STING regulates intracellular DNA-mediated, type I interferon-dependent innate immunity. Nature. 2009 Oct 8;461(7265):788–92.

39. Pedranzini L, Dechow T, Berishaj M, Comenzo R, Zhou P, Azare J, et al. Pyridone 6, A Pan-Janus-Activated Kinase Inhibitor, Induces Growth Inhibition of Multiple Myeloma Cells. Cancer Res. 2006 Oct 1;66(19):9714–21.

40. Korherr C, Gille H, Schäfer R, Koenig-Hoffmann K, Dixelius J, Egland KA, et al. Identification of proangiogenic genes and pathways by high-throughput functional genomics: TBK1 and the IRF3 pathway. Proc Natl Acad Sci USA. 2006 Mar

14;103(11):4240–5.

41. Becker S, Groner B, Müller CW. Three-dimensional structure of the Stat3beta homodimer bound to DNA. Nature. 1998 Jul 9;394(6689):145–51.

42. Clément J-F, Meloche S, Servant MJ. The IKK-related kinases: from innate immunity to oncogenesis. Cell Res. 2008 Sep 1;18(9):889–99.

43. Hemmi H, Takeuchi O, Sato S, Yamamoto M, Kaisho T, Sanjo H, et al. The roles of two IkappaB kinase-related kinases in lipopolysaccharide and double stranded RNA signaling and viral infection. J Exp Med. 2004 Jun 21;199(12):1641–50.

44. Tenoever BR, Ng S-L, Chua MA, McWhirter SM, García-Sastre A, Maniatis T. Multiple functions of the IKK-related kinase IKKepsilon in interferon-mediated antiviral immunity. Science. 2007 Mar 2;315(5816):1274–8.

45. Chiu Y-H, MacMillan JB, Chen ZJ. RNA polymerase III detects cytosolic DNA and induces type I interferons through the RIG-I pathway. Cell. 2009 Aug 7;138(3):576–91.

46. Shimada T, Kawai T, Takeda K, Matsumoto M, Inoue J, Tatsumi Y, et al. IKK-i, a novel lipopolysaccharide-inducible kinase that is related to IkappaB kinases. International Immunology. 1999 Aug;11(8):1357–62.

47. Suzuki T, Oshiumi H, Miyashita M, Aly HH, Matsumoto M, Seya T. Cell Type-Specific Subcellular Localization of Phospho-TBK1 in Response to Cytoplasmic Viral DNA. Guo H, editor. PLoS ONE. 2013 Dec 9;8(12):e83639.

48. Caldenhoven E, van Dijk TB, Solari R, Armstrong J, Raaijmakers JA, Lammers JW, et al. STAT3beta, a splice variant of transcription factor STAT3, is a dominant negative regulator of transcription. J Biol Chem. 1996 May 31;271(22):13221–7.

49. Schaefer TS, Sanders LK, Park OK, Nathans D. Functional differences between Stat3alpha and Stat3beta. Mol Cell Biol. 1997 Sep;17(9):5307–16.

50. Park OK, Schaefer LK, Wang W, Schaefer TS. Dimer stability as a determinant of differential DNA binding activity of Stat3 isoforms. J Biol Chem. 2000 Oct 13;275(41):32244–9.

51. Woo S-R, Fuertes MB, Corrales L, Spranger S, Furdyna MJ, Leung MYK, et al. STING-dependent cytosolic DNA sensing mediates innate immune recognition of immunogenic tumors. Immunity. 2014 Nov 20;41(5):830–42.

52. Corrales L, Glickman LH, McWhirter SM, Kanne DB, Sivick KE, Katibah GE, et al. Direct Activation of STING in the Tumor Microenvironment Leads to Potent and Systemic Tumor Regression and Immunity. Cell Rep. 2015 May 19;11(7):1018–30.

53. Melillo JA, Song L, Bhagat G, Blazquez AB, Plumlee CR, Lee C, et al. Dendritic Cell (DC)-Specific Targeting Reveals Stat3 as a Negative Regulator of DC Function. J

Immunol. 2010 Feb 17;184(5):2638–45.

54. Morgenstern JP, Land H. Advanced mammalian gene transfer: high titre retroviral vectors with multiple drug selection markers and a complementary helper-free packaging cell line. Nucleic Acids Res. 1990 Jun 25;18(12):3587–96.

55. Sanjana NE, Shalem O, Zhang F. Improved vectors and genome-wide libraries for CRISPR screening. Nat Meth. 2014 Jul 30;11(8):783–4.

56. Besser D, Bromberg JF, Darnell JE, Hanafusa H. A single amino acid substitution in the v-Eyk intracellular domain results in activation of Stat3 and enhances cellular transformation. Mol Cell Biol. 1999 Feb;19(2):1401–9.

57. Lawrence CL, Baldwin AS. Non-Canonical EZH2 Transcriptionally Activates RelB in Triple Negative Breast Cancer. Ahmad A, editor. PLoS ONE. 2016 Oct 20;11(10):e0165005.

CHAPTER 4: FUTURE DIRECTIONS AND CONCLUSIONS

In this Chapter, I examine how the discoveries described in this dissertation add to our current understanding of the roles and regulation of STAT3 in diseases, and present unpublished data to discuss future directions revealed by my research.

4.1 Roles and Regulation of STAT3 Activity in Diseases

4.1.1 Regulation of STAT3 activity: A balancing act

The ubiquitous expression of STAT3 and its activation by a number of cytokines and activators give STAT3 a central role in controlling the survival, proliferation, and function of cells. Consequently, dysregulation of STAT3 activity is associated with numerous diseases and disorders. In humans, STAT3 loss-of-function mutations lead to the immunodeficiency disorder AD-HIES as discussed in Chapter 1. AD-HIES patients have higher incidences of herpesvirus reactivation and viremia, and these symptoms have been partially attributed to T cell-intrinsic defects (1). My work presented in Chapter 2 showed that myeloid-specific STAT3 knockout mice are also more susceptible to HSV-1 (2,3). Specifically, these knockout mice exhibited an attenuated type I IFN response and defects in DC and NK cell activation, indicating that STAT3 is required by the myeloid cells to elicit effective innate immune responses against herpesvirus infections. On the other hand, STAT3 gain-of-function mutations cause lymphoproliferative disorders and cancers in human. It is also well established that constitutive STAT3 activation contributes to increased metastasis, resistance to therapy, and poor prognosis in a variety of cancers (discussed in Chapter 1). Thus, precise temporal and spatial regulation of STAT3

activity is crucial to maintaining homeostasis and establishing effective defense against pathogens.

Regulation of transcription factor activity can be achieved through several means, but regulation of activity by post-translational modification (PTM) offers the advantage of instantaneous response and flexibility in timespans. Several PTMs have been reported to fine-tune STAT3 activity, including K49 dimethylation, K685 acetylation, and S727 phosphorylation, all of which has been suggested to increase STAT3 activity (4-8). The S754 phosphorylation identified in Chapter 3 adds a novel inhibitory mechanism to the growing means of STAT3 activity regulation by PTM. The inhibitory effect of S754 phosphorylation on STAT3 activity suggests that it may modify cellular responses by regulating STAT3 target gene expression, necessitating the need to understand the gene expression profile affected by S754 phosphorylation of STAT3. It is unclear whether all STAT3 target genes or only a subset of targets are repressed by S754 phosphorylation. Although the DNA binding specificity of STAT3 is dictated by its DBD (9), it is still conceivable that S754 phosphorylation may modify the promoter preference of STAT3 by altering the interaction between STAT3 and other transcription factors or co-factors, and consequently change the selectivity of STAT3 toward specific target genes depending on the available transcription factors and co-factors at a given moment. Moreover, a transcriptional repression role of STAT3 has also been reported for some genes (10,11). Whether S754 phosphorylation has any impact on the transcriptional repression mediated by STAT3 remains to be determined. For future investigations, comparing the cytosolic DNA-induced promoter occupancy of STAT3 and gene expression of WT and S754A STAT3 reconstituted cells by ChIP-seq and RNA-seq may provide some clues to these questions.

4.1.2 Regulation of STAT3 activity in viral infection

The finding that cytosolic DNA restrains STAT3 activation by S754 phosphorylation raises several important questions: When and where does this occur *in vivo*, and what are the consequences? One possible scenario that may lead to STAT3 S754 phosphorylation is during DNA virus infection, which is known to activate the cytosolic DNA pathway. As a negative regulator of STAT1 and IFN response, STAT3 deficiency confers improved resistance to viral infections in cell culture (12), but permanent functional loss of STAT3 *in vivo* leads to impaired immune responses to bacterial and viral infections (Chapters 1 and 2). Therefore, a transient and controlled inhibition of STAT3 activity by S754 phosphorylation may be beneficial to the host defense without causing long-term detrimental effects. Indeed, my preliminary data showed that WT HSV-1 infection induced a modest STAT3 S754 phosphorylation in STAT3 reconstituted MEFs, although WT and S754A MEFs did not have a measurable difference in their intrinsic resistance to HSV-1 replication (data not shown). One possible explanation is that modest STAT3 inhibition is not sufficient to overcome the effective repression of TBK1 and IFN responses by HSV-1 (13,14), and using an attenuated strain of HSV-1 with reduced ability to inhibit TBK1 may help reveal the subtle differences between WT and S754A STAT3 cells. Additionally, it may be worth examining the gene expression profile in HSV-1 infected WT and S754A reconstituted cells, since differential gene expression, if involving cytokines and secreted factors, is likely to affect the course of viral pathogenesis and clearance *in vivo*.

4.1.3 Regulation of STAT3 activity in tumors and the tumor microenvironment

The tumor microenvironment is another possible scenario in which STAT3 can become phosphorylated at S754. It was known that cytosolic DNA can activate DC and act as a potent

adjuvant for vaccination before the molecular mechanism of the cytosolic DNA pathway was fully understood (2,3). Recent studies showed that DC in the tumor microenvironment are activated by tumor-derived DNA in a STING-dependent manner, resulting in IFNβ secretion and T cell recruitment to the tumor (4-8,15). Although these infiltrating T cells are often functionally repressed, this "T cell-inflamed" tumor microenvironment predicts better responses to check-point inhibitor immunotherapies (9,16). Since STAT3 is a negative regulator of DC activity (10,11,17), it is tempting to speculate that tumor-derived DNA may induce STAT3 S754 phosphorylation in DC to transiently inhibit STAT3 activity and relieve restraints on DC activation. Because bone marrow-derived dendritic cells (BMDC) from *Stat3*$^{fl/fl}$ LysM-Cre$^{+/+}$ mice have an incomplete deletion of STAT3 (Figure 4.1A), I used these cells to approximate the inhibitory effect installed by S754 phosphorylation. As expected, DNA transfection induced S754 phosphorylation in WT BMDC (Figure 4.1B). Cytosolic DNA-induced DC maturation was not affected by reduced STAT3 levels, as shown by comparable upregulation of stimulatory co-receptors CD80 and CD86 in WT and KO BMDC (Figure 4.1C; Table 4.1). Both WT and KO BMDC were able to maintain homeostatic T cell proliferation in a co-culture system in the absence of foreign antigen or stimulation, while DNA-stimulated BMDC had decreased capacity to support T cell proliferation, presumably due to T cell anergy in the absence of foreign antigens (Figure 4.1D). For future studies, it would be of interest to determine the capacity of DNA-stimulated STAT3 KO BMDC to activate T cells following pulsing with foreign antigens or tumor-derived neoantigens. An increase in T cell proliferation induced by STAT3 KO BMDC will justify further investigations on the regulation of STAT3 activity in DC in the tumor microenvironment.

Functional loss of the cytosolic DNA pathway is often observed in some commonly used cell-lines in the laboratory and primary tumors, suggesting that loss of this pathway confers survival or proliferation advantage to the cancers *in vivo* and perhaps also *in vitro*. DNA damage, which can be caused by aneuploidy in cancer cells or radiation therapy, also activates the cytosolic DNA pathway, resulting in IFNβ production and T cell-mediated anti-tumor immunity (12,18-21). As a result, functional loss of the cytosolic DNA pathway in cancer provides them an advantage *in vivo* by reducing T cell recruitment and anti-tumor immune responses. However, the cell-intrinsic effect of losing the cytosolic DNA pathway has not been fully explored. Constitutive STAT3 activation promotes survival and proliferation in many tumors, and inhibition of STAT3 activity by S754 phosphorylation would likely be unfavorable to tumors. Therefore, functional loss of the cytosolic DNA pathway may also confer a survival advantage at a cell-autonomous level by allowing unchecked STAT3 activation. To test this hypothesis, a study focusing on whether responsiveness to cytosolic DNA correlates with STAT3 activity in cancer cell-lines should be conducted. If genetic ablation of cGAS and STING promotes the proliferation and survival in a STAT3-dependent manner in cancer cell-lines that normally respond to cytosolic DNA, this would support the aforementioned hypothesis. Additionally, a particularly interesting case involves TBK1 and IKKε-dependent cancers, as discussed in Chapter 1. It would be of interest to determine if the cytosolic DNA pathway is preferentially lost in TBK1-dependent K-RAS transformed cells or IKKε-overexpressing breast cancers.

With its role in promoting tumorigenesis, STAT3 seems to be a rational target for cancer therapeutics. Several strategies have been adopted to develop STAT3 inhibitors, including small molecules and phosphotyrosyl peptides that interact with the SH2 domain of STAT3 to directly disrupt STAT3 dimerization (13,14,22-25). While these inhibitors demonstrated efficacy in

inhibiting STAT3 *in vitro*, their low affinity and promiscuous substrate specificity pose a major challenge for further applications (4-8,26,27). STAT3 decoy oligonucleotides with GAS sequences have also been developed to sequester STAT3 from the nucleus, but the potential interaction between this decoy and STAT1 may result in confounding effects (9,28,29). Targeting the upstream kinases that activate STAT3 is another approach. For example, Ruxolitinib is a JAK1/JAK2-specific inhibitor approved by FDA for myelofibrosis, but it also showed promising results in leukemia patients in a phase II trial through STAT3 inhibition (10,11,30). AG490, another JAK2-specific inhibitor, selectively blocks STAT3-driven proliferation and induces cell death in several cancer cell-lines (12,31-33), In tumors with EGFR mutation or amplification, the efficacy of anti-EGFR monoclonal antibodies and small molecules is also partially mediated by STAT3 inhibition (Reviewed in (13,14,34)). The case for using STAT3 inhibitors to treat cancers is also bolstered by the discovery that STAT3 negatively regulates the anti-tumor immunity of hematopoietic cells in the tumor microenvironment (2,35-37). If it is determined that STAT3 S754 phosphorylation by tumor-derived DNA increases the ability of DC to activate T cells in the tumor microenvironment, it will provide additional arguments to advocate for using STAT3 inhibitors as cancer therapeutics to not only curb tumor growth but also augment anti-tumor immunity.

4.2 The Mechanism of STAT3 Inhibition by S754 Phosphorylation

My work has demonstrated that S754 STAT3 phosphorylation restricts its transcriptional activity, but the molecular mechanism resulting in such inhibition remains to be determined. One possible explanation is that S754 phosphorylation modulates STAT3 activity by altering the interaction between STAT3 and its co-factors. Of note, one such co-factor, nuclear receptor

coactivator 1 (NCOA1), has been shown to promote STAT3 transcriptional activity through direct interaction with the amino acids 752-761 of STAT3 (15,38,39). Therefore, I hypothesized that S754 phosphorylation will disrupt the interaction between STAT3 and NCOA1. Unfortunately, I was unable to detect STAT3-NCOA1 interaction in THP-1 cells under basal condition or upon cytosolic DNA stimulation (data not shown). For future directions, comparing STAT3 interactomes under basal and cytosolic DNA-stimulated conditions by an unbiased proteomics approach may be useful to identify the interactions that are modulated by S754 phosphorylation. However, there are several caveats in this approach. For instance, the percentage of STAT3 being phosphorylated at S754 in a cell will directly affect the quality of the results. If only a small fraction of STAT3 in the cell is phosphorylated at S754, interactions that are phospho-S754-dependent may not be sufficiently distinguished from the background. The use of phosphomimetic mutants, S754D or S754E, may be an alternative solution, but it also risks the possibility of not fully reflecting the structural and functional change of a phosphorylation and fail to capture some of the phospho-S754-dependent interactions.

The decreased Y705 phosphorylation in S754 phosphorylated STAT3 and S754D mutant is in fact more consistent with another hypothesis regarding the stability of STAT3 dimers. Mutational analyses demonstrated that the cluster of negatively charged acidic amino acids in the C terminus destabilize STAT3 dimers, and the stability of STAT3 dimers correlates with the level of Y705 phosphorylation, since the phosphorylated residue is likely more vulnerable to phosphatases when the dimers are less stable (16,40). Therefore, the additional negative charges introduced by S754 phosphorylation may further destabilize STAT3 dimers, thereby reducing the level of Y705 phosphorylation and its transcriptional activity. To test this hypothesis, I assessed IL-6-induced STAT3 dimerization by blue native-PAGE (BN-PAGE). Because inactive STAT3

can also exist as dimers due to interactions mediated by the NTDs, deltaNTD-STAT3 (amino acids 125-770) was used to evaluate the effect of S754 phosphorylation on dimerization mediated by phospho-Y705 and the SH2 domain. As expected, S754D mutant showed a mild decreased in dimerization upon IL-6 stimulation (Figure 4.2). Because the stability of STAT3 dimers has a direct impact on its DNA binding activity (17,40), future investigations will focus on the dimer stability of full-length STAT3, and hence the DNA binding activity, in the presence or absence of S754 phosphorylation.

4.3 Concluding Remarks

In the first part of my dissertation (Chapter 2), I showed that myeloid STAT3 deficiency results in reduced IFNα expression in macrophages, and impaired DC and NK cell activation, making the mice more susceptible to HSV-1 infection. This demonstrates that STAT3 is required to mount an efficient anti-viral response through innate immunity at the early stage of viral infection, and may partially explain the susceptibility of human AD-HIES patients to herpesviruses. In the second part of my dissertation (Chapter 3), I revealed that cytosolic DNA restrains STAT3 activation through a TBK1-mediated inhibitory phosphorylation, and expanded our knowledge of regulation of STAT3 activity by PTM. In summary, my research contributes to our understanding of the roles and regulation of STAT3 in innate immunity. The discovery that STAT3 activity can be fine-tuned by the cytosolic DNA pathway also reveals potential implications in cancer biology. Future studies will be built on these findings to continue investigating the molecular mechanism of STAT3 regulation, and to explore the means of manipulating STAT3 activity for therapeutic purposes.

4.4 Materials and Methods

BMDC differentiation. The bone marrows of 12-week-old female mice were isolated as described in Chapter 2. Cells were cultured in BMDC differentiation media (RPMI 1640 with 10% FBS and Pen/Strep, supplemented with 20 ng/ml of GM-CSF (Biolegend)). On day 2 and 4 after isolation, half of the media was gently removed and replaced with fresh media. BMDC in suspension were collected after 6 days and analyzed by flow cytometry as >60% $CD11c^+$.

T cell isolation. Splenic T cells were isolated from a 13-week-old wild-type male mouse by magnetic T cell isolation kit (Stemcell #19851) according to manufecturer's instruction. The viability and purity ($CD3^+$) of isolated T cells were determined by flow cytometry as > 95%. The T cells were labeled with 2.5 μM of CFSE (Biolegend) at a density of $3.5x10^6$ cells/ml at room temperature for 4 minutes, and washed three times with RPMI1640 with 10% FBS.

DC and T cell co-culture. BMDC were plated in 96-well round bottom plates at $2.5x10^5$ or $0.5x10^5$ cells/well in 100 μl of BMDC media, and were left untreated or transfected with VACV70mer at 2 μg/ml with lipofectamine 2000 (Thermo Fisher) as described in Chapter 3. Next day, freshly isolated and CFSE-labeled T cells were added to the BMDC at $0.5x10^5$ cells/well in 100 μl of RPMI 1640 with 10% FBS and Pen/Strep. After 4 days of culture, cells were analyzed by flow cytometry, and viable proliferated T cells ($DAPI^-CD3^+$) were gated by their lower CFSE intensity.

BN-PAGE. BN-PAGE was carried out as described in (41). Flag-deltaNTD-STAT3 (amino acids 125-770) reconstituted MEFs were serum-starved overnight and treated with 100 U/ml of mouse IL-6 (Biolegend) for 30 minutes or left untreated. Cells were lysed with BN lysis buffer with 0.5% Triton X-100, protease inhibitor cocktail (Promega), phosphatase inhibitor cocktail (Sigma), and 1 μM of pervanadate, and spun at 13000 rpm at 4°C for 10 minutes to

remove cell debris. The protein concentration of the supernatants was adjusted to ~2-3 mg/ml with BN lysis buffer, followed by mixing with 2% Coomassie G-250 (Sigma) to a final detergent-to-Coomassie ratio of 8:1. Twenty-five μg of protein per sample was resolved in 10% BN-PAGE gel with 3.6% stacking gel together with native protein markers (Life Technology). The proteins were transferred to PVDF membranes by wet transfer (25 mM Tris, 192 mM glycine, 0.01% SDS, 10% methanol for 2h at 70V) and proceeded with regular immunoblotting using STAT3 antibody (Cell Signaling Technology #9139)

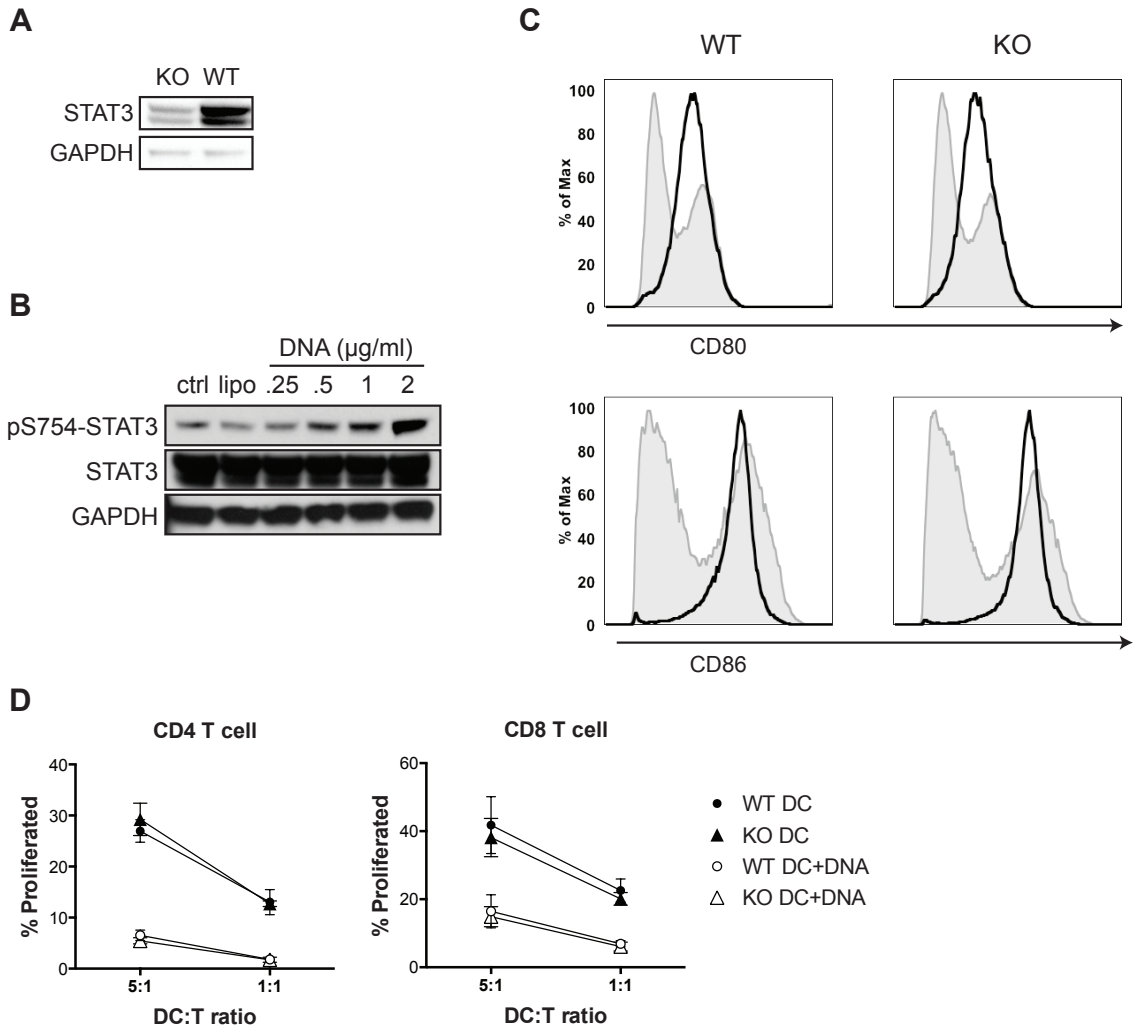

Figure 4.1 Cytosolic DNA induces STAT3 S754 phosphorylation and promotes DC maturation

(A) Immunoblotting of STAT3 in GM-CSF-differentiated BMDC derived from WT or KO mice. No differentiation block of BMDC was observed in *Stat3* knockout cells (not shown) (B) WT BMDC were transfected with increasing concentration of VACV70mer for 3 hours or left untreated, and analyzed by immunoblotting. (C) WT and KO BMDC were transfected with 2 μg/ml of VACV70mer or left untreated, and analyzed by flow cytometry to determine CD80 and CD86 expression after one day. Shaded area: untreated BMDC; Solid line: DNA-transfected BMDC. Data are representative of 3 mice per group. (D) WT or KO BMDC were transfected with 2 μg/ml of VACV70mer or left untreated. After 1 day of culture, BMDC were co-cultured with CFSE-labeled T cells at different ratios for 4 days. Proliferated T cells were determined by lower CFSE intensity. Data are shown as mean with standard deviation with 3 mice per genotype.

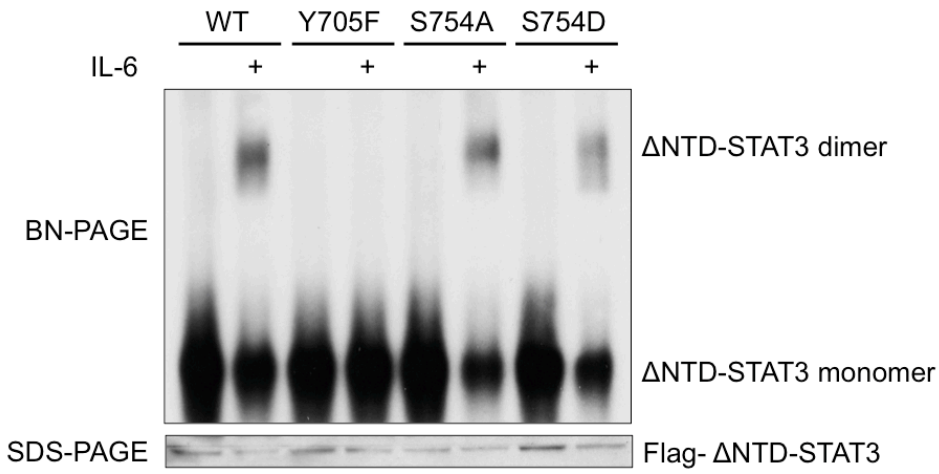

Figure 4.2 S754 phosphomimetic interferes with STAT3 dimerization
MEFs reconstituted with Flag-deltaNTD-STAT3 were treated with 100 U/ml of mouse IL-6 for 30 minutes, and lysates were subjected to BN-PAGE to analyze STAT3 dimerization.

Table 4.1 Upregulation of stimulatory co-receptors in BMDC by DNA transfection

Mouse (n=3)	Treatment	% $CD80^+$	%$CD86^+$
WT	Ctrl	42.7 ± 4.46	46.5 ± 5.48
KO	Ctrl	41.1 ± 1.31	46.3 ± 1.79
WT	DNA	76.9 ± 1.33	90.9 ± 1.55
KO	DNA	72.2 ± 2.15	95.1 ± 0.81

BMDC from STAT3 WT or KO mice were transfected with 2 μg/ml of VACV70mer or left untreated for a day. The percentage of $CD80^+$ or $CD86^+$ cells in $CD11c^+$ population was determined by flow cytometry.

REFERENCES

1. Siegel AM, Heimall J, Freeman AF, Hsu AP, Brittain E, Brenchley JM, et al. A critical role for STAT3 transcription factor signaling in the development and maintenance of human T cell memory. Immunity. 2011 Nov 23;35(5):806–18.

2. Hsia H-C, Stopford CM, Zhang Z, Damania B, Baldwin AS. Signal transducer and activator of transcription 3 (Stat3) regulates host defense and protects mice against herpes simplex virus-1 (HSV-1) infection. Journal of Leukocyte Biology. 2016 Dec 13.

3. Wang R, Cherukuri P, Luo J. Activation of Stat3 sequence-specific DNA binding and transcription by p300/CREB-binding protein-mediated acetylation. J Biol Chem. 2005 Mar 25;280(12):11528–34.

4. Yuan ZL. Stat3 Dimerization Regulated by Reversible Acetylation of a Single Lysine Residue. Science. 2005 Jan 14;307(5707):269–73.

5. Schuringa JJ, Schepers H, Vellenga E, Kruijer W. Ser727-dependent transcriptional activation by association of p300 with STAT3 upon IL-6 stimulation. FEBS Lett. 2001 Apr 20;495(1-2):71–6.

6. Wen Z, Zhong Z, Darnell JE. Maximal activation of transcription by Stat1 and Stat3 requires both tyrosine and serine phosphorylation. Cell. 1995 Jul 28;82(2):241–50.

7. Dasgupta M, Dermawan JKT, Willard B, Stark GR. STAT3-driven transcription depends upon the dimethylation of K49 by EZH2. Proc Natl Acad Sci USA. 2015 Mar 31;112(13):3985–90.

8. Horvath CM, Wen Z, Darnell JE. A STAT protein domain that determines DNA sequence recognition suggests a novel DNA-binding domain. Genes Dev. 1995 Apr 15;9(8):984–94.

9. Snyder M, Huang X-Y, Zhang JJ. Identification of novel direct Stat3 target genes for control of growth and differentiation. J Biol Chem. 2008 Feb 15;283(7):3791–8.

10. Zhang H, Hu H, Greeley N, Jin J, Matthews AJ, Ohashi E, et al. STAT3 restrains RANK- and TLR4-mediated signalling by suppressing expression of the E2 ubiquitin-conjugating enzyme Ubc13. Nat Commun. 2014;5:5798.

11. Ho HH, Ivashkiv LB. Role of STAT3 in type I interferon responses. Negative regulation of STAT1-dependent inflammatory gene activation. J Biol Chem. 2006 May 19;281(20):14111–8.

12. Christensen MH, Jensen SB, Miettinen JJ, Luecke S, Prabakaran T, Reinert LS, et al. HSV-1 ICP27 targets the TBK1-activated STING signalsome to inhibit virus-induced type I IFN expression. EMBO J. 2016 Jul 1;35(13):1385–99.

13. Ma Y, Jin H, Valyi-Nagy T, Cao Y, Yan Z, He B. Inhibition of TANK binding kinase 1

by herpes simplex virus 1 facilitates productive infection. J Virol. 2012 Feb;86(4):2188–96.

14. Ishii KJ, Kawagoe T, Koyama S, Matsui K, Kumar H, Kawai T, et al. TANK-binding kinase-1 delineates innate and adaptive immune responses to DNA vaccines. Nature. 2008 Feb 7;451(7179):725–9.

15. Deng L, Liang H, Xu M, Yang X, Burnette B, Arina A, et al. STING-Dependent Cytosolic DNA Sensing Promotes Radiation-Induced Type I Interferon-Dependent Antitumor Immunity in Immunogenic Tumors. Immunity. 2014 Nov 20;41(5):843–52.

16. Gajewski TF. The Next Hurdle in Cancer Immunotherapy: Overcoming the Non-T-Cell-Inflamed Tumor Microenvironment. Semin Oncol. 2015 Aug;42(4):663–71.

17. Melillo JA, Song L, Bhagat G, Blazquez AB, Plumlee CR, Lee C, et al. Dendritic Cell (DC)-Specific Targeting Reveals Stat3 as a Negative Regulator of DC Function. J Immunol. 2010 Feb 17;184(5):2638–45.

18. Härtlova A, Erttmann SF, Raffi FA, Schmalz AM, Resch U, Anugula S, et al. DNA damage primes the type I interferon system via the cytosolic DNA sensor STING to promote anti-microbial innate immunity. Immunity. 2015 Feb 17;42(2):332–43.

19. Ferguson BJ, Mansur DS, Peters NE, Ren H, Smith GL. DNA-PK is a DNA sensor for IRF-3-dependent innate immunity. eLife. 2012 Dec 18;1:e00047.

20. Zhang X, Brann TW, Zhou M, Yang J, Oguariri RM, Lidie KB, et al. Cutting Edge: Ku70 Is a Novel Cytosolic DNA Sensor That Induces Type III Rather Than Type I IFN. J Immunol. 2011 Apr 4;186(8):4541–5.

21. Kondo T, Kobayashi J, Saitoh T, Maruyama K, Ishii KJ, Barber GN, et al. DNA damage sensor MRE11 recognizes cytosolic double-stranded DNA and induces type I interferon by regulating STING trafficking. Proc Natl Acad Sci USA. 2013 Feb 19;110(8):2969–74.

22. Takeda K, Noguchi K, Shi W, Tanaka T, Matsumoto M, Yoshida N, et al. Targeted disruption of the mouse Stat3 gene leads to early embryonic lethality. Proc Natl Acad Sci USA. 1997 Apr 15;94(8):3801–4.

23. Schust J, Sperl B, Hollis A, Mayer TU, Berg T. Stattic: A Small-Molecule Inhibitor of STAT3 Activation and Dimerization. Chemistry & Biology. 2006 Nov;13(11):1235–42.

24. Siddiquee K, Zhang S, Guida WC, Blaskovich MA, Greedy B, Lawrence HR, et al. Selective chemical probe inhibitor of Stat3, identified through structure-based virtual screening, induces antitumor activity. Proc Natl Acad Sci USA. 2007 May 1;104(18):7391–6.

25. Turkson J, Ryan D, Kim JS, Zhang Y, Chen Z, Haura E, et al. Phosphotyrosyl peptides block Stat3-mediated DNA binding activity, gene regulation, and cell transformation. J Biol Chem. 2001 Nov 30;276(48):45443–55.

26. Ball DP, Lewis AM, Williams D, Resetca D, Wilson DJ, Gunning PT. Signal transducer and activator of transcription 3 (STAT3) inhibitor, S3I-201, acts as a potent and non-selective alkylating agent. Oncotarget. 2016 Mar 2.

27. Sanseverino I, Purificato C, Gauzzi MC, Gessani S. Revisiting the specificity of small molecule inhibitors: the example of stattic in dendritic cells. Chemistry & Biology. 2012 Oct 26;19(10):1213–4–authorreply1215–6.

28. Leong PL, Andrews GA, Johnson DE, Dyer KF, Xi S, Mai JC, et al. Targeted inhibition of Stat3 with a decoy oligonucleotide abrogates head and neck cancer cell growth. Proc Natl Acad Sci USA. 2003 Apr 1;100(7):4138–43.

29. Souissi I, Najjar I, Ah-Koon L, Schischmanoff PO, Lesage D, Le Coquil S, et al. A STAT3-decoy oligonucleotide induces cell death in a human colorectal carcinoma cell line by blocking nuclear transfer of STAT3 and STAT3-bound NF-κB. BMC Cell Biol. 2011 Apr 12;12:14.

30. Eghtedar A, Verstovsek S, Estrov Z, Burger J, Cortes J, Bivins C, et al. Phase 2 study of the JAK kinase inhibitor ruxolitinib in patients with refractory leukemias, including postmyeloproliferative neoplasm acute myeloid leukemia. Blood. 2012 May 17;119(20):4614–8.

31. Aoki Y, Feldman GM, Tosato G. Inhibition of STAT3 signaling induces apoptosis and decreases survivin expression in primary effusion lymphoma. Blood. 2003 Feb 15;101(4):1535–42.

32. Rahaman SO, Harbor PC, Chernova O, Barnett GH, Vogelbaum MA, Haque SJ. Inhibition of constitutively active Stat3 suppresses proliferation and induces apoptosis in glioblastoma multiforme cells. Oncogene. 2002 Dec 5;21(55):8404–13.

33. Meydan N, Grunberger T, Dadi H, Shahar M, Arpaia E, Lapidot Z, et al. Inhibition of acute lymphoblastic leukaemia by a Jak-2 inhibitor. Nature. 1996 Feb 15;379(6566):645–8.

34. Johnston PA, Grandis JR. STAT3 signaling: anticancer strategies and challenges. Mol Interv. 2011 Feb;11(1):18–26.

35. Wang T, Niu G, Kortylewski M, Burdelya L, Shain K, Zhang S, et al. Regulation of the innate and adaptive immune responses by Stat-3 signaling in tumor cells. Nat Med. 2003 Dec 21;10(1):48–54.

36. Kortylewski M, Kujawski M, Wang T, Wei S, Zhang S, Pilon-Thomas S, et al. Inhibiting Stat3 signaling in the hematopoietic system elicits multicomponent antitumor immunity. Nat Med. 2005 Nov 20;11(12):1314–21.

37. Kortylewski M, Xin H, Kujawski M, Lee H, Liu Y, Harris T, et al. Regulation of the IL-23 and IL-12 balance by Stat3 signaling in the tumor microenvironment. Cancer Cell. 2009 Feb 3;15(2):114–23.

38. Zhao H, Nakajima R, Kunimoto H, Sasaki T, Kojima H, Nakajima K. Region 752–761 of STAT3 is critical for SRC-1 recruitment and Ser727 phosphorylation. Biochem Biophys Res Commun. 2004 Dec;325(2):541–8.

39. Giraud S, Bienvenu F, Avril S, Gascan H, Heery DM, Coqueret O. Functional interaction of STAT3 transcription factor with the coactivator NcoA/SRC1a. J Biol Chem. 2002 Mar 8;277(10):8004–11.

40. Sasse J, Hemmann U, Schwartz C, Schniertshauer U, Heesel B, Landgraf C, et al. Mutational analysis of acute-phase response factor/Stat3 activation and dimerization. Mol Cell Biol. 1997 Aug;17(8):4677–86.

41. Swamy M. Blue Native Polyacrylamide Gel Electrophoresis (BN-PAGE) for the Identification and Analysis of Multiprotein Complexes. Science's STKE. 2006 Jul 18;2006(345):pl4–pl4.